2017

Characterization of the Effect of Aeration on a Commercially Available Fibrin Sealant for Use in Wound Therapy

Adam Robert Marek
Loyola University Chicago

LOYOLA UNIVERSITY CHICAGO

CHARACTERIZATION OF THE EFFECT OF AERATION ON A COMMERCIALLY AVAILABLE FIBRIN SEALANT FOR USE IN WOUND THERAPY

A DISSERTATION SUBMITTED TO

THE FACULTY OF THE GRADUATE SCHOOL

IN CANDIDACY FOR THE DEGREE OF

DOCTOR OF PHILOSOPHY

PROGRAM IN MOLECULAR PHARMACOLOGY & THERAPEUTICS

BY

ADAM R. MAREK

CHICAGO, IL

AUGUST 2017

ACKNOWLEDGEMENTS

I would like to begin by thanking my main advisor, Richard Kennedy, Ph.D. Dr. Kennedy was instrumental in my graduate education from its beginning. It was with his tutelage that my industrial Ph.D. program came about, and he was with me during the good and bad times that came along with it. As the years progressed, Dr. Kennedy was still in reach after his move from Loyola, and he was always there to give insight into any situation.

Next, I would like to thank my Baxter advisors, Shawn Bairstow, Ph.D. and John Barry, Ph.D. – these two scientists were my main mentors throughout the years with the company. Dr. Bairstow was there for me week in and week out to help me perform to the best of my scientific abilities. Dr. Barry always brought the industrial aspect to discussions and taught me a lot about these intricacies. I have gained a plethora of knowledge spanning cellular biology to surgical sciences and engineering from them both.

I would also like to thank the remainder of my committee – from Loyola, Kenneth Byron, Ph.D. and Richard Gamelli, M.D. and from Baxter, Mark Doty, Ph.D. and Marcus Schabacker, M.D., Ph.D. These great minds influenced my program and learning both in the academic setting as well as the industrial one. With their guidance throughout my doctoral career, I feel very confident in my future.

In addition, I would truly like to thank my friends and colleagues throughout the time spent at Baxter. From my Advanced Surgery team to the dozens of others that I had the pleasure of working with and learning from, I am very thankful for each and every one of them. They helped me to improve my scientific techniques and taught me so much about the technical side of the healthcare industry. I am appreciative of the time I had with them all.

Thank you to the faculty, students, and staff of the Molecular Pharmacology and Therapeutics Program at Loyola University Chicago as well as all colleagues that I have been fortunate enough to interact with over my years with the university. I would also like to thank the Jones Laboratory for their contributions to the murine wound model.

Lastly, I would like to thank my family and friends. They have been with me at each and every step along my extensive educational journey. Without their influence and encouragement, I would not be where I am today.

To my Theodore

TABLE OF CONTENTS

LIST OF TABLES

LIST OF FIGURES

LIST OF ABBREVIATIONS

3D	Three-dimensional
AB	AlamarBlue
ASTM	American Society for Testing and Material
FF	Fibrin foam
HSA	Human serum albumin
HUVEC	Human umbilical vein endothelial cells
ISO	International Organization for Standardization
IU	International unit
LDH	Lactate dehydrogenase
NHDF	Normal human dermal fibroblasts
NHEK	Normal human epidermal keratinocytes
NPWT	Negative-pressure wound therapy
PU	Polyurethane foam
SEM	Scanning electron microscopy
TEG	Thromboelastography

ABSTRACT

Wound care affects millions of people worldwide each year, and the need for an effective wound therapy still exists. The aim of this study was to characterize a novel, aerated biopolymer, fibrin foam, which is generated through a patented mixing process using a commercially-available fibrin sealant. This research developed a distinct preparation of fibrin foam that creates a porous environment with improved wound healing properties. With this fibrin foam, characterization assessments were performed, including evaluation of mixing parameters, biocompatibility, and biomechanical strengths.

Fibrin foam is created by performing six passes through a mixing device, which generates a foam matrix with a mean pore size of 155 micrometers. Cellular viability assays utilizing lactate dehydrogenase and AlamarBlue reagents demonstrated that primary endothelial cells, fibroblasts, and keratinocytes were all viable and metabolically active on and within fibrin foam. Though fibrin foam produced slightly weaker tensile and wound closure strengths from a biomechanical standpoint compared to the fibrin sealant, the aeration process provides additional structural properties. These include higher fluid permeability and greater porosity.

In addition to characterizing the biodegradable fibrin foam, efficacy was assessed in an *in vivo* wound healing model. For this, a biopsy punch model was utilized whereby full-thickness dorsal skin wounds were generated in mice. The wounds were treated with fibrin foam, and wounds were evaluated 7 and 14 days post-surgery. The fibrin foam-

treated wounds showed significantly superior wound closure compared to the other treatments. In summary, this study characterized an aerated fibrin preparation generated from a commercially-available fibrin sealant and demonstrated its superior efficacy as a novel wound therapy.

CHAPTER ONE

INTRODUCTION

Wound care has evolved substantially over the years for the treatment of patients worldwide. The annual global prevalence of skin wounds is staggering – 114 million acute wounds, 40 million chronic wounds, and over 10 million burn wounds.[1,2] These wounds have a major clinical and economic impact on the patients. To treat and close wounds, a number of options are available, including sutures, staples, surgical sealants and glues, and energy- and negative-pressure-based wound closure techniques.[3-5] These products and procedures are designed to facilitate the multiphase wound healing process. Wound healing consists of four main stages – hemostasis, inflammation, proliferation, and remodeling.[6,7] However, complications of wound healing can arise and range from pain, scarring, and dehiscence to the more severe evisceration, hemorrhage, and infection.[8,9]

More recent wound care treatments have progressed to aid in more efficacious wound healing and to avoid the consequences of improper or impaired wound healing. Modern wound care treatments include stem cell treatment, gene therapy, and light-emitting diode-based treatment; however, these are still in early development.[1] One particular wound healing advancement, tissue engineering, seeks to mimic regeneration by employing bioengineered scaffolds to create suitable cellular microenvironments. The optimal matrix should have the following characteristics: 1) biocompatible; 2) biodegradable; 3) allows for cellular infiltration; 4) allows for gas and fluid transfer; 5)

antibacterial/antimicrobial; 6) strength to resist shear and fragmentation stresses; 7) reduces heal-time; and 8) fully-incorporates into surrounding tissue.[10-12] Current tissue engineering scaffolds have been developed from materials, such as collagen, hyaluronic acid, polyesters, acellular matrices, and fibrin – each with their respective advantages and disadvantages.[13-15]

Fibrin has been well-characterized as a therapy in hemostasis and wound healing. Fibrin also has a critical role in cellular and matrix interactions, inflammation, angiogenesis, and neoplasia.[16] This is due to its inherent binding sites for cellular receptors, integrins, and clotting and growth factors.[17-19] By having a dual function of contributing to the biologically active clot during hemostasis and creating a viable matrix with specific-binding sites during the wound healing process, fibrin is crucial to tissue repair.[20-22] Thus, fibrin sealants have been investigated as scaffolds to promote wound healing.

ARTISS is a fibrin sealant indicated for use as a tissue glue to adhere/seal subcutaneous tissue in plastic, reconstructive, and burn surgeries, as a replacement or an adjunct treatment. Additionally, ARTISS is indicated as an adjunct to hemostasis on subcutaneous tissue surfaces.[23] Fibrin foam is a novel fibrin biopolymer that is generated when ARTISS is aerated using a patented mixing process.[24-28] Compared to ARTISS, fibrin foam has greater viscosity, can polymerize in a temperature-independent manner, and can be applied to both vertical and inverted surfaces without dripping. Additionally, the foam mixing process generates an open-pore fibrin clot structure compared to the dense, closed structure of typical fibrin sealants.[24-27]

This prior research has presented fibrin foam as a candidate for uses in specific surgical procedures, including acute and chronic wound treatments, where standard tissue sealants have historically had poor performance. Based on these preliminary findings, I hypothesized that this novel fibrin sealant preparation would gain advantageous physical attributes from aeration, which would allow fibrin foam to function as a superior wound therapy. Therefore, this study set out to characterize fibrin foam.

The first aim of this study was to determine the impact of aeration on the physical, biomechanical, and biocompatibility properties of fibrin foam. The process and formulation for fibrin foam were initially tested to generate an optimal foam. From here, I used the optimal foam in additional characterization experiments. Biomechanical and structural attributes were measured, including tensile strength, porosity, and permeability. To determine the biocompatibility of fibrin foam, both qualitative (scanning electron and confocal microscopies) and quantitative (lactate dehydrogenase and AlamarBlue assays) experiments were used.

The second aim of the study focused on the use of fibrin foam as a novel wound therapy. Utilizing an *in vitro* three-dimensional assay to mimic a wound, I was able to visually assess cellular migration and proliferation on and within fibrin foam. Moving from these results, a murine skin wound model was used to elucidate the *in vivo* efficacy and performance of fibrin foam as a wound therapy. Lastly, fibrin foam was tested for its use and feasibility in a negative-pressure wound therapy system.

Results from this work indicate that fibrin foam is a biodegradable and biocompatible polymer with advantageous structural characteristics. Fibrin foam was also shown to be effective in the three-dimensional *in vitro* wound model as well as

having superior wound-closure ability in the murine model. Following this study, it can be established that fibrin foam is an appropriate candidate for future research as a novel wound healing therapy.

CHAPTER TWO

LITERATURE REVIEW

Skin and Wounds.

The skin is a multilayered organ within the integumentary system. It is the largest organ in this system and is important in the balance of human health and disease. The skin contains three, main layers within its structure (Fig. 1). They are the epidermis, dermis, and hypodermis (or subcutaneous layer).[1,3] The epidermis is the outer most layer of the skin and is divided into five additional layers. The stratum corneum is the top layer of the epidermis and contains mainly flat squamous cells and keratinocytes. These cells serve as a barrier to prevent water loss and entrance of bacteria into the host system. The stratum lucidum is a layer present only in human palms and soles; it is composed of several layers of dead cells, which act as an additional barrier. The next layer of the epidermis is the stratum granulosum. This thin, granular layer of cells is important in the secretion of lamellar granules, which aid in the binding of keratin fibers. Specialized cuboidal cells interacting with desmosomes are found in the stratum spinosum. This layer contains multiple layers of keratins that support the epidermal layer. The last and deepest layer in the epidermis is known at the stratum basale. This layer is comprised of columnar cells that are continuously undergoing cell division and proliferation into new keratinocytes. The stratum basale also contains melanocytes and Langerhans cells, which are important in the skin's overall immune function.[4,5,29]

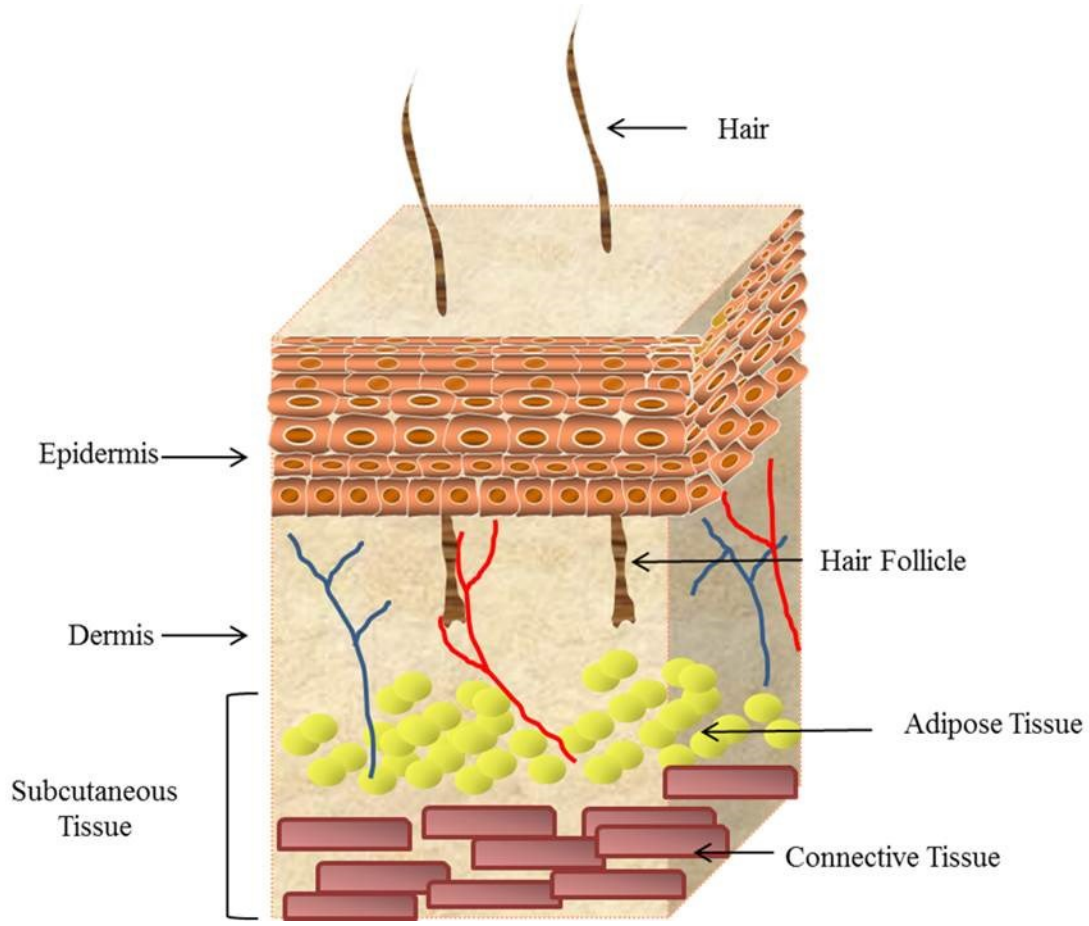

Figure 1. Anatomy of the Skin. The skin is composed of two main layers. First, the epidermis, which is comprised of closely-packed epithelial cells, and secondly, the dermis, made of dense, irregular connective tissue. The dermis houses hair follicles, sweat glands, blood vessels, and other structures. The subcutaneous tissue lies underneath the dermis, which is composed mainly of adipose and underlying connective tissues. Adapted from Grice et al.[30]

The dermis is the next layer in human skin. This middle layer contains many more cells and cellular elements than the epidermis. Collagen and elastin as well as other connective tissues are housed within the dermis. Cells, such as fibroblasts, are located here as well. Hair follicles, nerves, lymphatic and blood vessels, and sweat and sebaceous glands are also found in this layer. The dermis acts to cushion the skin from external forces and also eliminates waste. The bottommost layer of the skin is the hypodermis, or subcutis/subcutaneous tissue layer. The subcutaneous layer is comprised

of adipose tissue. These deposits of fat allow for the protection from external injury as well as insulation of body heat.[29] This is the final layer before reaching the underlying muscle, bone, and ligaments.

These combined layers of the skin have a multitude of functions that are vital to the human body. Externally, the skin provides protection from foreign objects as well as ultraviolet radiation. The dermal layer regulates temperature by either dilating or constricting the blood vessels, which are innervated by the sympathetic nervous system. Langerhans cells within the epidermis are important in recognition of microbial antigens in support of our immune system. Additionally, the skin has functions in insulation and storage of fat tissues, sensations of external movements, and internal vitamin D synthesis.[31-33]

While the skin serves as a protective barrier, it can be subjected to injury in the form of a wound. These disruptions of the skin can be classified as acute (surgical or traumatic) or chronic (pressure or diabetic) wounds. The annual global prevalence of these skin wounds is astounding with 114 million acute wounds, 40 million chronic wounds, and over 10 million burn-related wounds.[1] In the United States alone, these numbers are overwhelming. In 2009, there were a reported 60 million major and minor wound incidents, 13 million traumatic wounds, and 4 million pressure- and ulcer-causing wounds.[2] Each year since, these numbers have been growing with the increases in the aged population as well as the increased incidence of diabetes and obesity worldwide.

The first two cases of wounds – surgical and traumatic – are acute wounds and are typically classified based on their etiology. Surgical wounds occur as a result of a cut due to a sharp instrument, which often occurs during a surgical procedure. Traumatic

wounds include lacerations (tissues are torn apart), abrasions (wound results from friction or scraping away) and contusions (wound results from a direct blow). Included in the traumatic grouping are also burn wounds, amputations, and the more rare disorders, such as necrotizing fasciitis.[8,34]

Chronic wounds typically persist for significant amounts of time, can reoccur, and can develop deep within soft tissues. Within the chronic wound classification are pressure ulcers, diabetic ulcers, and venous and arterial ulcers. These wounds manifest upon one or more of the following factors: lack of blood flow, malnutrition, trauma, immobility, excessive moisture, and lack of sensation. Pressure ulcers are the most common chronic wound and result in tissue ischemia after long periods of applied pressure to a tissue.[1] Venous ulcers can be caused by several conditions including, deep vein thrombosis, peripheral neuropathy, and obesity. Arterial ulcers are often caused by diabetes mellitus, aging, and peripheral vascular disease. However, these are commonly treated with surgical intervention or pharmaceuticals. The final classification of chronic wounds is diabetic ulcers. Due to irregular blood glucose levels and impaired immune defenses, diabetic patients are often prone to this type of chronic ulcer. Diabetic ulcers can manifest on the lower limbs and feet of patients and heal slowly and poorly due to the delayed healing and infection-prone phenotype of diabetic patients.[2,3]

Proper therapies are in place to treat both acute and chronic wounds; however, complications can arise within a wound. When wounds fail to heal properly, minor adverse effects, such as scars and dehiscence, can occur. Scars are a naturally occurring process of wound healing; however, abnormal scarring can result in the formation of keloid or hypertrophic scars, which are caused by excessive inflammatory response and

fibrin formation.[1] Dehiscence is the partial or total splitting open, or separation, of wound layers. This most commonly occurs before collagen formation and can also be caused while removing particular wound healing treatments, such as sutures. More severe consequences include hemorrhage and infection. Hemorrhage occurs when the initial phase of hemostasis is unable to stop the bleeding. This can be caused by a slipped surgical suture, a dislodged clot, infection or erosion of a blood vessel by a foreign object. Lastly, infections, which can be quite serious, are a significant detriment to the wound healing process. Bacterial infections can inhibit wound healing and can lead to discomfort, deformity, disability, and even death.[4,5]

Wound Healing.

The human body begins to heal wounds within seconds after the insult or injury. Wound healing is a multi-phase process that includes the processes of hemostasis, inflammation, proliferation, and remodeling/maturation (Fig. 2).[6,7,9] However, wound healing is much more complex than the simple progression of phases details. There is extensive overlap between the phases, and within each phase, there are a plethora of reactions occurring among the cells, matrices, and chemical mediators (Fig. 3).[35]

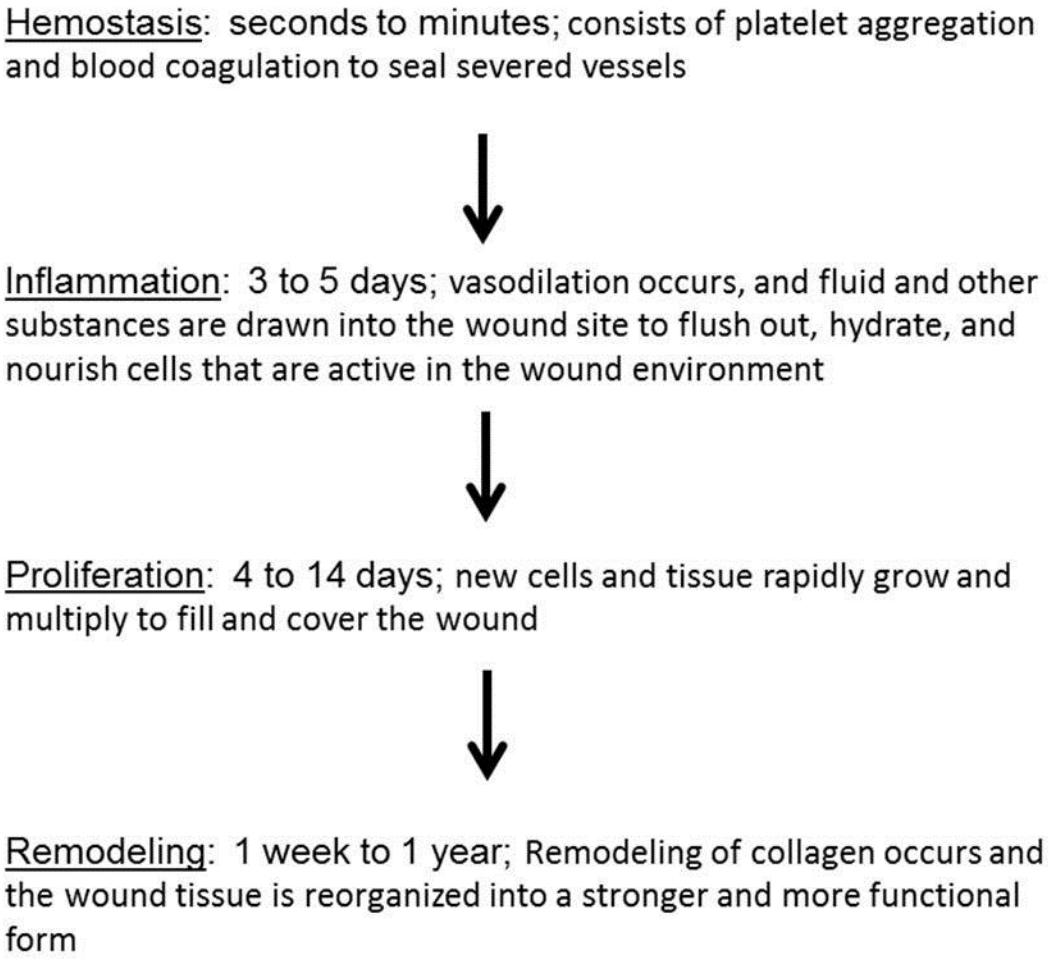

Figure 2. Phases of Wound Healing. The sequential wound healing process with its four main phases, including hemostasis, inflammation, proliferation, and remodeling. Collagen exposed during wound formation activates hemostasis and the inflammatory phase. The fibrin clot formed during hemostasis serves as a scaffold for cells, such as neutrophils, monocytes, fibroblasts, and endothelial cells. Fibrin also serves to concentrate the influx of cytokines and growth factors. During the proliferation phase, processes, such as epithelialization, angiogenesis, and granulation tissue formation are rapidly occurring. Lastly, in the remodeling phase, collagen deposition into well-organized networks occurs for up to a year following wounding. Adapted from Broughton et al.[36]

The initial step in the wound healing process is hemostasis. Hemostasis begins immediately after the injury has occurred, resulting in blood vessel constriction.[37] Following this vasoconstriction, two simultaneous reactions begin to generate a clot at the wound site. The extrinsic pathway of the coagulation cascade is activated and leads to the generation of a stabilized fibrin clot. At the same time, local endothelium and platelets become active and aggregate. This platelet aggregation forms a physical barrier to prevent further blood loss. Once this clot has been generated, the fibrin, platelets, collagen, and other factors begin to release cytokines and growth factors into the interstitium. The clot also serves as a vital scaffold for incoming cells, such as fibroblasts, neutrophils, monocytes, and endothelial cells.[18]

After injury and following the formation of the clot, inflammatory factors and mediators are released from cellular membranes and clotting factors at the wound site.[7] Blood vessel dilation leads to the accumulation of these factors and results in overall inflammation. Neutrophils will next enter the wound site and begin to eradicate bacteria and cellular debris. Metalloproteinases remove damaged extracellular matrix from the wound site to clear the way for new cellular structures. Lastly, macrophages begin to work within the wound cavity.[38] Macrophages secrete enzymes and cytokines, such as vascular endothelial growth factor (VEGF) and fibroblast growth factor (FGF), which stimulate debridement of the wound, promotion of angiogenesis, and proliferation of keratinocytes.[39,40] These actions by the macrophages serve as a crucial gateway into the third phase of wound healing – proliferation.

Proliferation occurs at the wound site from approximately day 4 through day 14 post-wounding. The key processes of epithelialization, angiogenesis, granulation tissue formation, and collagen deposition occur throughout these days (Fig. 3).[36]

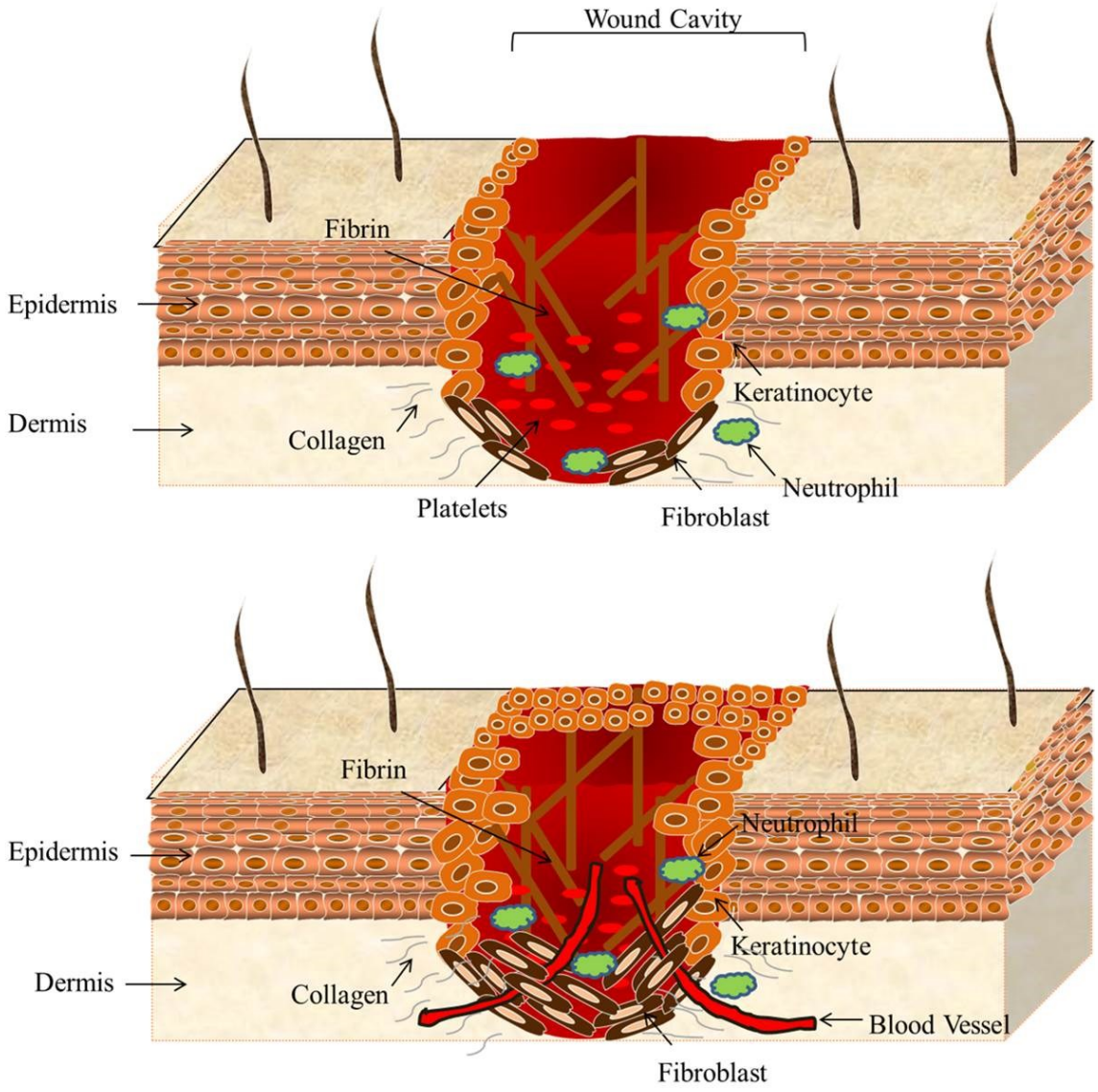

Figure 3. Wound Environment and Key Players. The key players within the wound environment. (Top) Within minutes after wounding, coagulation occurs and the fibrin clot is formed within the wound cavity. Inflammation is induced, characterized by entry of neutrophils and macrophage accumulation. (Bottom) Fibroblasts enter the region in subsequent days. Granulation tissue is established and angiogenesis occurs. In the final steps, epithelialization is initiated, collagen is deposited, and the extracellular matrix undergoes remodeling. Adapted from Broughton et al.[7]

Epithelialization is stimulated during the inflammatory phase and begins shortly thereafter. Fibroblasts that entered the wound as a result of macrophage stimulation begin to secrete keratinocyte growth factor (KGF).[40] This factor stimulates the nearby keratinocytes to migrate into the wound area, proliferate, and differentiate into new extracellular matrix and epidermis. Endothelial cells and fibroblasts have additional roles within the proliferation phase. Stimulated endothelial cells begin to form new blood vessels within the wounded region as part of angiogenesis. Within the final portion of the proliferation phase, migrated fibroblasts will become activated, proliferate, and begin to synthesize collagen and form granulation tissue. Collagen deposition begins and is the transitional step into the final phase of wound healing, maturation and remodeling.

As the name implies, remodeling and organization of the collagen matrix is the key aspect of this phase. The initial granulation tissue and collagen results in thin strands, which are not highly organized. As the weeks progress, however, the thin collagen fibers are reabsorbed and thicker, denser collagen is deposited into the wound by fibroblasts. Maturation and remodeling begins to occur roughly a week after wounding, but can last upwards of a year, as the tissues within the wound regain their original pre-wound strength.[36,41,42]

Perturbations to the highly-systematic wound healing process can occur as a result of several effectors. These include age, nutrition, illness, smoking, and other environmental factors. These influences can affect the wound healing process greatly. For instance, infections can lead to a prolonged inflammatory phase and interference with epithelialization and collagen deposition. This combined effect can cause lack of wound closure and possible wound contamination moving forward. Smoking has debilitating

effects on the wound healing environment. Nicotine is a vasoconstrictive molecule that has been shown to decrease proliferation of the critical wound healing cells, macrophages and fibroblasts.[7,36]

Often times, the canonical wound healing process, as mentioned previously, refers to the processes that happen as a result of an acute wound. However, medical conditions, such as diabetic or pressure ulcers, result in situations of chronic wound healing. Chronic wound healing differs from that of the acute process in several ways.[43,44] First, chronic wounds often have a large accumulation of inflammatory cells within the wound site. These cells lead to such negative effects as increased reactive-oxygen species and increased degradation of extracellular matrix. These combine to generate a state of habitual inflammation. Secondly, fibroblasts in these wound situations have been shown to have a lower mitogenic response to growth factors and cytokines. This, in turn, impedes the formation of granulation tissue and collagen deposition. Keratinocytes are also affected as a result of a chronic wound state. In diabetic patients, keratinocytes exhibit impaired migration, which leads to a failure to epithelialize the wounded region. Lastly, the abundance of inflammatory cells causes a continual state of extracellular matrix degradation. Collagen deposition and maturation within the remodeling phase of wound healing is prevented as the inflammatory cells deter the processes from occurring.[44] Together, these effects found in chronic wounds lead to the formation of poor- or non-healing wounds for their patients as a result of the sustained inflammation and lack of epithelization of the wound.

While there are clear differences between acute and chronic wound healing pathways in humans, there are also major similarities and differences in wound healing among species. In scientific research, porcine and murine models are used most widely to relate pre-clinical wound healing studies to humans. Pigs have similar anatomy and physiology of the skin, blood supply to the skin, and wound healing characteristics when compared to humans.[45] Porcine skin also has similar lipid profiles, epidermal cell turnover, and carbohydrate metabolism within the epidermis. Due to their highly-translational ability, pigs are frequently used in pre-clinical studies for wound healing and plastic surgery. An additional similarity between humans and pigs is the fixed skin. Fixed skin allows for wound healing by reepithelialization.

Unlike pigs and humans, mice primarily heal through contraction of the skin. To overcome this disadvantage, researchers have developed splinted-wound models, which force the mice to heal through granulation and reepithelialization and mimic human wound healing.[46] Murine skin also contains far greater amounts of hair follicles, while having a thinner epidermal layer when compared to human skin. Even with these few dissimilarities, mice are still readily used in scientific research due to their abundance, ability to reproduce data, and low cost – all of which are advantages to using murine models over pigs. Additionally, and while mice share 95% of the same genes as humans, mice can easily be genetically modified to study particular disease states, which is highly attractive for any translational research situation, including wound healing.[47]

Hemostasis and Coagulation Cascade.

Hemostasis is a crucial first step in wound healing, but it also is a highly-regulated and important homeostatic process within the human body. Hemostasis is

required for everyday functioning and to prevent blood loss after tissue injury or trauma. There are three main phases that occur during hemostasis: 1) vascular phase 2) platelet phase and 3) coagulation cascade.[48]

The vascular phase of hemostasis begins immediately after injury, which causes spasm of the smooth muscles in the vessel walls and results in retraction of severed arteries and vasoconstriction of arteries and veins, thus decreasing the rate of blood flow.[49] This occurs as the pericytes, which are cells that function in the regulation of blood flow, proliferate and differentiate into endothelial and smooth muscle cells. Additional factors, such as reflexes initiated by local pain/nervous system receptors, and chemicals released by endothelial cells and platelets such as von Willibrand's factor (vWF), adenosine diphosphate (ADP), thromboxane, and serotonin, can lead to further vasoconstriction of the blood vessels. This vascular phase can significantly reduce blood loss for over an hour, which provides time for the formation of the platelet plug and blood coagulation.[50,51]

After the vasoconstriction of the blood vessels at the site of injury, the platelet phase begins and results in ultimate formation of a soft platelet plug.[52] In normal physiological conditions, platelets are small anucluer cells that do not adhere to surfaces or aggregate with one another.[53] However, in the case of injury to a tissue or blood vessel, platelets are exposed to the subendothelial matrix and various platelet adhesive proteins and activators. The von Willebrand factor is an abundant platelet adhesion protein, which interacts with other adhesive proteins, such as collagen.[54] The circulating platelets bind to collagen via the glycoprotein Ia/IIa receptors located on their cell surface. This adhesion process leads to the activation of the platelets.[55] Once activated,

platelets begin to aggregate at the site of injury through fibrinogen bridges, which link glycoprotein IIb/IIa receptors located on adjacent platelets, as well as collagen binding. Additionally and upon activation, platelets can release the contents of their storage granules, which include ADP, thromboxane A2, and serotonin, which are critical to platelet aggregation and activation.[56] These granules activate additional circulating platelets, which lead to further aggregation, and activation of coagulation. These aggregating platelets adhere and create the soft platelet plug at the site of injury.[57,58] Although the platelet plug initially stops bleeding, a supplemented and more stable fibrin clot is required. This fibrin clot is formed during the coagulation cascade.

Simultaneous to the above-mentioned platelet phase, the coagulation cascade occurs at the wound site (Fig. 4). The coagulation cascade is a complex process that occurs to stabilize the platelet plug through the generation of a fibrin clot. The coagulation cascade is comprised of two distinct pathways – the extrinsic and intrinsic pathways. Both pathways ultimately converge on an identical enzymatic reaction that leads to formation of the clot.[48]

The extrinsic, or tissue factor, pathway is activated when the endothelial lining of the blood vessel becomes damaged.[59] This damaging of the vessel wall allows for collagen and tissue factor (TF) to be exposed and released to the surrounding tissues and blood. TF is expressed by smooth muscle cells, cells surrounding blood vessels (i.e. fibroblasts) as well as white blood cells. TF is a cell surface receptor for factor VIIa. When TF is exposed after injury, the TF/VIIa complex forms. This complex can then convert factor X to its active form, Xa. After the activation of factor X, both extrinsic and intrinsic pathways of the coagulation cascade converge at the common pathway –

activation of X to Xa (Fig. 4). After factor Xa is active, factor Xa, factor V, and calcium form the tenase complex that is required to convert prothrombin to thrombin. Thrombin is a serine protease that converts soluble fibrinogen into insoluble strands of fibrin.[60] Factor XIIIa catalyzes the formation of covalent bonds between amino acid residues in fibrin. These covalent bonds increase the stability of the fibrin clot by crosslinking the fibrin polymers.

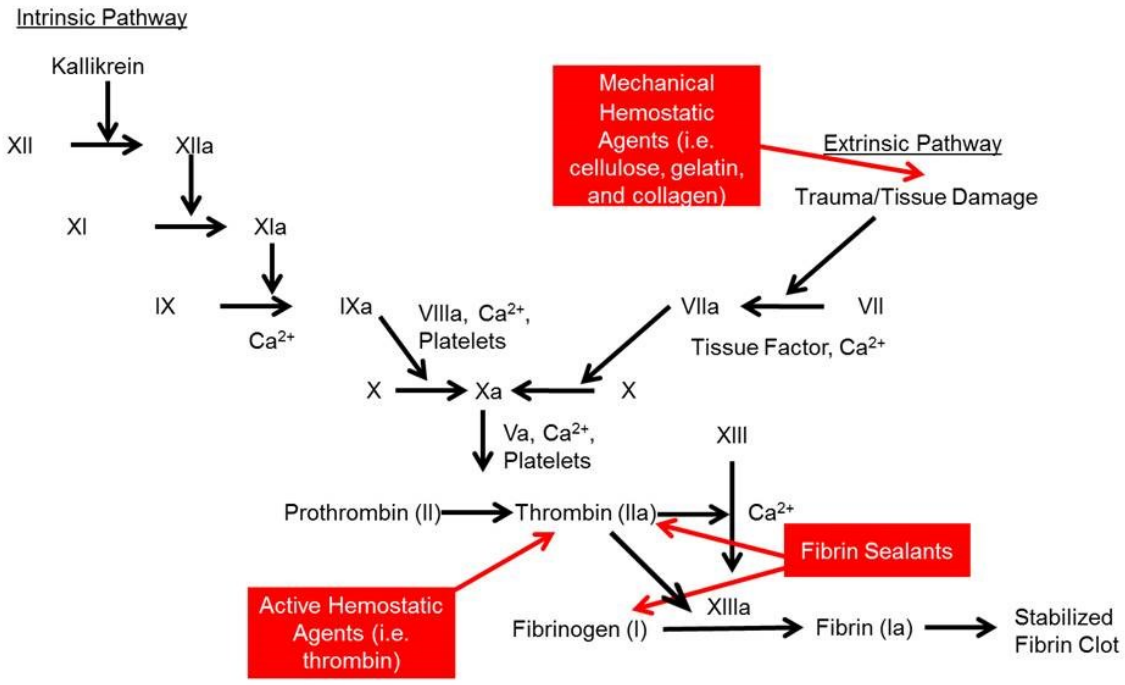

Figure 4. The Coagulation Cascade. The intrinsic and extrinsic pathways of the coagulation cascade. The intrinsic cascade is initiated when contact is made between blood and exposed negatively-charged surfaces. The extrinsic pathway is initiated upon vascular injury which leads to exposure of tissue factor, a cell-surface glycoprotein that binds phospholipids. These two pathways converge at the activation of factor X to Xa – the common pathway. Active factor Xa activates prothrombin (II) to thrombin (IIa). Thrombin then converts fibrinogen to fibrin and activates factor XIII to XIIIa. Factor XIIIa cross-links fibrin polymers creating a final fibrin clot. Roman numerals refer to the specific coagulation factors. Black arrows indicated the cascade events; red arrows indicate where the hemostatic agents act within the pathway. Adapted from Monroe et al.[50]

In contrast to the extrinsic pathway, the intrinsic, or contact pathway, is typically less significant to overall hemostatic balance. The intrinsic pathway is linked to abnormal physiological states, such as hyperlipidemia and bacterial infections.[61-63] Contact activation within the intrinsic pathway can occur through interactions with phospholipids, lipoprotein particles, and negatively-charged surfaces as well as with surface proteins and fatty acids on bacteria. This pathway contains more functional proteins than the extrinsic pathway (Table 1). After activation, the intrinsic pathway is initiated with the formation of a complex of high-molecular-weight kininogen (HMWK), prekallikrein, and factor XII (Fig. 4). The formation of this complex converts both prekallikrein to kallikrein and XII to XIIa – their active forms. Factor XIIa goes on to convert XI into XIa, and subsequently XIa activates IX.[48] Factor IXa, along with its co-factor VIIIa and calcium, forms a complex with their combined substrate, factor X. Factor X is converted to Xa, and the common pathway of the coagulation cascade is activated with the ultimate arrival at a fibrin clot formed through conversion of fibrinogen to fibrin by thrombin.

However, thrombin has other functions that are vital for maintaining hemostasis. Additionally, thrombin acts to convert factor XI to XIa, VIII to VIIIa, and V to Va. These conversions are considered positive feedback mechanisms by which amplification of the coagulation cascade can occur. Thrombin can also activate factor XIII to XIIIa. In addition to its activity in the coagulation cascade, thrombin promotes platelet activation and aggregation.[64]

Factor/Name	Function(s)
Factor I (fibrinogen)	Converted to fibrin by Factor IIa (thrombin). Creates fibrin clot.
Factor II (prothrombin)	Converted to thrombin by Factor X. Factor IIa converts fibrinogen to fibrin.
Factor III (tissue factor, TF)	Initiates the extrinsic pathway. Interacts with Factor VII.
Factor IV (calcium)	Is required for activation of Factors II, VII, IX, X, and XIII.
Factor V (Proaccelerin)	Essential for activation of thrombin.
Factor VI (Accelerin, Va)	Also known as Factor Va
Factor VII (Proconvertin)	Binds to TF and is essential for the activation of Factor X.
Factor VIII (Antihemophilic globulin)	Important to the activation of Factor X.
Factor IX (Christmas factor)	Essential to the activation of Factor X and the common pathway.
Factor X (Stuart-Prower factor)	Converts prothrombin to thrombin.
Factor XI (Plasma thromboplastin antecedent)	Activates Factor IX in intrinsic pathway.
Factor XII (Hageman/contact factor)	Essential to the intrinsic pathway and the activation of Factor XI.
Factor XIII (fibrin-stabilizing factor)	Aids in the final fibrin clot formation through stabilization of fibrin fibers.
Kallikrein	Essential for Factor XII activation, necessary in Factor XIIa activation of XI.

Table 1. Factors of the Coagulation Cascade. Adapted from Moss et al.[65]

The hemostatic pathway is a critical physiological pathway; however, it is in a constant state of homeostasis. As the fibrin clot is being formed throughout the coagulation cascade, the fibrinolytic system is already beginning to disrupt it.[51,66] The fibrinolytic system functions to dissolve blood clots in healthy blood vessels (i.e. prevent thrombosis) and during the wound healing process. Plasmin is the key effector in this system. Plasmin is a zymogen that is generated from its inactive precursor, plasminogen. Plasminogen is converted into plasmin by two proteases – tissue-type plasminogen activator (tPA) and urokinase-type plasminogen activator (uPA).[67] For balance, these PAs are regulated by plasminogen activator inhibitors. However, after plasminogen is

activated to plasmin, it cleaves fibrin at specific lysine and arginine residues, which ultimately results in dissolution of the clots.

Working alongside these proteases is thrombin-activated inhibitor of fibrinolysis (TAFI). TAFI is also a zymogen that can be activated by either plasmin or thrombin. While the fibrin clot is being degraded, C-terminal lysine residues are exposed and can enhance activation of plasmin and further fibrin degradation. TAFI, however, removes these lysine residues from fibrin fibers and inhibits any further plasmin(ogen) activation. Taken together, the effectiveness and balance of the hemostasis depends on both the procoagulation reactions of the coagulation cascade as well as the clot-dissolving process in the fibrinolytic system.[68,69]

The fibrin clot functions in a variety of important physiological processes throughout the body.[16] The most known function of fibrin is within the coagulation cascade. Upon injury, fibrin and its constituents are formed, processed, and degraded in a highly-defined pathway. Due to the influence of the coagulation cascade and hemostasis on wound healing, fibrin has been shown to play an important role in the healing phases. Hemostasis is the first phase in wound healing. The network of insoluble fibrin fibers that is created as a result of the coagulation cascade stabilizes the platelet plug.[22] This fibrinous matrix acts as a scaffold during wound healing for a plethora of cell types. Because of the integrin and non-integrin bindings site of fibrin, cells such as endothelial cells, smooth muscle cells, and fibroblasts can easily attach and migrate to the fibrin matrix to initiate the wound-healing response.[17,18]

After these initial contacts, fibrin can also bind monocytes and leukocytes, which are two prominent cell types for the secondary, inflammation phase of wound healing.[70,71]

These cells eliminate debris and bacteria from the wound site.[72,73] In line with the wound healing phases, fibrin also serves as a provisional matrix for endothelial cells and fibroblasts. The endothelial cells, upon stimulation by growth factors, proliferate and migrate into the wound site. There, they begin to generate new vasculature.[74,75] Following the proliferative phase of wound healing, remodeling of the wound area occurs. Fibroblasts initially use the fibrin matrix as a scaffold for migration and proliferation. Once the fibroblasts have entered the wound, they begin to create collagen as well as other extracellular matrix proteins to regenerate the tissue.[76,77] At each step along the wound healing process, fibrin has been shown to be an integral factor. Fibrin has critical roles in hemostasis, inflammation, and revascularization due to its inherent binding sites for cellular receptors, integrins, and clotting and growth factors.[17-19]

Although the hemostatic and wound healing phases are sequential and regulated, medical and clinical indications can manifest causing perturbations to this normally-balanced pathway. Surgical or accidental trauma as well as genetic predispositions can alter hemostasis through abnormal (or lack of) formation of the platelet plug or fibrin clot.

To combat these clinical situations of excessive or abnormal bleeding, the medical field has several hemostatic therapies at its disposal (Table 2).[78] These include mechanical, energy-based, and chemical methods to control bleeding – each with their own specific indications and impact on coagulation (Fig. 4).[65] Mechanical methods, such as direct pressure, gauze, sponges, and sutures/staples are often used. These measures rely on the physical strength and barrier formation to prevent further blood loss. Thermal and energy-based hemostatic methods (e.g. electrosurgery, ultrasound, and lasers) have

been employed for their use in achieving hemostasis. Electrosurgery utilizes high-frequency alternating currents to cut, coagulate, and vaporize tissues; while ultrasound devices covert electrical energy into mechanical energy that can seal blood vessels. Additionally, lasers use highly concentrated light energy to cauterize bleeding tissues. The thermal and energy-based hemostatic techniques must, however, be used by properly trained medical professionals due to their complex equipment and functionalities.[79,80]

Mechanical	-Direct pressure -Gauze, sponges -Sutures, staples
Thermal & Energy-based	-Electrosurgery -Ultrasound -Laser
Chemical -Pharmacological -Hemostatic Agents	 -Epinephrine -Vitamin K, Vitamin K analogs -Protamine -Desmopressin -Lysine analogs -Mechanical • Collagen • Gelatin • Cellulose -Active (Thrombin) -Sealants • Fibrin • Polyethylene glycol (PEG) • Albumin, glutaraldehyde

Table 2. Methods for Achieving Hemostasis. Adapted from Samudrala et al.[78]

The final means for (re-)establishing hemostasis is through the use of chemical methods. Both pharmacological and hemostatic products are used in cases where the mechanical and thermal methods are impractical or otherwise contraindicated, such as instances of bleeding over multiple vessels or areas of the body. Pharmacological

treatments, as named in Table 2, are primarily used to improve final fibrin clot formation through either preventing anticoagulation or increasing the platelet aggregation to the bleed site. Mechanical (or passive) hemostatic agents stop the flow of blood by either providing a scaffold for the rapid formation of a native clot, or by physically acting as a barrier to stop the bleeding. In contrast, active hemostatic agents, such as thrombin products and fibrin sealants act to recapitulate the endogenous coagulation cascade and fibrin clot formation.[80,81]

Fibrin and Fibrin Sealants.

Fibrinogen is cleaved by thrombin to generate a fibrin clot during the final step of the coagulation cascade (Fig. 4). This single step within hemostasis has a far greater reach over the physiological processes within the human body. Not only is fibrin critical to clot formation during hemostasis, but fibrin is an important factor in wound healing, inflammation, angiogenesis, and neoplasia.[16] Fibrinogen is a 340 kilodalton (kD) glycoprotein that consists of a dimeric structure composed of 2Aα, 2Bβ, and 2γ chains. The Bβ and γ chains make up the D-region of fibrinogen and create an alpha-helical structure, while the Aα chains of the E-region are globular (Fig. 5).[82]

Thrombin is a serine protease of the trypsin family of proteins that is generated from its zymogen, prothrombin. During the coagulation cascade, prothrombin is cleaved into thrombin by factors Xa and Va. Cleavage of prothrombin into thrombin occurs with two sites and can be generated through two possible pathways (Fig. 5). Initial cleavage yields N-terminal fragments 1 and 2 (F1.2) and the zymogen, prethrombin, which is further cleaved to yield the disulfide linked thrombin (left pathway of Fig. 5A). Alternatively, cleavage in the opposite order generates an immediate, meizothrombin,

prior to processing into the active thrombin (right pathway of Fig. 5A). Thrombin, in its active form of α-thrombin, is a 36 kD protein. Thrombin is known to act as a procoagulant and anticoagulant enzyme with the human body. Thrombin elicits a response during the coagulation cascade to form a fibrin clot and also activates platelet activation during the earlier stages of hemostasis.[83] For anticoagulation, thrombin has been shown to interact with thrombomodulin, which is a required molecule for the activation of protein C – an inactivator of factors Va and VIIIa leading to down regulation of thrombin generation.

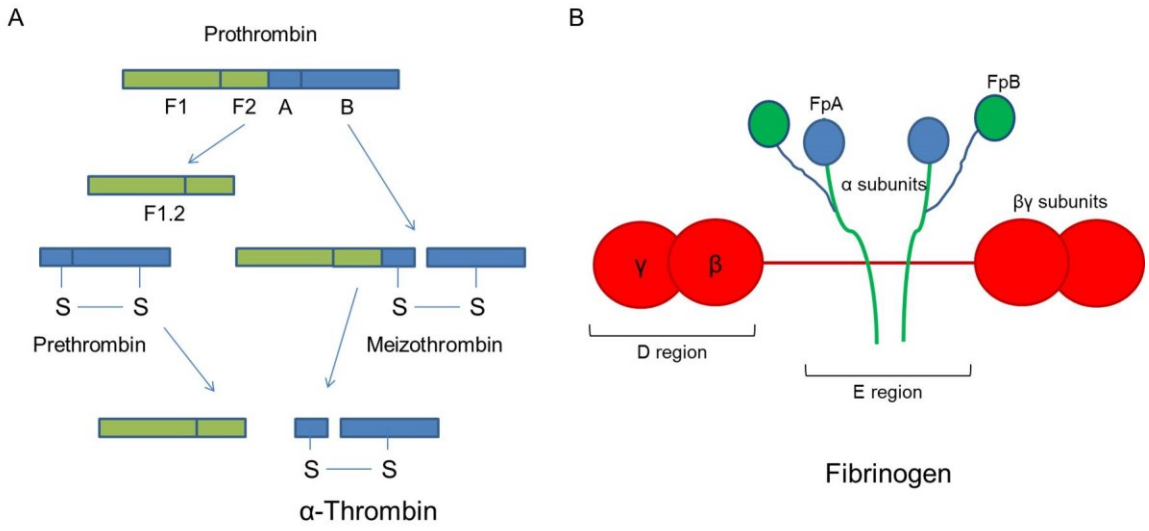

Figure 5. Structures of Thrombin and Fibrinogen. A) α-thrombin is generated by the autocatalytic and factor Xa cleavage of prothrombin. α-thrombin, the active form of thrombin, is covalently linked through disulfide bridges. B) Fibrinogen is dimeric glycoprotein composed of 2Aα, 2Bβ, and 2γ chains. Fp: Fibrinopeptides. Adapted from Wood et al and Undas et al.[82,84]

When fibrin formation occurs, fibrinogen is converted to fibrin by thrombin (Fig. 6). Thrombin cleaves fibrinopeptides (Fp) A and B from the Aα and Bβ chains in fibrinogen. The release of these peptides contributes to the lateral aggregation of the initial fibrin clot. Cross-linking and expansion of the fibrin clot occur after the inclusion of factor XIII. Factor XIII allows for the crosslinks of the γ-chains and overall expansion

of the final, stabilized fibrin clot. This overall fibrin clot structure is dependent on many variables, including pH, salt concentration, thrombin concentration, factor XIII concentration, and fibrinogen cross-linking. pH changes can affect the fibrin fiber thickness, with more basic pH environments leading to thinner fibers. Increased salt and thrombin concentrations increase clotting rate, which leads to thinner fibrin fibers as well. Factor XIII and fibrinogen alterations can cause changes in branching and polymerization in the final fibrin clot. Each of these factors may lead to variations of the fibrin clot and can impact the function of the clot itself.[82,85]

The fibrin clot also possesses unique biomechanical and viscoelastic properties. Fibrin clots have the tensile strength to stop bleeding and hold tissues together; while also having burst pressure to withstand the forces of arterial blood flow. Fibrin is elastic and viscous as well. It can deform and withstand shear forces within the body while remaining fluid due to its high elasticity.[85] Fibrin clots also possess unique structural qualities as well. Fibrin contains a structure encompassing a spectrum of porous void spaces – from a few nanometers to 50 μm.[86] This porosity is crucial to fibrin functioning and has a direct impact on cell migration on fibrin, air/fluid transfer through the clot, and overall permeability.

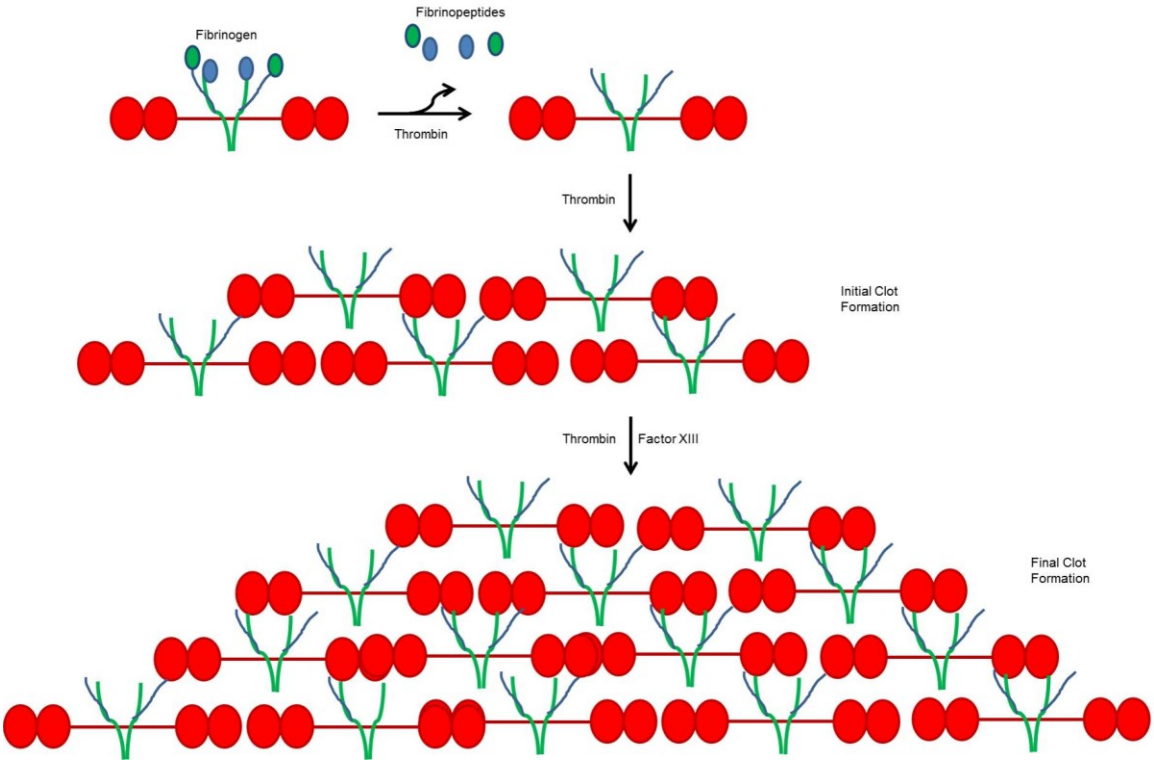

Figure 6. Fibrin Clot Formation. Schematic of fibrin clot formation. Fibrin polymerization is initiated by the action of thrombin, which cleaves the fibrinopeptides from the middle of fibrinogen to produce fibrin. These initial oligomers lengthen with the additional monomers to make protofibrils, which aggregate to form fibrin fibers. These fibers branch into a three-dimensional fibrin network, which is finally stabilized by the formation of covalent bonds introduced by the plasma transglutaminase, factor XIII. Adapted from Undas et al.[82]

Due to the impact of fibrin on multiple human systems, its biocompatibility, and advantageous biomechanical attributes, fibrin has been well-characterized and used in the medical field for a variety of applications for over a hundred years.[87] Fibrin sealants are two-component medical devices that contain fibrinogen and thrombin. These agents are combined and generate a fibrin clot. Variations of fibrin sealants exist as well – including alterations to the formulation (i.e. increasing or decreasing thrombin concentrations, use of human, bovine, or synthetic proteins), addition of constituents (i.e. other hemostatic agents), and freeze-drying.[88]

Each preparation of a fibrin sealant is created for a particular use. Fibrin sealants can be used as hemostatic agents, sealants, or adhesives.[89] Hemostatic agents (e.g. hemostats) are the canonical use of a fibrin sealant, whereby their use is dependent on a bleed and fibrin to generate a clot. A sealant creates a barrier between surfaces to prevent leakage of liquids and gases. Lastly, fibrin sealants functioning as adhesives are used for ability to glue structures together. With each preparation, the indications for a particular fibrin sealant become apparent. Hemostats can be used in most surgical situations where bleeding occurs. Sealants can be used as wound therapies and to repair tissue anastomoses, while adhesives are employed for use in reconstructive surgeries, such as burn and skin grafts.[87,90,91]

While the aforementioned practices of fibrin sealants are ever-abundant in the medical field, newer and more innovative uses for fibrin sealants are being studied. In recent years, fibrin sealants have been altered to serve as a template for cellular migration. Their matrix interactions with various cell types, such as those in wound healing, allows for a candidate scaffold for wound repair. Additionally, fibrin sealants have been widely studied for their use as a delivery system. Pharmaceutical drugs, growth factors and cytokines as well as cells have been incorporated into fibrin matrices for use in a spectrum of medical applications.[92-94]

Lastly, fibrin sealants have gained appeal in the field of tissue engineering. Due to their cellular and protein interactions, fibrin sealants are considered active cellular matrices. Along with their mechanical and biochemical properties, fibrin sealants are attractive candidates for further applications in tissue engineering and as matrices for

cellular differentiation. By combining fibrin with other stimulating factors, these sealants could be used as highly-customizable scaffolds.[90,92]

Wound Therapy.

To promote proper wound healing and prevent the possible risks caused by inadequate healing, a variety of wound closure treatments and dressings are available for clinicians (Table 3).[95] These wound therapies range from the components of the therapy to the mechanism by which the therapy acts to close the wound. Traditional wound therapies include gauze, sutures, staples, and wound-closure strips. These therapies have been used for many decades and rely on their mechanical strength to hold and seal the wounds. While reliable in most skin wounds, the use of these agents is often limited to their reach and placement on the wound. Additionally, these traditional therapies can often lead to dehiscence and improper sealing of the wound.[1,2]

There are two main classes of sealants used for wound healing: biologic (e.g. albumin, collagen, and fibrin sealants) and synthetic (e.g. hydrogels, cyanoacrylate, and polymers). The biologically-derived sealants products have inherent hemostatic properties to decrease blood flow and allow for adherence to the tissue. Synthetic sealants elicit tissue adherence within minutes without the use of sutures or staples. These sealants are also biodegradable and slough off or become resorbed by the body once the underlying wound site has fully healed. These materials chemically bind to tissue, provide immediate sealing of tissues with significant tensile strengths and without the risk of immunogenicity.[2,4]

Polymers have also been used to synthesize gauze, foams, and other dressings. Polyurethane dressings are used in the treatment of acute and chronic wounds. These

wound dressings are permeable to both gases and fluids, including wounds with moderate-to-heavy exudates. Moreover, polyurethane dressings are biocompatible, have relatively low toxicity, and can be fashioned to a specific pore size matrix. These specific matrices can be utilized in different therapies and can enhance reepithelialization while providing mechanical stability to the wound site. A common disadvantage to these polymer dressings is their limited biodegradability. These dressings must be changed or removed periodically during the wound treatment process, which ultimately can lead to delayed healing.[96]

Physical and energy-based processes have also been coupled to wound closure methods to aid in wound healing. One of which is negative-pressure wound therapy (NPWT), which utilizes a subatmospheric vacuum system to improve wound healing. This technique is often used in hard-to-close acute and chronic wounds because of its ability to seal the wound edges and remove excess exudate from the site of injury. NPWT involves the use of polyurethane foam or gauze to cover the wound site and is ever-growing in popularity for patients with skin grafts, dehisced surgical wounds, and pressure ulcers. NPWT-treated wounds often require debridement of the polyurethane wound dressings after several days of treatment due to the tissue ingrowth. This leads to pain, discomfort, and re-wounding of the tissue.[2,95]

Class/Type	Characteristics
Gauze	Cotton fiber; inexpensive material; requires frequent changes on the wound
Sutures	Absorbable or non-absorbable; variable tensile strength; may enable infections
Staples	Stainless steel or titanium based; technique needed for application
Tapes/Films	Cost-effective; not suitable for wounds with heavy exudates
Hydrogels	Water- or glycerin-based gels; non-adherent to wound
Hydrocolloids	Pectin- or gelatin-based gels; adherent and may cause damage to skin
Foams	Polyurethane based; can absorb moderate exudate
Alginates	Suitable for wounds with heavy exudate; some hemostatic activity
Sealants	Human-, animal-, or synthetic based platforms; ability to seal wound; protect wound from infection
Silver Dressings	Contain broad-spectrum antimicrobial activity; should be used for infected wounds
Vacuum	Removes exudate from wounds; mechanical seals wounds; increasing perfusion

Table 3. Classification of Wound Therapies. Adapted from Janis et al.[6]

Ultrasonic and radiofrequency are two energy-based therapies that have gained recognition for use in wound healing. Ultrasonic wound therapy uses ultrasonic frequencies to fuse and seal tissues together. Similarly, radiofrequency techniques, or electrosurgery, can generate high temperatures from radio waves to be used to cauterize the wounded tissues. These energy-based techniques have become more popular over the traditional sutures and staples because of their ability to create a leak-proof seal in the wound. The requirement of specialized tools and training to use such devices, though, is a larger disadvantage to their use.[2]

While all available wound therapies have their respective advantages and disadvantages for use in clinical situations, the ideal wound therapy or dressing still eludes the scientific community. This optimal wound therapy has been postulated to require the following attributes[10,95]:

- Ease of application
- Reduce heal time
- Biocompatible to tissue
- Biodegradable
- High mechanical strength and elasticity
- Fluid and gas permeability
- Non-toxic and non-antigenic
- Affordable and long shelf life
- Resistant to bacterial/microbial infection

Researchers in the later part of the 20th century began generating more modern wound therapies to try and meet these requirements and provide superior wound healing therapies for patients worldwide. These include the use of stem cell therapy, gene therapy, and tissue engineering. Stem cells have been favored as they are critical to tissue regeneration and wound healing in the body. Stems cells recapitulate wound regeneration and provide daughter cells that can replenish the lost or damaged tissues through cellular differentiation.[14]

Gene therapy has been a novel wound therapy as it allows for the implantation of genes/transgenes into recipient cells. These genes, often encoding growth factors or cytokines, can be used to promote wound healing through the added recruitment of cells

and other tissue factors. For example, virally-transferred epidermal growth factor (EGF) could be implanted at a wound site for the downstream effect of leading to the proliferation of epidermal and mesenchymal cells; whereas platelet-derived growth factor (PDGF) would allow for the chemotactic response and matrix production of macrophages and fibroblasts, respectively. Downsides to this potential therapy are immunological or toxic side effects as well as the risk of tumor development.[97] Additionally, these therapies apply one gene encoding one cytokine or growth factor, with limited effects. A typical wound environment has dozens of factors present. While stem cells and gene therapies are promising, very few have reached clinical trials.

Lastly, tissue engineering has been at the forefront of recent studies in wound healing research. Tissue engineering aims to mimic the structural and cellular elements of a tissue to promote the repair and regeneration of that tissue, which is appealing for a wound healing situation. Current tissue engineering scaffolds vary on the test material and range from collagen, fibrin, and hyaluronic acid to acellular matrix and biodegradable polymers.[13,14]

Tissue Engineering.

Tissue engineering has gained interest over the past twenty years for its versatile role in many clinical situations, including wound healing, due to the highly-customizable ability of tissue-engineered scaffolds. Tissue engineering's goal is to mimic tissue regeneration by creating suitable cellular microenvironments. The scaffolds restore the cellular microstructures and mechanical properties of the tissues by possessing critical attributes, including porosity, biocompatibility, and biomechanical strength – making them ideal therapies for medical intervention.[10,14]

The porosity of the scaffolds is one of the most important attributes to its success. The pore sizes of a scaffold can be manipulated for a given clinical indication. Pore sizes affect different cell types and cellular processes depending on their sizes (Table 4).[15,98,99] Due to the ability of tissue-engineered-scaffolds to be customized, researchers may alter their scaffold's pores to fit and treat a particular problem.

Cellular Process	Cell Type/Model Used	Pore size (μm)
Angiogenesis	*In vivo* rat implantation	160-270
Adipogenesis	Bone marrow stem cells, adipose-derived stem cells	70-110
Cellular infiltration	Dermal fibroblasts	100
Chondrogenesis	Porcine chondrocytes, rabbit mesenchymal stem cells	70-120, 200-500
Osteogenesis	*In vivo* mouse implantation	150-400
Proliferation	Human fibroblasts	100-250
Skin regeneration	Guinea pig dermal and epidermal cells	20-125
Smooth muscle cell differentiation	Canine bone marrow stem cells	50-200

Table 4. Pore Sizes Required for Various Cellular Processes. Pore sizes required for various cellular processes. Pore sizes (μm) detail the approximate range required for a scaffold's structure to support the cellular processes listed. Adapted from Loh et al.[15]

The porosity of a scaffold also affects its permeability. Permeability of these scaffolds plays a significant function in its overall effectiveness. The scaffolds must be able to allow for cellular migration and infiltration, but also for nutrient, waste, and fluid transport in and out of the structure. Additionally, the scaffolds must possess biomechanical strengths to support tissue growth and movement.[99]

Tissue-engineered scaffolds can come in all shapes and sizes and can be created from a variety of substrates to accomplish the goals of tissue regeneration. Biocompatibility and biomechanical strength go hand-in-hand with the chosen substrate

for the particular scaffold. The ideal matrix is biocompatible, promotes regeneration and cellular integration, and fully incorporates into the tissue.

Collagen is often used for tissue engineering and wound healing situations. It is biocompatible, non-immunogenic, and is readily absorbed into the tissue site. Due to its similar structural properties to extracellular matrix proteins, collagen-based scaffolds can be used in a variety of regenerative applications, including bone, skin, and wound repair.[100] Another often-used scaffold is hyaluronic acid. This polysaccharide is present in connective tissues within the body and, while biocompatible, is readily digested. Because of its impact in connective tissues, hyaluronic acid scaffolds are sought after for use in cartilaginous repair and wound healing.[101]

Chitosan is an aminopolysaccharide found in the exoskeleton of insects, shellfish, and fungi.[102] Chitosan, while porous, biocompatible, and biodegradable, is often combined, in practice, with hyaluronic acid and collagen-based scaffolds for use in a variety of applications.

Fibrin, often utilized as a surgical sealant, is a versatile scaffold in tissue engineering.[103] Fibrin-based scaffolds have excellent biocompatibility and have been fabricated with additional cells, growth factors, and pharmaceutical drugs to improve tissue regeneration.

Acellular matrices are derived from animal tissue for which the living cells have been removed. This matrix is appealing for tissue engineering because of its several advantages. These matrices are biocompatible and biodegradable, but are also morphologically identical to the tissue structures. This allows for improved cellular migration and infiltration. Additionally, acellular matrices have similar biomechanical

strengths to the surrounding tissues.[104] Due to these attributes of decellularized matrices, their use in organ transplant has been a recent hub of tissue engineering research. Acellular matrices have been employed in many clinical indications, including as artificial skin scaffolds as well as human tracheal matrices for use as bronchial transplants.[105]

While natural and biological materials have the added attributes of biocompatibility and similar structural characteristics to the native tissues, synthetic polymers have gained appeal in recent years for their use in tissue engineering. These scaffolds can be generated from many polymers, including polyesters, polylactic acid, polyglycolide, poly(lactic-co-glycolic acid), and others.[106] These polymers are biodegradable and have additional advantages as well. The polymers have added biomechanical strength over natural materials, can be processed to meet exact porosity requirements, and have controlled degradation rates over time. As long as the degradation byproducts are non-toxic, these polymeric scaffolds can be fabricated to treat a wide array of tissue engineering-related issues.

Because of the capacity to influence all properties of the scaffolds, researchers have also manipulated the above materials through addition of cells, growth factors, and other molecules to aid in improved tissue regeneration.[107] Stem cells, for instance, have been implanted in these matrices to allow for improved healing and growth of tissues. The tissue engineering field is continuing to grow in hopes of finding optimal scaffolds for tissue regeneration, wound healing, bone growth, and other medical issues.

ARTISS Fibrin Sealant.[23]

ARTISS is a fibrin sealant marketed by Baxter Healthcare Corporation. ARTISS was first approved by the FDA for use in the United States in 2008. ARTISS is a fibrin sealant preparation made from pooled human plasma, where both components (fibrinogen and thrombin) are formulated as two sterile, deep-frozen solutions. These solutions are presented in two, separate pre-loaded chambers of a single device that mixes those two components at the syringe tip (Fig. 7). ARTISS is generated in a deep-frozen, vapor-heated and solvent detergent-treated state that has a two-week shelf life once thawed at room temperature.

The two components of ARTISS fibrin sealant are denoted as the sealer protein solution (i.e. fibrinogen) and thrombin solution. The sealer protein contains active ingredients as listed in Table 5. The sealer solution contains addition excipients (per 1 mL): human serum albumin (10-20 mg), histidine (10-25 mg), sodium citrate (4.8-9.7 mg), Polysorbate 80 (0.6-1.9 mg), nicotinamide (3-9 mg), and water for injection q.s. to 1 mL. Of these added excipients, human serum albumin acts as a protein stabilizer and buffer to pH. Polysorbate 80 is an emulsifier, while histidine, sodium citrate, and nicotinamide are used for buffering and pH agents. The thrombin solution contains two active ingredients as listed in Table 6. The thrombin solution contains the addition excipients (per 1 mL): human serum albumin (45-55 mg; protein stabilizer) and sodium chloride (3.5-5.5 mg, buffer).

Figure 7. ARTISS Fibrin Sealant. Photograph of a pre-filled dual-component syringe of a 10 mL preparation of ARTISS fibrin sealant (Baxter Healthcare Corporation). Source of image: Baxter Healthcare Corporation.[23]

Active Ingredient	Quantity/Amount
Fibrinogen	72-110 mg
Factor XIII	1.2-10 IU
Synthetic Aprotinin	2250-3750 KIU

Table 5. Sealer Protein Active Ingredients. KIU: Kallidinogenase Inactivator Unit.

Active Ingredient	Quantity/Amount
Thrombin	3.2-5 IU
Calcium Chloride	36-44 μmol

Table 6. Thrombin Solution Active Ingredients.

The two-component system, when mixed, acts to mimic the final step of the coagulation cascade – formation of a fibrin clot. Thrombin converts fibrinogen to fibrin. This process is repeated as the fibrin fibers begin to polymerize. The polymerized network of fibrin fibers is crosslinked by the native (or added) factor XIII to form the

final fibrin clot (Fig. 4). This clotting process, however, takes approximately one minute to begin and two hours to generate a full-strength clot due to the low thrombin concentration within the thrombin solution.

Because of this slower set time compared to other fibrin sealants, ARTISS is indicated for use as tissue glue to adhere/seal subcutaneous tissue in plastic, reconstructive and burn surgery, as replacements or adjuncts to sutures or staples. Additionally, ARTISS is indicated as adjunct to hemostasis on subcutaneous tissue surfaces. ARTISS is contraindicated for use in replacing skin sutures intended to close surgical wounds. ARTISS, by itself, should not be used for the treatment of massive arterial or venous bleeding, and the sealant can never be applied intravascularly for risk of thromboembolism.

ARTISS has been well-studied and was investigated in human clinical trials, including use for the fixation of skin grafts in burn patients and for the adherence of skin flaps in facial rhytidectomy surgeries. In the burn patients, ARTISS proved to be non-inferior to staples with respect to wound closure at 28 days after wounding using a one-sided 97.5% confidence interval on the difference in the proportion of test sites successfully treated (ARTISS 43.3% of wounds closed at Day 28 compared to 37.0% of wounds using staples). Additionally, a facial rhytidectomy trial was performed to investigate the adherence of skin flaps using ARTISS. A standardized drain was placed on the face of each patient where the skin flap was placed to compare adherence. At 24 hours post-operation, ARTISS-treated skin flaps had a significantly lower volume of drainage, correlating to better overall adherence ($p<0.0001$). ARTISS-treated skin flaps also resulted in significantly less incidence of hematoma/seroma when compared to the

standard of care ($p<0.05$). Depending on the indication, ARTISS also comes with different application equipment. Cannulas are often employed for use in small wounds or for the edges of skin grafts. A spray set is also offered. The spray set is highly recommended for use in large surface areas requiring tissue adherence.

Foams: Properties and Uses.

Foams are universal in everyday life – from soap bubbles, detergents, packaging, and foods and beverages to firefighting and biomedical foams.[108] Foams are substances generated by trapping gas in either liquid or solid, resulting in an aqueous or dry foam, respectively. Foams can additionally be characterized by their pore structure. Open-cell foams have interconnected pores that allow for rapid movement of gas and liquids across the foam. Closed-cell foams, on the other hand, trap gas within individual pockets and thereby restrict the flow of gas and liquids. The more commonly studied foams are the ones generated from liquid and gas – aqueous foams.[109]

Aqueous foams, in general, may be made through several techniques, including 1) blowing gas through a small hole/nozzle into a liquid, 2) sparging, or blowing gas into a liquid through a porous plug, 3) nucleation of gas bubbles in a supersaturated liquid, and 4) mechanically shaking or beating the liquid.[108] The formation and breakdown of foams occurs in phases as well (Fig. 8). First, bubbles are formed and grow through the aqueous foam (Fig. 8A). As the bubbles grow, they begin to cream and deform onto one another generating a distinct polyhedral shape. Following the creaming process, drainage occurs once the bubbles are more tightly packed. Drainage refers to the liquid passing through the intricacies between bubbles. As the bubbles begin to form distinct borders with one another, the bubbles coarsen, or form larger bubbles, when the borders between

the bubbles merge. Lastly, as the bubbles become larger and larger, the final process in the lifecycle of an aqueous foam is rupture (Fig. 8E). The borders between bubbles collapse leading to the dissolution of the foam.[108,110,111]

Several factors are needed to generate an aqueous foam. As mentioned, this type of foam is created when a gas is mixed into a liquid. However, often times a surfactant is required to generated and stabilize the foam. A surfactant, or surface active compound, is typically concentrated on the surface of foams and reduces the surface tension/energy associated with the foam surfaces. Additionally, a surfactant stabilizes an aqueous form from rupture.[108,112] Surfactants, such as emulsifiers, detergents, and wetting agents, are amphiphilic molecules – a molecule that contains both a hydrophobic and hydrophilic end. These molecules act to lower the interfacial tension between the bubbles in the foam. The surfactants stabilize the bubbles through the Marangoni Effect, which occurs when bubbles coarsen and increase their local surface area between the lamellae.[108,110]

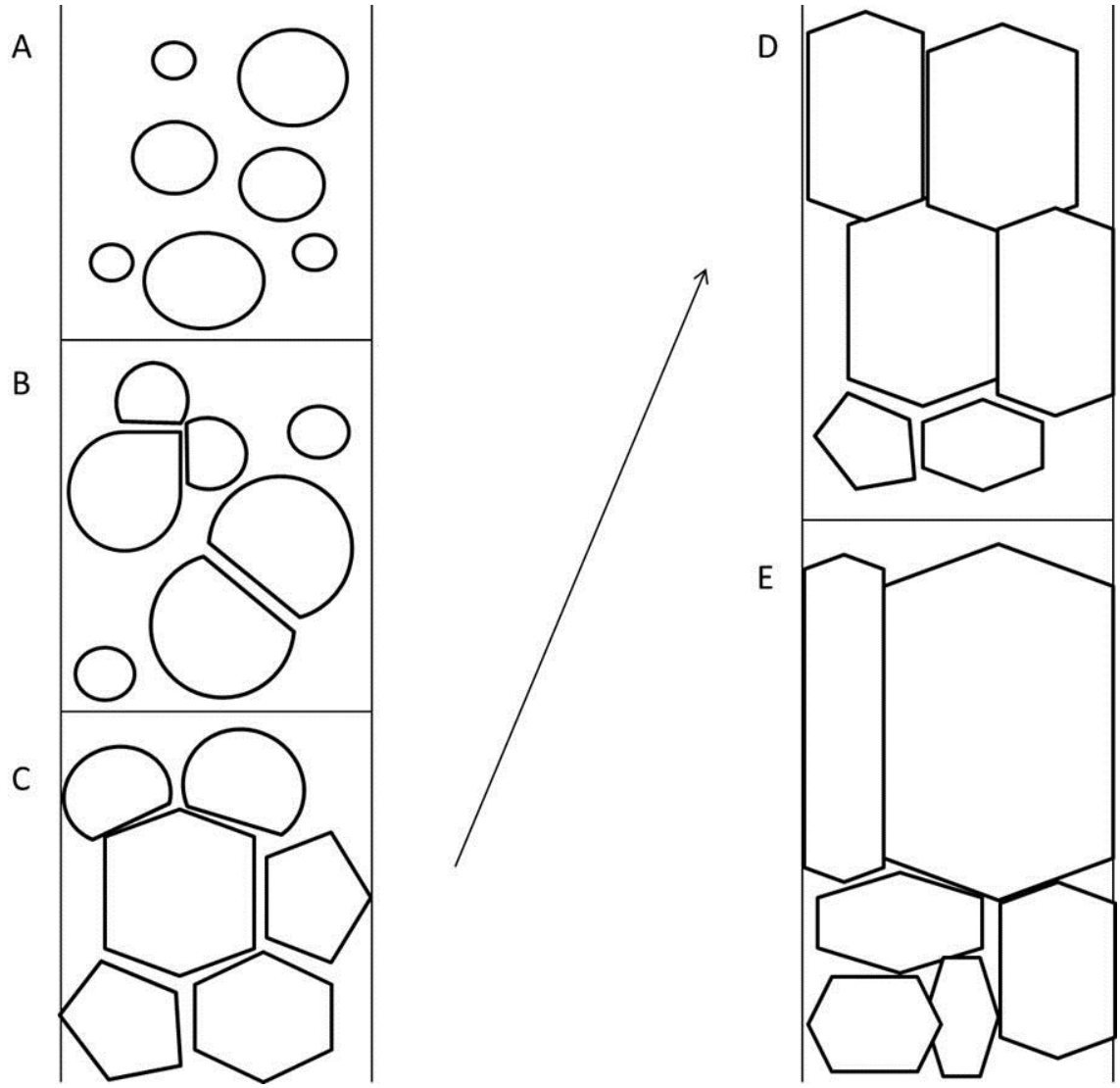

Figure 8. Foam Formation and Lifecycle. A) Foam formation begins as smaller bubbles dissolve, while larger ones grow in size by diffusion of gas. B) As bubbles begin to cream, segregation occurs between the foam layer and liquid layer. C) Next, bubbles deform one another leading to the polyhedral foam structure of the bubbles. D) Coarsening occurs as liquid drains among bubbles and bubbles become larger. E) Finally, the lamellae between bubbles begin to rupture yielding only few remaining, large bubbles. Adapted from Weaire et al.[108]

The versatility of foams – both liquid and solid foams – has never been more ubiquitous. Foams are found on a daily basis and can be generated from many different organic and inorganic materials. Even animals, insects, and plants have been studied for their ability to create foam structures.[108] The spittlebug, for instance, produces a bubbled

spit to protect its body from the sun and predators. The Cork Oak tree contains highly-elongated cells, which generates the porous cork material that is a familiar commodity. More recently, biomedical foams have become widely used in various applications. These biocompatible and biodegradable foams also have substantial mechanical properties. Additionally, biomedical foams can be manipulated, designed, and manufactured to exact specifications for use in medical situations. Because of this appealing quality to scientific researchers, foams have been used in: porous biomedical devices, *in vitro* scaffolds, *in vivo* tissue regeneration, and as drug-delivery vehicles.[113]

Biomedical foams have evolved over the years. Initially these foams were created from metals – for their longevity and high mechanical strengths. In recent years, foams have been more commonly generated from ceramics, such as glass and carbon, to inorganic (polyesters) and organic (lipids, polysaccharides) polymers. Lastly, composite foams have been used to overcome the often problematic issue on incompatibility between tissue/recipient and the foam. Composites, such as collagen and fibrin, are naturally-occurring and can provide an excellent balance between mechanical strength and biocompatibility.[113]

Fibrin Foam.

Fibrin foam is a novel biopolymer generated from the aeration of the fibrin sealant, ARTISS. The processes for making the foam and the devices are both patented and owned by Baxter Healthcare Corporation.[24-27] Several embodiments for creating a foam from fibrinogen and thrombin are detailed in their patents, such as dual-chambered syringes and other mixing apparatuses. However, one such embodiment (Fig. 9A) was pursued in preliminary studies. This process for generating fibrin foam has been

previously described by Baxter researchers. In short, two syringes with male 6% luers are filled using constituents from ARTISS. One syringe contains thrombin (with or without air) while the other syringe contains fibrinogen (with or without air). At least one syringe must contain air to allow for foam formation. Between the syringes is a patented mixing device, which consists of two female luer locks and a porous mixing disc. The mixing device is known as Mix-F (Fig. 9B), while the porous disc is called Vyon-F. The porous disc is produced by Porvair (UK) and is a sintered porous polyethylene disc. The disc (Ø3.8 x 1.5 mm) has a porosity of 38.9% and an average pore size distribution of 60 μm (Fig. 9C).[28]

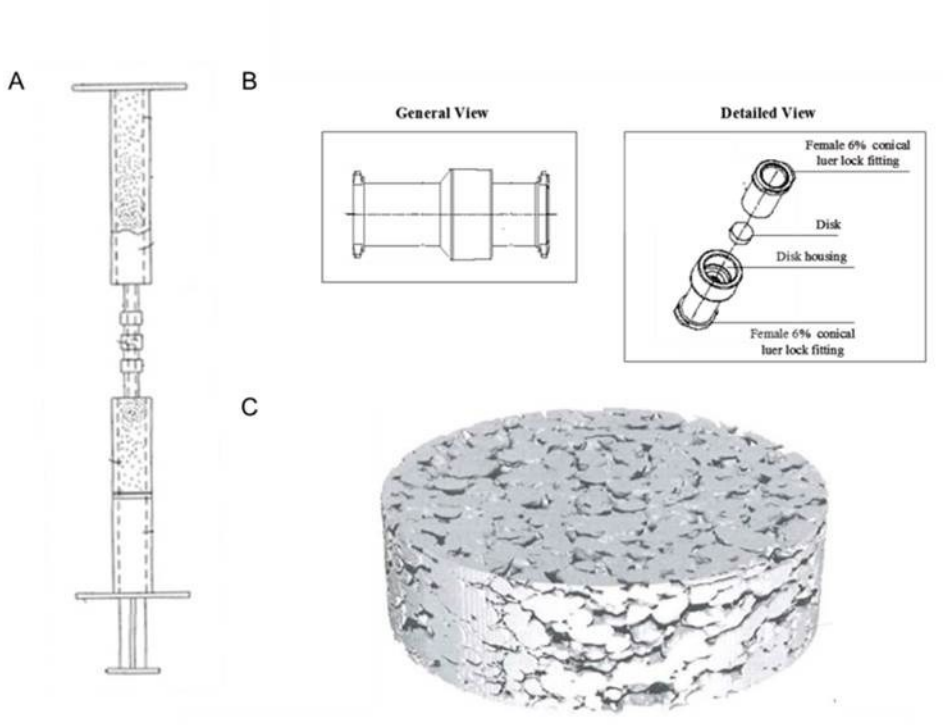

Figure 9. Preparation Apparatus and Device for Generation of Fibrin Foam. Preparation of fibrin foam using ARTISS fibrin sealant. A) Dual syringes containing either thrombin (+ air) or fibrinogen (+ air) are mixed through a patented mixing device, Mix-F (B). C) CAD model of the Vyon-F mixing disc housed inside Mix-F device. Images obtained from Baxter patents and internal documentation.[24-28]

To generate the foam, the fibrin components are repetitively passed through the mixing device, from one syringe to another. Thus, this aeration and manual mixing

through the Mix-F device allows for a homogenous combination of fibrinogen and thrombin constituents into the foamed matrix. While the patents detail a wide array of potential uses and treatments of fibrin foam, only limited characterization has been performed on the mixing device and the foam itself. The foam, when compared to ARTISS, has similar degradation and alpha-chain crosslinking formation. However, fibrin foam has greater viscosity, can polymerize in a temperature-independent manner, and can be applied to both vertical and inverted surfaces without dripping. Also, the mixing process to generate the foam causes the fibrin structure to be an open, porous clot compared to the dense, closed structure of ARTISS (Fig. 10A, 10B).

However, this internal research was only performed in initial stages of conceptual design. Due to its porous structure and fibrin matrix, fibrin foam has the potential to be an applicable wound therapy in specific surgical settings. The foam has a clot structure that could allow for cellular migration and infiltration that would promote improved wound healing. Moreover, the foam's advantage of increased viscosity could permit treatment of hard-to-treat wounds, such as diabetic foot ulcers or bed sores, which must be treated from vertical or inverted angles. These attributes would provide multiple advantages over current wound therapies. And it is with this research, that I aimed to optimize the fibrin foam preparation while also characterizing the foam and assessing its untapped potential as an innovative wound therapy.

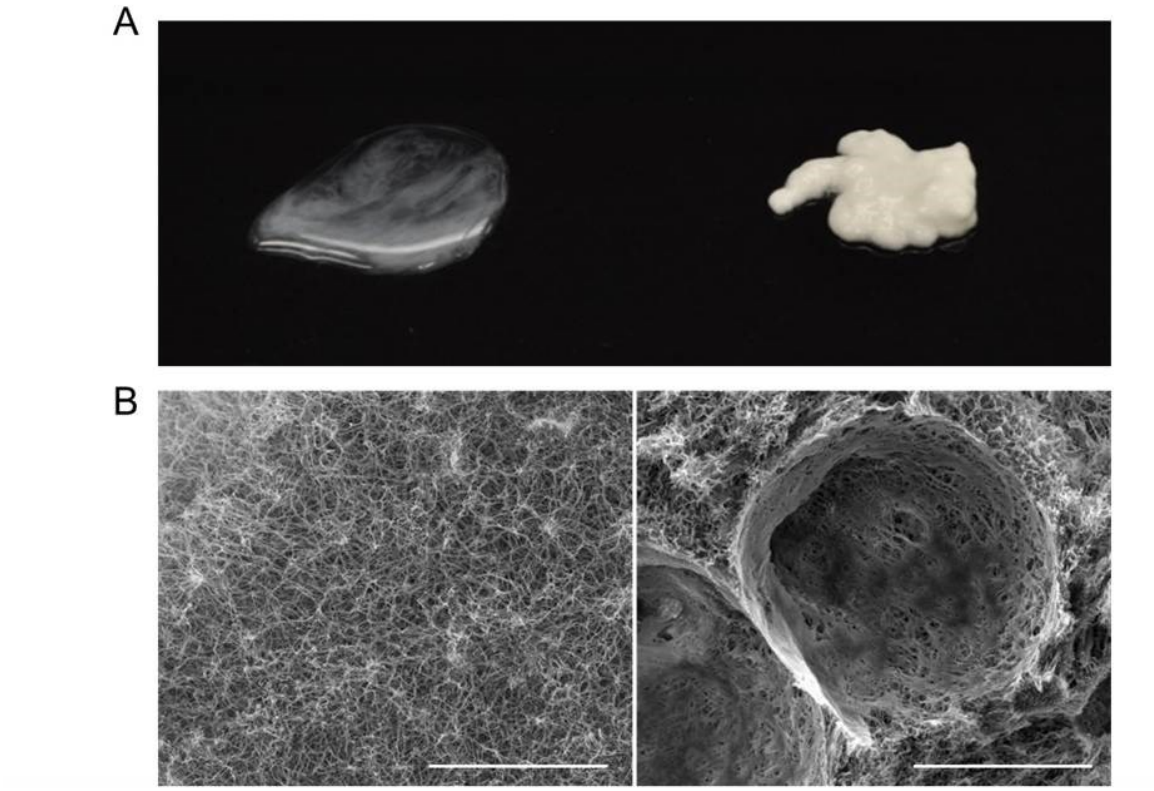

Figure 10. Macroscopic and Microscopic Images of ARTISS and Fibrin Foam. A) ARTISS fibrin sealant (left) and fibrin foam (right) gross images after being manually prepared. B) SEM images of ARTISS (left) and fibrin foam (right). Scale bars for SEM images: 50 μm.

Wound Care Market.

The wound care market is ever-expanding and continues to see growth in revenue and scientific research. The global wound care market was estimated at $15.8 billion in 2013.[2] It is expected to reach $22.1 billion by later this year.[4] The key drivers of this rise are: aging population, obesity, and incidence of diabetes, which are all escalating around the world. Additionally, factors such as burns and surgical-related wounds demand the use of wound care products, thereby increasing revenue in this market. The wound care market involves many types of treatments and dressings as previously described. Each of the key classes of wound healing treatments has a different outlook in the current and

future markets. The traditional wound dressings segment continues to dominate the total wound care market and was at $3.3 billion in 2013.[1] Low cost, local availability, and ease of use and maintenance are the primary reasons for gauze and bandages dominating this segment, especially in the Asia-Pacific and BRIC (Brazil, Russia, India, and China) countries. Wet dressings are perceived to be best suited for quicker wound healing at an affordable price. The market in hospital care has been driven by increased sales volume. It is expected to generate $2.9 billion in revenue by 2018.[2,5] However, traditional (sutures or staples) and wet dressings (dry-to-wet gauze) come with several consequences that often impair wound healing, such as risk of evisceration and infection. These wound care markets are in need of products that can minimize these risks and improve sealing of tissues. Thus, future needs of wet dressings include products that provide a moist environment for cell repair and products that reduce pain during dressing changes.

There is a shift in preference for advanced wound care products from traditional dressings in developed countries such as the U.S. Both antimicrobial dressings and active therapies, such as fibrin sealants and bioactive dressings, are emerging segments, especially in developing countries. Improved clinical results and faster healing rates are driving the demand for these products. The expensive nature of these treatments makes them feasible in only developed countries or in private hospitals in those developing countries. The growth of minimally-invasive surgeries is also driving expansion towards advanced wound care products that will allow for improved efficacy during these technical surgeries. A model product for the minimally-invasive surgery sector would allow for treatment in small, enclosed areas, and the product would be able to be applied in all spatial directions.[2,4]

Currently, there are approximately 50 million reported cases globally of patients suffering from chronic and hard-to-close wounds, which have created a severe cost burden to the world's healthcare system.[3,5] Additionally, the demand for portable and easy-to-use devices is expected to grow over the coming years. Negative-pressure wound therapy (NPWT) is the fastest growing product segment in developing countries. This therapy is used to treat an array of wound situations, including traumatic, dehisced wounds, partial-thickness burns, ulcers (e.g. diabetic, pressure or venous), flaps, and grafts. The NPWT sector of the advanced wound care market is growing – the NPWT segment generated revenue of $1.7 billion in 2013 and is expected to reach $2.1 billion by 2018.[2] This segment has several unmet needs as researchers are looking to improve wound healing methods. These include the ability of new products to reduce the size of the wound throughout treatment with the vacuum, and the need to minimize or remove pain caused by debridement during dressing changes. An ideal product for the NPWT sector would allow for cellular in-growth into a biocompatible and biodegradable material while being able to withstand the subatmospheric pressure treatment.[1]

Taken together, there are several unmet needs in the wound therapy field. Both acute and chronic wound care segments have untapped potential for where an optimal wound therapy is needed. Traditional and modern wound therapies have been able to satisfy wound healing situations for many years; however, there is the current trend to tissue regeneration and healing through the use of tissue-engineered and bioactive dressings.

CHAPTER THREE

METHODS

Preparation of Fibrin Foam.

ARTISS (4 IU thrombin, Baxter Healthcare Corporation) and TISSEEL (500 IU thrombin, Baxter Healthcare Corporation) fibrin sealants were prepared as per manufacturer's instructions for use. Fibrin foam was generated by separating the fibrinogen and thrombin components from the prefilled syringes of ARTISS into individual syringes. As an example, 1 mL of fibrinogen was placed in one syringe and 1 mL of thrombin plus 2 mL air was taken up into another syringe. The Mix-F mixing device (Baxter AG) was placed between the two syringes. The constituents were then manually passed back and forth through the Mix-F device, with one pass equaling moving through the Mix-F once. The number of passes through the Mix-F (ex. 2, 4, 6, 8, etc.), concentration of thrombin (4 IU, 20 IU, 50 IU), and addition of supplemental constituents, including human serum albumin (MP Biomedicals, LLC) and Tween 80 (Sigma Aldrich), were parameters varied during the analysis of fibrin foam preparations. Preparation parameters and their results are listed in the subsequent Results section.

Fibrin Foam Kinetics Assay.

Fibrin foam was prepared as per above utilizing 1 mL of fibrinogen and 1 mL of thrombin plus 2 mL of air in respective syringes. Six passes were used to generate fibrin foam for the kinetics assessment. Once mixed, fibrin foam was applied to a vertical glass

surface at 5 second intervals – starting at t = 0 seconds and finishing at t = 30 seconds. Five hundred microliters (500 μL) of fibrin foam was dispensed from the syringe at each time point. To evaluate the formation of fibrin foam at each time point, a visual yes-or-no conclusion was given based on the following: yes: foam-like consistency and ability to be applied to vertical/inverted surface without dripping/running; no: liquid consistency and inability to be applied to vertical/inverted surface without dripping/running. A yes-or-no designation was given at each time interval. The experiment was repeated for a total of eight samples at each time interval.

Cell Culture.

Cell culture was performed on primary human umbilical vein endothelial cells (HUVEC), primary normal human dermal fibroblasts (NHDF), and primary normal human epidermal keratinocytes (NHEK) purchased from PromoCell. Cells were maintained in respective growth media in a humidified atmosphere of 5% CO_2 in air at 37°C. When subculturing, cells were washed with HEPES-HBSS (PromoCell), suspended in trypsin/EDTA (0.025%/0.01%, PromoCell) for 5 minutes, and neutralized with respective growth media. Cells were spun down at 130 x g for 4 minutes using a swinging bucket centrifuge. Cells were counted using TC20 BioRad Cell Counter and seeded in new tissue culture flasks containing fresh growth media. Cells were passaged every three to four days during use.

Scanning Electron Microscopy and Pore Size Analysis.

ARTISS and fibrin foam clots were prepared and fixed with glutaraldehyde buffer (Electron Microscopy Sciences), containing 0.2 M HEPES and MilliQ water, for SEM preparation. For cell morphology analysis, 5 x 10^4 cells were seeded on ARTISS and

fibrin foam clots for 24-48 hours prior to fixation in buffer. Subsequently, clots were washed, serially dehydrated with ethanol, and dried with hexamethyldisilizane (Alfa Aesar). Clots were allowed to air dry overnight thereafter. Clots were then mounted on aluminum sample supports with carbon adhesive tape. Samples were sputter coated with palladium gold in a Denton Desk IV Sputter/Etch Unit and analyzed in a FEI Quanta 650 FEG Scanning Electron Microscope.

Pore size analysis was performed on cross-sectional cuts of fibrin foam clots. Briefly, SEM images were uploaded into FIJI ImageJ imaging software. Feret's diameter was measured for pores in each sample. Mean pore size was obtained for each fibrin foam preparation. The numbers of pores measured to calculate mean values are shown in the Results section. Percent porosity of ARTISS, fibrin foam, and polyurethane foam samples was calculated using SEM images analyzed with FIJI ImageJ. Sample images were assessed for mean gray scale values over a 300 x 300 pixel area. Two, independent measurements were taken per image with at least three images per sample. Percent porosity was calculated per equation 1. A total of 12 fibrin foam, 6 ARTISS, and 12 polyurethane foam (KCI) measurements were analyzed.

$$\text{Porosity} = \text{mean gray scale} / 255 \times 100\% \qquad \text{Eq (1)}$$

Tensile and Wound Closure Strengths Testing.

For tensile strength testing, a specially designed dog-bone-shaped mold was used to create ARTISS and fibrin foam clots of identical size and volume. The sample thickness was 2 mm and had a width at the narrow middle part of 4 mm. The total volume of the mold was 3.0 mL. Samples were allowed to cure in the mold for 15 minutes, and then placed in phosphate-buffered saline (PBS, HyClone) until use.

Tensile testing was performed on MTS Criterion Model 42 (MTS Systems Co.). The larger ends of each dog-bone-shape mold were placed into the pneumatic grips of the MTS machine. Tensile loading was applied at a crosshead speed of 12.70 mm/min. The maximum load at the sample failure and stress-strain curve was obtained; tensile strength and elastic modulus were measured using the MTS Test Suite software version 3.0.1. Six samples of each group were analyzed.

Wound closure strength was assessed using ASTM F2458 – 05 (Reapproved 2010), Standard Test Method for Wound Closure Strength of Tissue Adhesives and Sealants.[114] Briefly, porcine skin was cut into 10 cm long x 3 cm wide pieces. Pieces were placed vis-à-vis along the 3 cm width margin. ARTISS and fibrin foam were prepared and applied to a 0.5 cm region on each porcine skin piece along that same margin. ARTISS and fibrin foam were measured at 3 mm thickness on the porcine skin using a non-calibrated ruler. Samples were allowed to cure for 1 hour in PBS at 37°C. Samples were loaded into the pneumatic grips of the MTS machine and tensile loading was applied at a rate of 50 mm/min or until a full break occurred. Wound closure strength and modulus measurements were obtained using the MTS software. The type of break was recorded for each sample. Four samples from each group were measured.

Thromboelastography and Shear Strength.

Clot formation kinetics and strength were determined with thromboelastography (TEG) using Thromboelastograph® Hemostasis Analyzer Model 5000 (Haemonetics Co.) with the following deviations. Three-hundred sixty microliters (360 µL) of ARTISS or fibrin foam were prepared per sample. For ARTISS, the samples were placed into the assay cups and allowed to cure for 30 seconds before the analysis was started. For fibrin

foam, the samples were mixed at t = 0 seconds, then allowed to sit in a syringe for 30 seconds prior to application into cups to normalize to ARTISS. The TEG analyses were started at 30 seconds for both sets of samples and run at 37°C. The thromboelastograph was calibrated with quality control samples before each use. TEG Analytical Software version 4.2.3 was used to calculate the time to clot initiation (R, minutes), time to clot firmness (K, minutes), alpha angle (α, degrees), maximal clot strength (MA, maximum amplitude, mm), and shear elastic modulus strength (G, dynes/cm^2). Analyses were performed for at least 30 minutes or until the operating software had calculated all mentioned parameters.

Shear modulus was further calculated from MA values in TEG to dynes/cm^2 and kilopascals (kPa) as per equation 2, where G has units of dynes/cm^2 and 10,000 dynes/cm^2 is equal to 1 kPa.[115] Fourteen samples of ARTISS and sixteen samples of fibrin foam were measured for TEG and shear strength.

$$G = 5000 \cdot MA / (100\text{-}MA) \qquad \text{Eq (2)}$$

Permeability Analysis.

Sample fluid permeation was assessed using previously described techniques with the following exceptions.[116,117] The permeation coefficient (K_s) was calculated per equation 3, where η is the viscosity of the liquid (water, 0.001 Pascal seconds), L is the length of the sample (mm), Q is the flow rate in time t, S is the surface area of the sample (mm^2), and P is the average pressure in the system (98 Pascals). To assess the fluid permeability, ARTISS, fibrin foam, and polyurethane foam samples were fit to a cylindrical apparatus and allowed to cure for 30 minutes. Two milliliters (2 mL) of water stained with bromophenol blue (Sigma Aldrich) was applied to the top of each sample.

Permeability was assessed after 1 hour when the sample radius, thickness of sample, and height of permeabilized/dyed area were measured using a ruler. Lower values of K_s indicated reduced permeability and smaller pore size in the matrixed network. Eight samples were measured per group.

$$K_s = \eta \cdot L \cdot Q / S \cdot P \qquad \text{Eq (3)}$$

Clot Compaction Assessment.

Compaction experiments were performed as previously described.[116] Briefly, 1.5 mL microcentrifuge tubes were precoated with cooking oil spray (Conagra Brands) and dried with a cotton swab. ARTISS and fibrin foam were prepared, and 1.0 mL was dispensed into each tube. Clots were incubated at room temperature for 2 hours. After 2 hours, the clots were centrifuged at 4200 x g for 30 seconds. The supernatant volume was removed and measured with a Hamilton syringe (Hamilton Co.). Percent compaction was calculated as the ratio of the expelled supernatant volume to the original clot volume (1.0 mL). Eight samples were measured per group.

Non-Invasive *In Vivo* Degradation Assay.

To measure the kinetics of *in vivo* degradation, fluorescently-conjugated fibrin in either fibrin foam or ARTISS fibrin sealant was subcutaneously implanted in nude mice. For this purpose, fibrin clots of defined volume (200 µL) were labeled by integration of fluorescently-conjugated fibrinogen (125 µg/mL; Alexa Fluor 546 conjugate; Invitrogen). The experiments were approved by the local animal research committee (Amt der Wiener Landesregierung, Vienna, Austria) and animals were treated according to the National Institute of Health guidelines. A total of 6 nude mice (BALB/C nu/nu; female; 20-30 g; Institut für Labortiertechnik und Gentechnik, Austria) were implanted with fibrin clots

under the skin over each shoulder and proximal to each hock. Animals were treated preoperatively and on the following 3 days with carprofen (2.5 mg/kg Rimadyl, Pfizer, Austria). The fluorescence of the fibrin matrix was non-invasively followed and quantified over 14 days using a multispectral imaging system (Maestro Imaging System, CRI Inc.). The images were acquired using the CCD frame at 2 x 2 binning and resulting spectral data series unmixed using the identical spectral library for every cube. This *in vivo* degradation analysis was performed by the Ludwig Boltzmann Institute on behalf of Baxter Healthcare Corporation.

Lactate Dehydrogenase Cell Viability Assay.

ARTISS fibrin sealant, fibrin foam, and polyurethane foam samples were prepared and placed in 24-well plates and set in a 37°C/5% CO_2 incubator for 30 minutes. A specific number of cells from each cell line (HUVEC, NHDF, and NHEK) were isolated to give a final concentration of 2 x 10^4 cells per well. Cells were cultured on the samples, allowed to attach for 1 hour, and then additional media was placed into the wells. At 2, 24, and 48 hours after cell seeding, lactate dehydrogenase (a marker of cellular death) was analyzed using a colorimetric assay and per manufacturer's instructions (Promega). Briefly, 50 µL of supernatant was removed from each well, placed into a 96-well plate, mixed with 50 µL of substrate solution, and allowed to incubate for 30 minutes at room temperature. Fifty microliters (50 µL) of STOP solution (solution within LDH cell viability kit) was added to all wells after the 30 minute incubation. Wells were then analyzed for absorbance at 490 nm on a SpectraMax M5e microplate reader. Cell viability was quantified by the average absorbance at each time

point for the various cell conditions. Eight samples were measured for each cellular condition.

AlamarBlue Metabolic Assay.

HUVEC, NHDF, and NHEK cells were cultured and isolated to a final concentration of 5 x 10^4 cells per well. Cells were cultured on ARTISS fibrin sealant, fibrin foam, and polyurethane foam for 1 hour in a 24-well plate before an additional 900 µL of media was added to each well. After 4 hours of incubation at 37°C/5% CO_2, 100 µL of AlamarBlue reagent (Invitrogen, Thermo Fisher Scientific) were added to each well. At 2, 24, 48, and 72 hours after the addition of AlamarBlue, 50 µL of supernatant was removed, placed into a 96-well plate, and read in fluorescence mode with an excitation wavelength of 570 nm and emission wavelength of 585 nm. Readings were performed on a SpectraMax M5e microplate reader. Cellular metabolism and viability was assessed using average fluorescence units at each time interval. Four samples were measured per cell condition.

Confocal Microscopy for Cell Viability.

One milliliter of ARTISS fibrin sealant or fibrin foam was placed into a 24-well plate. Primary HUVEC, NHDF, and NHEK cells at a final concentration of 1 x 10^5 cells per well were seeded on the clots for 48 hours in a 37°C/5% CO_2 incubator. After 48 hours, clots containing cells were transferred and inverted onto MatTek dishes. Two milliliters of HBSS (PromoCell) were added to each sample. ReadyProbes® Cell Viability live/dead and wheat germ agglutinin stains (Thermo Fisher Scientific) were added to the HBSS solution. Samples were covered from light and incubated at room temperature for 15 minutes. Images of the samples were taken using a Nikon A1R

Confocal Microscope at magnifications noted in the images. Image manipulation and compilation was performed using Nikon NIS-Elements Software Version 3.10.

Cytotoxicity Assay.

NCTC clone 929 cells (ATCC #CCL1) were cultured at a concentration of 1.3 x 10^5 cells per well. Cells were incubated for 24 hours in a humidified atmosphere of 5% CO_2 in air at 37°C. After 24 hours and according for ISO 10993-5 – Biological Evaluation of Medical Products – fibrin foam samples were placed on top of the cells.[118] Positive control (powder free latex gloves, Rubbercare) and negative control (Baxter polyolefin material) were also tested and placed on cells. Cells and test samples were incubated for an additional 24 hours. After this elapsed time, test samples were removed from each well and 2% Crystal Violet solution (Sigma Aldrich) was added to each well to stain the cells. The cells were examined microscopically based on the ISO guidelines of toxicity ratings (below). Six fibrin foam samples were tested, and three positive and three negative controls were also analyzed.

Rating	Pass/Fail	Description
0	Pass	No detectable zone around or under the specimen
1	Pass	Some degenerated cells under the specimen
2	Pass	Zone of degenerated cells limited to the area under the specimen
3	Fail	Zone of degenerated cells extends specimen size up to 1.0 cm
4	Fail	Zone of degenerated cells extends farther than 1.0 cm beyond specimen

Table 7. Toxicity Ratings for ISO 10993-5. Adapted from ISO 10993-5.[118]

Three-Dimensional *In Vitro* Wound Assay.

Six hundred microliters (600 µL) of 5 mg/mL PureCol EZ Gel (Advanced BioMatrix, Inc., Sigma Aldrich) collagen gels were formed in a 24-well plate. Gels were incubated at 37°C/5% CO_2 for 90 minutes to allow for full polymerization of the collagen. Primary HUVEC, NHDF, and NHEK cells were trypsinized. A specific number of cells from each line were isolated to give a final concentration of 3×10^4 cells per gel and stained with Vybrant DiO (Life Technologies of Thermo Fischer Scientific). After staining, the cells were washed three times with media, and then seeded onto the collagen gels. After 4 hours, a 2 mm biopsy punch (V. Mueller) was used to punch regions out of the collagen gel. Careful pipetting was used to remove remainder of the collagen debris from the punch region. The regions were then filled with PureCol EZ Gel, ARTISS fibrin sealant, fibrin foam, or polyurethane foam and supplemental media was placed on gels. Gross migration of cells was assessed at 24 and 48 hours using a Nikon Eclipse LV100 Upright Microscope with Nikon Camera. Images were taken at 4x magnification at each time point to analyze the migrated cells and wound margins.

Murine Wound Model.

A dermal skin excision wounding model was performed as follows with the assistance of the W. Keith Jones Laboratory from Loyola University Chicago in collaboration with Baxter Healthcare Corporation. BKS.Cg-Dock7m +/+ Leprdb/J (db/-) mice (Jackson Laboratories, male, 8-12 weeks of age) were anesthetized using isoflurane (1.5 L/min) and buprenorphine (0.5 mg/kg i.p.) to effect. The dorsal aspect of the thorax was shaved, draped, and three butadiene scrubs were performed. A 6 mm biopsy punch was used to make four excision wounds (1 cm apart) in the sterile field. Each of the four

wounds was treated separately and covered using experimental materials and dressings (Fig. 11). Briefly, ARTISS fibrin sealant and fibrin foam were two treatments, compared to control (no dressing) and polyurethane foam dressing (KCI). Tegaderm (3M Medical, USA) and/or cohesive tape were put on the mice to prevent access to the wounds, and the mice were individually caged to prevent damage by other animals to the wound site. Dressings were changed and wounds measured and photographed at days 3, 7, 10, and 14 and depilatories used to remove growing hair as needed. At day 3, day 7, and day 10, mice were anesthetized and dressings changed. While uncovered, photographs with ruler were taken to document wound size. The wounds were re-dressed and the animals recovered and housed as above. At day 7 or day 14, mice were anesthetized using isoflurane and ketamine/xylazine (10 mg/mL and 0.2 mg/mL i.p.). When non-responsive to toe pinch, the dorsal aspect of the thorax, including the wounds, was excised, then prepared and fixed for histological analysis. The hearts were also harvested resulting in death of the mice.

Animal procedures were approved by Loyola University Chicago Institutional Animal Care and Use Committee (IACUC) and conducted in accordance with the Guide for the Care and Use of Laboratory Animals and applicable United States animal welfare regulations in an AAALAC-accredited facility. The animals utilized in this experiment all received humane care.

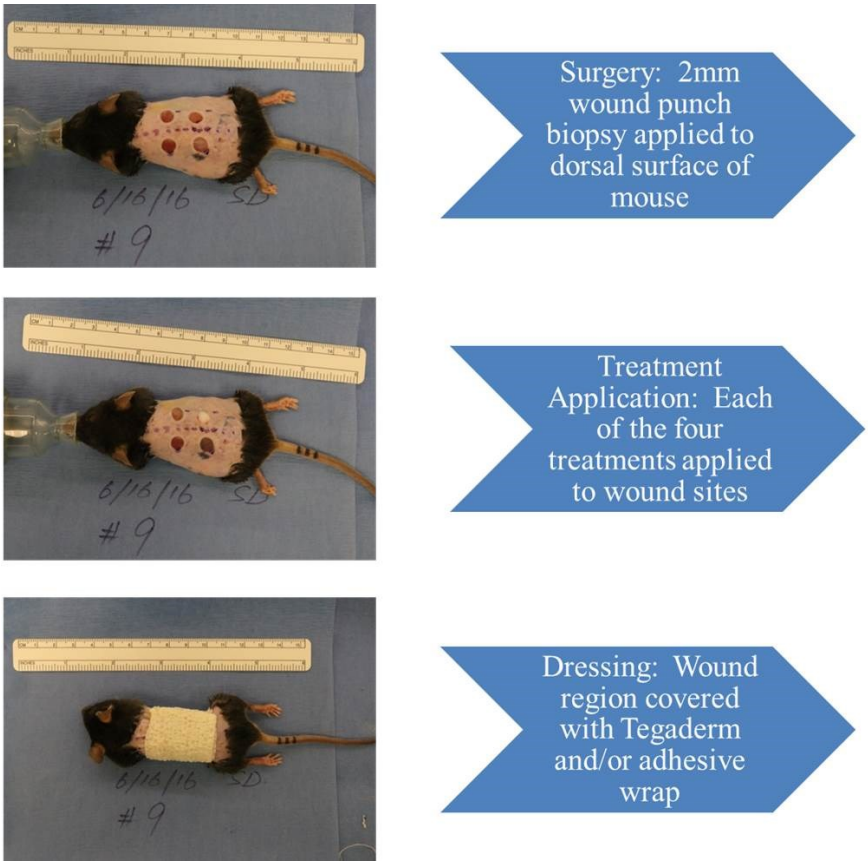

Figure 11. Overview of Murine Model Surgical Procedure. Photographical representation of surgical procedure and treatment of mice during murine model. Mice were subjected to 2 mm punch biopsies on their dorsum. Each would was treated separately with one of four treatment options. The dorsal surface of the mice was them covered to prevent any disruption to wound and treatment sites.

Wound Closure Measurement.

Using a digital camera, images of the wounds were obtained after wounding, after treatments, and at each scheduled dressing change (days 0, 3, 7, 10, and 14). Images were uploaded to a computer, and using imaging software (FIJI ImageJ), the wound area was measured. FIJI ImageJ imaging software was used to blindly measure the wound area by tracing the wound margin with a fine-resolution computer mouse and calculating the pixel area.[119] Wound size area (cm^2) from each day was measured as compared to

day 0. A wound was considered completely closed when the wound area was equal to zero (grossly). All area measurements are in cm^2.

Histological and Pathological Analyses.

The wounds and surrounding tissue were collected and placed in formalin for histopathologic evaluation on days 7 and 14. Polyurethane foam dressings were collected for histopathologic evaluation on dressing changing days (days 3, 7, and 10) and submitted to Loyola University Medical Center's Histology and Pathology departments. Histopathologic evaluation was performed on the collected tissue and samples. Analysis, including hematoxylin & eosin (H&E) and Masson's Trichrome staining, was read by an independent and blinded pathologist at Loyola University Medical Center.

The main histological parameters analyzed for wound healing were: reepithelialization, neovascular proliferation, acute and chronic inflammation, and collagen deposition. These parameters were scored on a 0-3 scale (below).[120] A total of 12 samples were analyzed per treatment per time point for all parameters except collagen deposition (n = 4 per treatment per time point). Each histological slide contained 4-6 slices of wound sample with scores being representative for the sample overall.

Parameter	0	1	2	3
Reepithelialization	None	Partial	Complete, but immature/thin	Complete; mature
Neovascular Proliferation	None	Up to 5 vessels per field	Up to 6-10 vessels per field	More than 10 vessels per field
Acute Inflammation	None	Scant	Moderate	Abundant
Chronic Inflammation	None	Scant	Moderate	Abundant
Collagen Deposition	None	Scant	Moderate	Abundant

Table 8. Histological Parameter Scoring for *In Vivo* Wound Model. Scoring scale adapted from reference Abramov et al.[120]

Additionally, epithelial maturation, granular tissue formation, and granular tissue maturation were assessed on a yes-or-no basis. The degree of granular tissue formation/maturation was determined by the structure and alignment of fibroblasts in the wound area.

Negative-Pressure Wound Therapy Feasibility.

Porcine skin samples (obtained from Baxter R&D) were thawed and cleaned, and hair was removed. A 12-mm full-thickness biopsy punch was created in the porcine skin. ARTISS or fibrin foam was prepared and placed into the wound punches. Samples were allowed to cure for 5 minutes, 30 minutes, 1 hour, and 2 hours in the wounds. At each time point, V.A.C. Freedom NPWT System (KCI) was placed over the treated wounds and vacuum pressure (-200 mmHg) was applied for 2-5 minutes. Images of the system apparatus, wounds, and treatment were taken using Nikkor 42x Wide Optical Zoom ED VR Cool Pix P510. At least three samples were performed for each treatment group at each time point.

Statistical Analysis.

All data collected in this body of work was expressed as mean ± SD. Sample sizes are stated within each experimental results section. Pairwise differences between products were evaluated using the Wilcoxon Mann Whitney test. For the murine model, the means and standard deviations of wound size were calculated initially and at follow-up time points for each treatment for 12 or 24 mice. A linear mixed effects model was specified to predict wound size as a function of treatment, time, and the treatment by time interaction, and included a random intercept for mice to account for possible correlation due to repeated measures. The effect of treatment at each time point was tested. Least squares mean differences in wound size by treatment were presented at day seven to assess differences due to treatment. P-values < 0.05 indicate samples are significantly different. Statistical analyses were performed with the support of Baxter Healthcare Corporation Biostatistics and Loyola University Chicago Biostatistics Core.

CHAPTER FOUR

RESULTS

Aim 1: To determine the impact of aeration on the physical, biomechanical, and biocompatibility properties of fibrin foam.

Optimal preparation of fibrin foam. The preparation of fibrin foam has several variables which could be changed to generate a variety of fibrin foam entities. Fibrin foam is created using a dual-syringe apparatus (Fig. 9A), where the fibrin sealant constituents are passed through the mixing device (Fig. 9B). This aeration process yields a foam-like, porous fibrin network compared to the dense fibrin matrix of commercially-available sealants (Fig. 10). To optimize the preparation of fibrin foam, I varied three, key factors. These included the number of passes through the Mix-F mixing device, thrombin concentration for speed of clot formation, and additional foaming agents (i.e. HSA and Polysorbate 80). With each preparation variant, the acceptance criteria were the following: 1) manual ease of mixing 2) foam-like, porous consistency 3) mean pore size < 200 μm. The pore size criterion was chosen based on several critical cellular processes that have been noted in the literature that require a mean pore size distribution less than 200 μm, including angiogenesis, skin regeneration, and fibroblast cell migration/proliferation, which have optimal pore size ranges from 160-270 μm, 20-125 μm, and 100-250 μm, respectively.[15]

Previous Baxter research dealing with the mixing of fibrin foam indicated either syringe could contain the air and an even number of passes was to be used to have equal mixing between the syringes.[24-27] This research had shown six or eight passes to be ideal for fibrin foam generation, which was solely based on the void volume remaining in the syringes during mixing and included no other acceptance criteria. At six or eight passes, the void volume was zero, meaning all constituents were incorporated into the foam. However, and to assess all possible parameters, the experimental variants used in the preparation, mixing, and pore size analyses are shown in Tables 9 and 10.

Fibrin Foam Preparation	4 passes	6 passes	8 passes	Failure Point
4 IU	Y	Y	Y	14
20 IU	Y	Y	Y	9
50 IU	Y	Y	N	6
4 IU + 10% HSA	Y	Y	Y	14

Table 9. **Gross Mixing Assessment of Fibrin Foam Preparations.** Y = total number of passes were achieved; N = total number of passes not achieved (i.e. clogging of device or failure to mix). Failure point was the maximum passes reached during mixing over the samples tested. Six total samples were measured for each preparation.

First, to assess ease of mixing with the various preparations, fibrin foam was prepared and subjected to differing number of passes through the Mix-F mixing device and the maximum number of passes before mixing failure (i.e. clotting/clogging). For all mixing experiments, the setup in Figure 9 was used with the following ratio of constituents – 1 mL thrombin + 2 mL air in one syringe; 1 mL fibrinogen in the second

syringe. From a gross and human factors perspective, the number of passes and added constituents to create fibrin foam was tested. The number of passes was varied from 2, 4, 6, 8, and maximum passes achievable. An even number of passes was chosen for all experiments as to have the thrombin and fibrinogen constituents equally mixed in the two syringes.

Higher concentrations of thrombin and human serum albumin (HSA) were also tested in this portion of the study. Thrombin concentration, which dictates the speed at which the fibrin clot forms, was varied from 4IU (current ARTISS formulation) up to 50 IU. HSA was adjusted to a final concentration of 10% or 50% HSA greater than that of the current formulation. HSA was a chosen constituent to adjust because of the ability of albumin to stabilize the fibrin clot and increase foaming abilities. Polysorbate (Tween) 80, a known surfactant, was also tested but failed mixing feasibility assessment as this preparation clogged the Mix-F device and did not allow for proper mixing through the device. Therefore, Tween preparations were not included in further analyses.

As shown in Table 9 (and A1), the 4 IU thrombin preparation of fibrin foam was able to be passed through the mixing device up to 14 times before failure of the device occurred. Failure was constituted as clogging of the Mix-F device. The 20 IU and 50 IU thrombin samples, however, clotted too rapidly and only were able to achieve a maximum of 9 and 6 passes through the device, respectively.

The microscopic matrix of fibrin foam was assessed next via scanning electron microscopy. SEM was used to measure the pore sizes of the various fibrin foam preparations (Fig. 12). Pore size is a crucial determinant in the overall structure and

function of matrices and scaffolds, as mentioned previously. Too small and the cell migration is limited; while too large of pores can reduce ligand density.

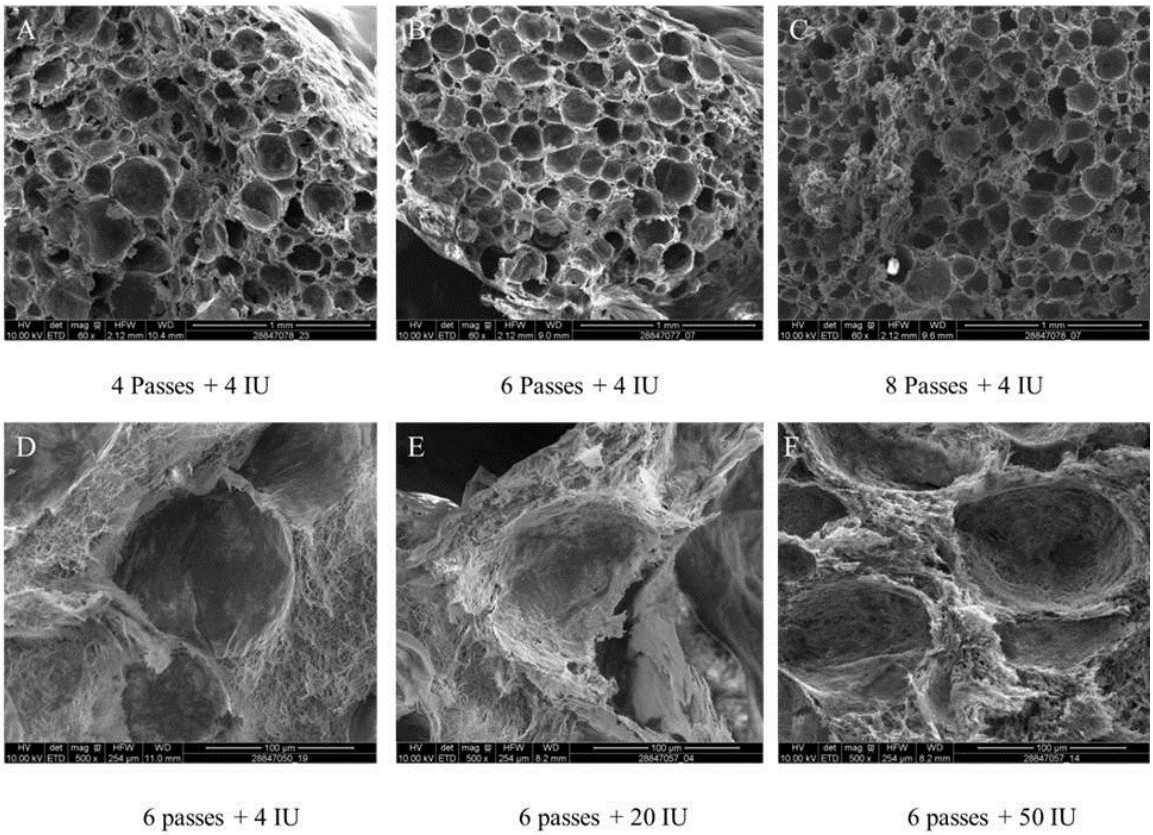

Figure 12. SEM Micrographs of Fibrin Foam Preparations. SEM micrograph images of several fibrin foam preparations. Preparations were varied by either the number of passes through mixing device or by additive constituents (i.e. increase in thrombin concentration). A) 4 Passes + 4 IU fibrin foam B) 6 Passes + 4 IU fibrin foam C) 8 Passes + 4 IU fibrin foam D) 6 Passes + 4 IU fibrin foam E) 6 Passes + 20 IU thrombin fibrin foam and F) 6 Passes + 50 IU thrombin fibrin foam. Scale bars: 1 mm (A-C), 100 μm (D-F).

The measured pore size distributions for all fibrin foam preparations are shown below in Figures 13 and 14. Table 10 displays the quantified means for all preparations (in microns) and the number of pores analyzed, which is visually shown in Figure 14. While the distributions vary from large distributions of pores in the lower number of passes to more tightknit pore sizes as the passes increase, it was noted that all preparations have mean pore sizes that fall below the accepted range of 200 μm (Table

10). Due to the large standard deviations for each distribution, there was no statistical difference among the groups.

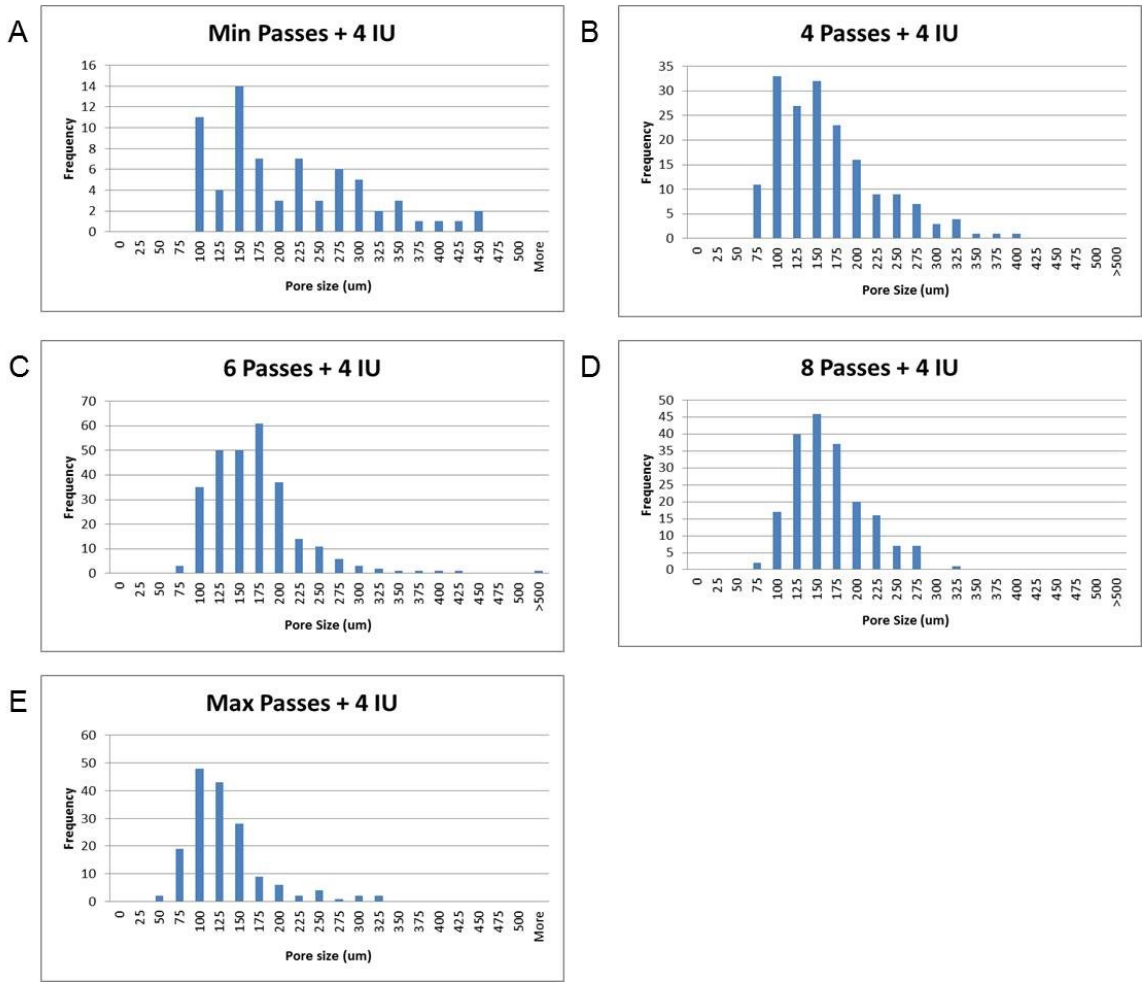

Figure 13. Pore Size Measurements of Fibrin Foam Preparations (Passes Varied). Histogram representations of pore size distributions for A) Minimum (2) Passes + 4 IU fibrin foam B) 4 passes + 4 IU fibrin foam C) 6 Passes + 4 IU fibrin foam D) 8 Passes + 4 IU fibrin foam and E) Maximum passes (14) + 4 IU fibrin foam. Quantified data for Figure 13 is found in Table 10.

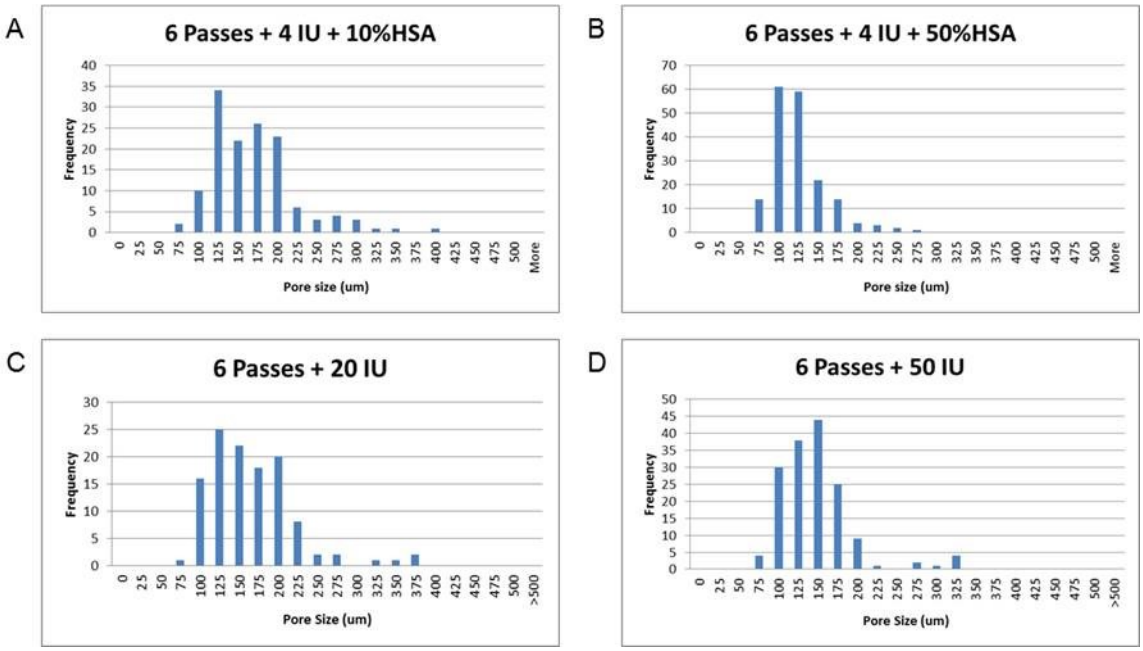

Figure 14. Pore Size Measurements of Fibrin Foam Preparations (Additives Varied). Histogram representations of pore size distributions for A) 6 passes + 4 IU + 10% HSA fibrin foam B) 6 Passes + 4 IU + 50% HSA fibrin foam C) 6 Passes + 20 IU thrombin fibrin foam and D) 6 Passes + 50 IU thrombin fibrin foam. Quantified data for Figure 14 is found in Table 10.

As the previous Baxter studies detailed, the number of passes to incorporate all constituents into the foam was 6 or 8 passes. The 20 IU preparation reached 9 passes and the 50 IU only reached 6 passes, respectively. These failure points were too close to the optimal range of passes (e.g. 6 to 8), which would not allow for a margin of error in a surgical use and preparation of the foam. Clogging and other mixing failures would likely occur at a higher frequency with these preparations. Thus, to ensure no future human factor issues with mixing and preparation of fibrin foam, the higher concentration thrombin preparations were eliminated from consideration. Next, I took into consideration the pore mean distribution of all foam preparations. As shown in Figure 15, there was no discernable difference in pore size distributions among the fibrin foam preparations.

All preparations met the mean pore size parameter; however, and after factoring in the mixing analyses and acceptance criteria, the 6 passes + 4 IU preparation was the optimal choice for fibrin foam. This preparation would allow for ease in generating the foam in a surgical situation and is well within the acceptable range for mean pore size (155 μm) for use in wound healing applications. There was no added effect(s) from HSA throughout this initial characterization, thus it was excluded from any major analyses moving forward.

	Min (2 Passes) + 4 IU	4 Passes + 4 IU	6 Passes + 4 IU	8 Passes + 4 IU	Max (14 Passes) + 4 IU	6 Passes + 20 IU	6 Passes + 50 IU	6 Passes + 4 IU + 10% HSA	6 Passes + 4 IU + 50% HSA
Mean Pore Size (μm)	199.3 ± 93.8	152.2 ± 66.8	155.5 ± 58.9	151.8 ± 46.0	117.2 ± 49.7	152.6 ± 54.8	134.5 ± 46.7	156.7 ± 55.3	113.21 ± 35.2
Pores Counted	70	177	277	193	166	118	158	136	180

Table 10. Mean Pore Sizes of all Fibrin Foam Preparations. The quantified mean pore size distributions (± SD) for all fibrin foam preparations are shown. The numbers of pores counted for each preparation are detailed as well. No significant differences were found among preparations. IU: international units of thrombin; HSA: human serum albumin.

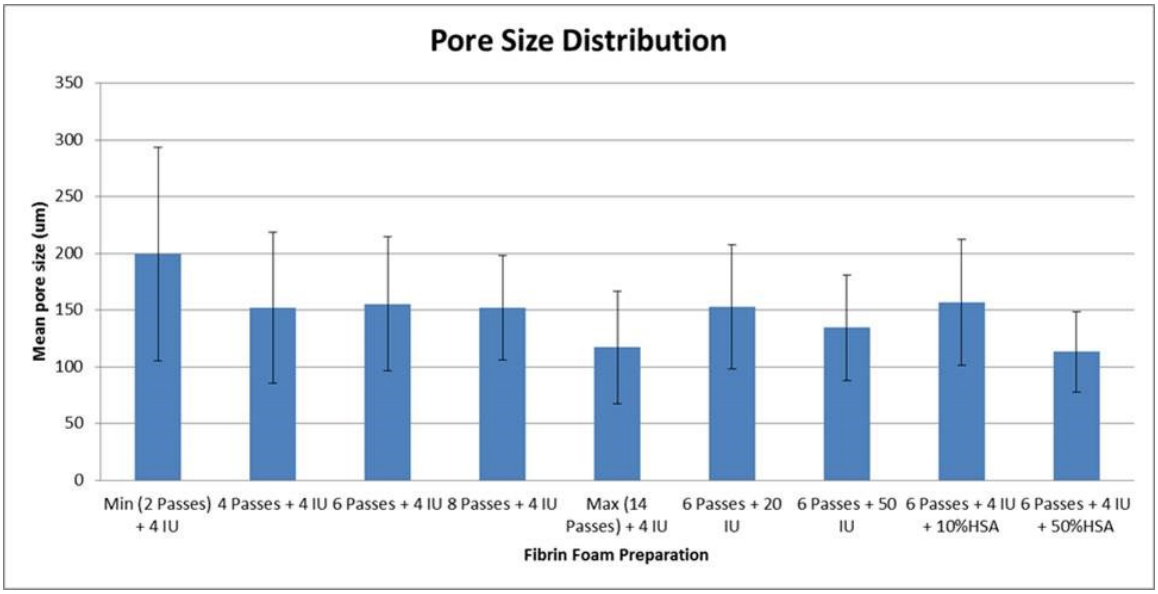

Figure 15. Mean Pore Sizes of Fibrin Foam Preparations. Mean pore size distributions (± SD) for all fibrin foam preparations (Table 10) are shown. No significant differences were found among groups.

Once chosen as the optimal preparation, further analyses in this study were performed on the 6 passes + 4IU fibrin foam. First, as seen in Figure 16, the rate of formation of fibrin foam was assessed in order to confirm that exact preparation procedure for the generation and application of fibrin foam. This test was performed by preparing fibrin foam, then waiting 0-30 seconds at 5 second intervals before applying the foam to a vertical surface. Per this experiment, an acceptable outcome was a foam having the viscosity to remain on a vertical surface without dripping or running, as this is one of the differentiating characterisitcs of fibrin foam compared to ARTISS and other fibrin sealants. Figure 15 details the number of positive outcomes at each time point (n = 8 per time point). After 20 seconds post-mixing, fibrin foam is able to be applied with 100% positive outcomes from a consistency standpoint. Thus, this 20-second set time prior to application was another step in the preparation of the 6 passes + 4 IU optimal fibrin foam.

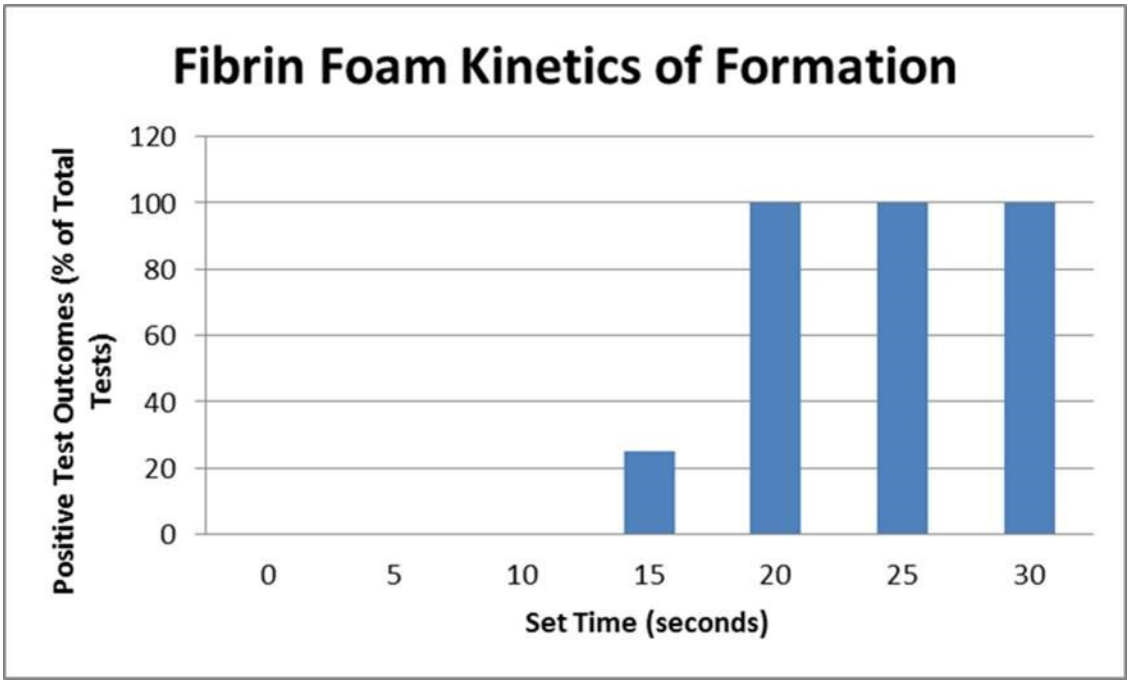

Figure 16. Kinetic Assessment of Fibrin Foam Formation. Fibrin foam (6 passes + 4 IU) was prepared and allowed to set in syringe for multiple time intervals. Fibrin foam was applied to a vertical surface and each sample's consistency was noted. An outcome was deemed positive based on formation of foam-like consistency and ability to hold on vertical surface without running. Percent of total positive outcomes is shown at each time point. A total of eight samples were analyzed at each time interval.

Taken together, the optimized fibrin foam preparation is generated from the components of the commercially-available fibrin sealant, ARTISS. The constituents of ARTISS are used at a ratio of 1 mL fibrinogen to 1 mL of 4IU thrombin + 2 mL of air to create fibrin foam as it is passed six times through the Mix-F mixing device. This preparation has a mean pore size of 155 μm and is allowed to set in the syringe for 20 seconds prior to application. Hereafter, this specific preparation of fibrin foam was used for all subsequent experiments and testing, and it will be referred to as solely as "fibrin foam".

Biomechanical and structural characterization of fibrin foam. With the fibrin foam preparation optimized to 6 passes + 4IU thrombin, biomechanical testing was performed to study the impact of aeration on fibrin foam as compared to that of ARTISS fibrin sealant. The following portion of the study details both biomechanical and structural analyses of fibrin foam.

Thromboelastography (TEG) is a coagulation assay used to evaluate the efficiency of clot formation and clot viscoelastic properties. TEG analyzes a set of specific parameters associated with clot kinetics and formation. These include: reaction time (R), or time until initial fibrin formation; clot formation time (K), or the measure of rapidity to reach clot strength; α angle, or the speed of clot strengthening; maximum amplitude (MA), or ultimate clot strength; and shear elastic modulus strength (G), or the clot firmness.[121] TEG was employed to understand any perturbations in clot formation and kinetics through the aeration process of ARTISS into fibrin foam and the impact of these changes.

Figure 17 depicts a thromboelastograph readout of fibrin foam versus ARTISS. The TEG analyses were normalized to time of preparation as described in the Methods section. This figure shows fibrin foam (green) with a much steeper angle to clot formation than ARTISS, as reflected in the significantly higher alpha angle (Table 11, $p<0.001$). Table 11 (and Table A1) shows the remaining TEG parameters as compared between ARTISS and fibrin foam preparations with significant differences ($p<0.001$) in the R and K values as well leading to the conclusion of faster clot kinetics for fibrin foam compared to ARTISS. There were similar measured values for maximum clot strength (MA) and shear elastic modulus strength (G), which shows fibrin foam and ARTISS,

have comparable clot strengths even after aeration. Expanding from the TEG analysis, a shear strength computation was performed to extrapolate additional data on the biomechanical attributes of fibrin foam. As referenced in the literature, shear strength, G, is often measured in a magnitude of Pascals.[115] Table 12 (shear strength) details similar values for G of both fibrin foam and ARTISS as would be expected from the values in the TEG analysis. These values, however, are used to correlate between this study and published literature for which the values of ARTISS and fibrin foam are consistent. Through literature searches and previous research, the shear strengths for fibrin sealants are on average 1-2 kPa.[115,121]

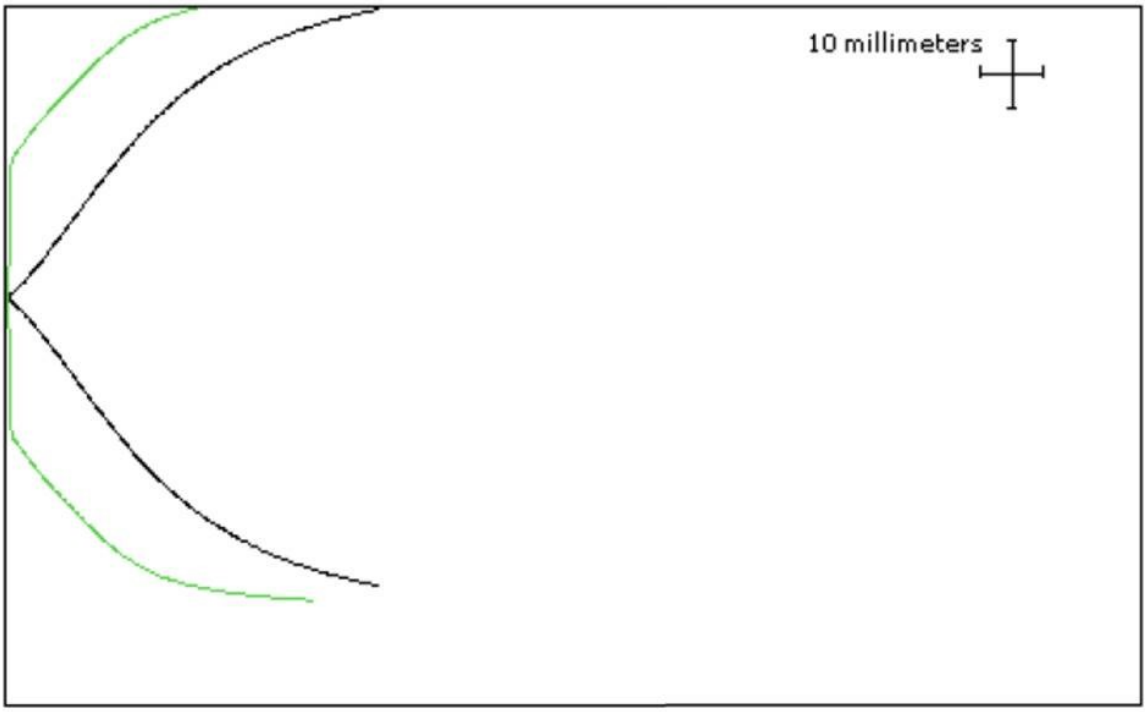

Figure 17. Thromboelastography Assessment of Fibrin Foam. Thromboelastography comparison of fibrin foam versus fibrin sealant. Fibrin foam (green) and ARTISS fibrin sealant (black) were analyzed on a thromboelastograph for 30 minutes. Associated parameter data from the plot found in Table 11.

Parameter	Fibrin Foam	ARTISS Fibrin Sealant
R (clot formation, min)	0.2 ± 0.0*	0.6 ± 0.4
K (degree of elasticity, min)	0.8 ± 0.0*	4.5 ± 1.8
Maximum amplitude (MA; clot strength, mm)	88.1 ± 1.8	85.0 ± 6.6
G (shear modulus, dynes/cm^2)	38.0 ± 6.5	35.5 ± 18.9
α-angle (clot kinetics, degrees)	86.0 ± 0.7*	49.8 ± 11.4

Table 11. Thromboelastography Parameter Measurements of Fibrin Foam. Thromboelastography results obtained for fibrin foam and commercially-available fibrin sealant. Fibrin foam showed decreased time to initial fibrin clot formation (R) and a lower degree of elasticity (K), which indicates faster clotting. Additionally, fibrin foam had larger α-angles correlating faster clot-forming kinetics. The fibrin sealant, however, had slightly greater clot (MA) and shear strengths (G) comparatively. Sample size: n = 16 for fibrin foam, n = 14 for ARTISS. *Significant difference ($p < 0.001$).

The mechanical properties of fibrin foam were also examined to show its ability to function as a proper wound therapy, including having elasticity to permit motion within tissue, ability to resist linear and shear stresses, and tensile strength to resist fragmentation.[14] Tensile strength and elastic modulus were examined using two, similar methods. First, a dog-bone-shaped mold apparatus was used to measure tensile strength and modulus. The tensile strength of fibrin foam (0.40 ± 0.07 MPa) was significantly lower than ARTISS (0.87 ± 0.27 MPa) (Fig. 18A); however, ARTISS (0.076 ± 0.01 MPa compared to fibrin foam 0.047 ± 0.01 MPa) was shown to be significantly stiffer with its higher elastic modulus ($p < 0.05$) (Fig. 18C). Similar results were noted in an ASTM wound closure experiment that utilized vis-à-vis porcine skin samples with either sealant preparation serving as a wound treatment holding the porcine skin pieces together. ARTISS, again, had a significantly greater wound closure strength ($p < 0.05$), but no observable difference was noted in wound closure elastic moduli (Fig. 18B, 18D). The tensile and wound closure strengths as well as associated moduli values are comparable

with previous research performed on fibrin sealants. The range for tensile and wound strengths is 3 kPa to 0.2 MPa and 1 kPa to 0.13 MPa for elastic moduli.[122,123] Thus, fibrin foam – even with decreased biomechanical strengths relative to ARTISS – should be considered a viable and mechanically-sound wound therapy candidate based on data from previous data on fibrin sealants.[122,123]

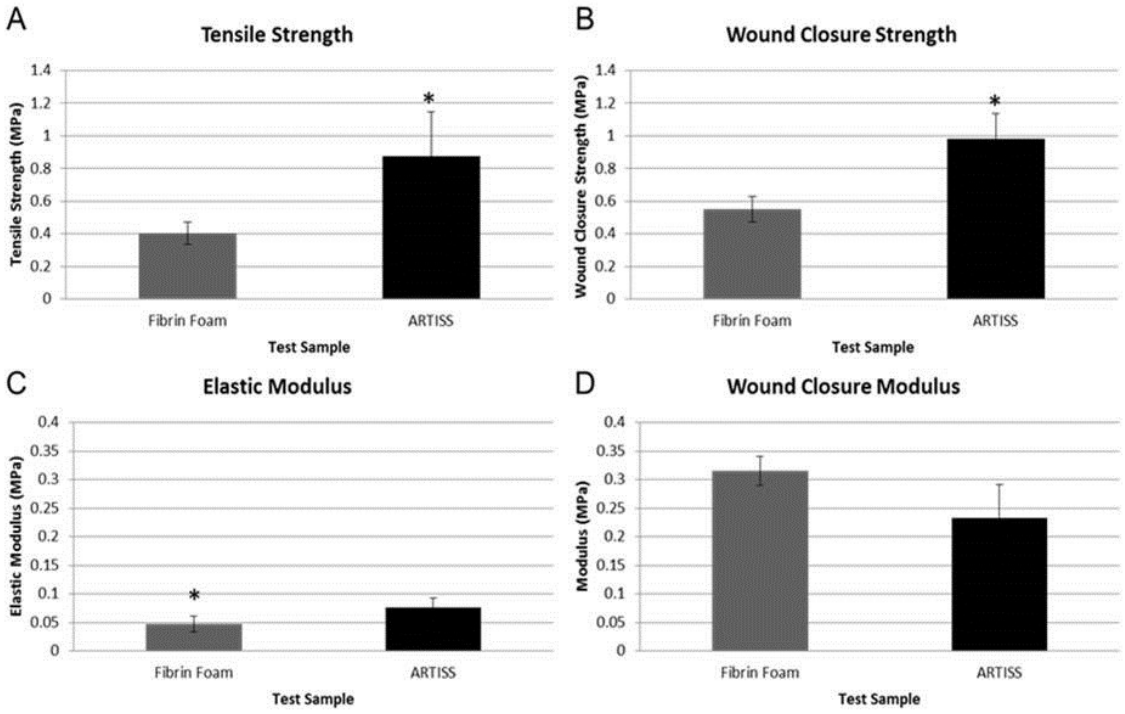

Figure 18. Biomechanical Comparison of Fibrin Foam and ARTISS Fibrin Sealant. Tensile strength and elastic modulus were obtained using a Materials Testing System for the tensile strength test. Wound closure strength and modulus were analyzed through use of ASTM F2458-05, which used porcine skin segments as scaffold to recreate a wound environment. A) Significant differences between ARTISS and fibrin foam for tensile strength (*$p < 0.05$) B) and wound closure strength (*$p < 0.05$). C) Significant increase in elasticity of fibrin foam compared to ARTISS observed for elastic modulus (*$p < 0.05$). D) No significant differences were shown for wound strength modulus. Sample sizes: tensile strength and modulus ($n = 6$ per group); wound closure strength and modulus ($n = 4$ per group).

While the biomechanical properties are important for wound therapy, I also assessed the effects of the aeration process on the structural characteristics of ARTISS

used to generate fibrin foam. In the following assessments, ARTISS (non-aerated fibrin sealant) and polyurethane foam dressing (a current wound therapy) were examined for comparison purposes. Polyurethane foam dressings (KCI, Inc.) are often used in negative-pressure wound therapy applications because of their highly porous scaffold structure (pore sizes: 400-600 μm). SEM images of each of the three test samples are displayed in Figure 19. As seen in these micrograph images, the polyurethane foam dressing sample has vastly larger pore sizes compared to that of fibrin foam and ARTISS. Fibrin foam does display its evenly dispersed range of pores in this cross-sectional sample, while ARTISS shows its tightly-bound fibrin network.

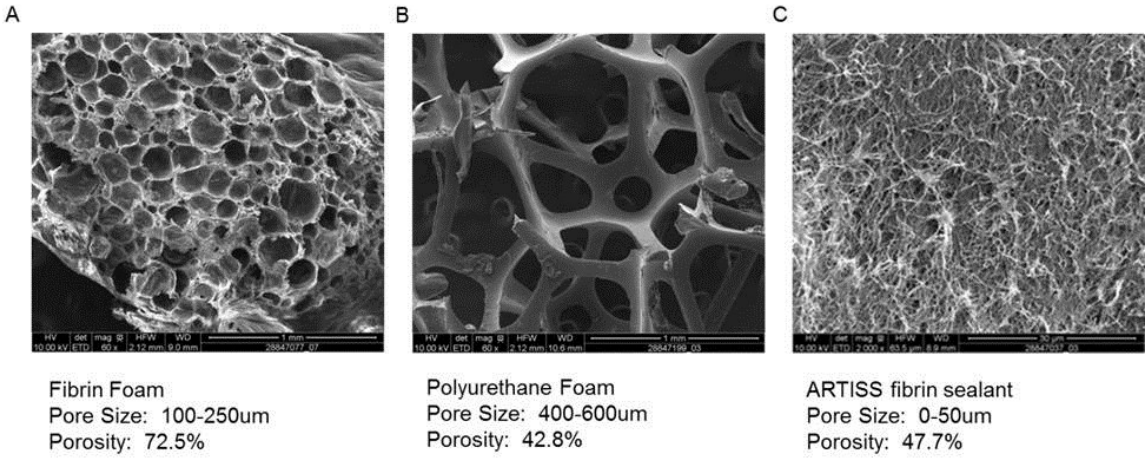

Figure 19. SEM Analysis of Wound Treatments. SEM images of each wound treatment. A) Fibrin foam. B) Polyurethane foam dressing. C) ARTISS fibrin sealant. Each treatment image is labeled with respective pore size (via SEM/FIJI ImageJ analysis) and porosity percentage. Scale bars: 1 mm (panels A, B), 30 μm (panel C).

The focus then shifted to studying the three-dimensional structure of fibrin foam. This entailed analysis of permeability, which is a crucial attribute for wound healing biomaterials. Permeability, in the instance of fibrin foam/sealant, is dependent on fibrin density and porosity. These properties were additionally studied through compaction and porosity experiments. As shown in Table 12 below, fibrin foam had a significant

increase in compaction percentage (24.7 ± 1.6% compared to 7.4 ± 1.4% of ARTISS) indicating a more porous fibrin matrix within the foam, as would be expected through the aeration process. Porosity (72.5 ± 8.3% compared to 47.7 ± 6.8%) and fluid permeability ($8.3 \times 10^{-8} \pm 2.3 \times 10^{-9}$ mm^2 compared to $6.1 \times 10^{-8} \pm 1.2 \times 10^{-8}$ mm^2) were also significantly higher ($p < 0.05$) in fibrin foam compared to the fibrin sealant. While polyurethane had significantly better fluid permeability ($K_s = 1.3 \times 10^{-7} \pm 1.0 \times 10^{-8}$ mm^2 of polyurethane compared to $8.3 \times 10^{-8} \pm 2.3 \times 10^{-9}$ mm^2 of fibrin foam, $p < 0.05$), fibrin foam was significantly more porous (72.5 ± 8.3% to 42.8 ± 5.4%, $p < 0.05$) due to the thicker fibers in the polyurethane matrix.

The results of the fluid permeation experiments displayed significant differences between ARTISS and fibrin foam, and polyurethane foam compared to both fibrin foam and ARTISS. This permeability trend among the three test samples is directly related to the increases in pore size from ARTISS (0-50 μm) to fibrin foam (100-250 μm) to polyurethane foam (400-600 μm) (Figure 19). All measured permeability constants fall within range of other tissue engineering and wound healing scaffolds (ex. range: 1×10^{-7} to 1×10^{-10} mm^2).[116,117] These combined results show fibrin foam is able to withstand the stresses and forces within a wound cavity, and fibrin foam also obtains advantageous attributes after aeration, such as increased fluid permeability and porosity, from that of commercially-available fibrin sealants and current wound therapies.

	Shear Strength (kPa)	Compaction (%)	Permeability (K, mm²)	Porosity (%)
ARTISS Fibrin Sealant	3.6 ± 1.9	7.4 ± 1.4	$6.1 \times 10^{-8} \pm 1.2 \times 10^{-8}$	47.7 ± 6.8
Fibrin Foam	3.8 ± 0.65	24.7 ± 1.6*	$8.3 \times 10^{-8} \pm 2.3 \times 10^{-9}$**	72.5 ± 8.3***
Polyurethane Foam	ND	ND	$1.28 \times 10^{-7} \pm 1.0 \times 10^{-8}$@	42.8 ± 5.4

Table 12. Structural Assessment of Fibrin Foam. Shear strength, fibrin compaction percentage, fluid permeability, and percent porosity of ARTISS fibrin sealant and fibrin foam. Shear strength indicates no significant difference between the two conditions. However, significant increases in compaction percentage (*p = 0.0009), fluid permeability (**p = 0.0034) and percent porosity (***p = 0.0012 FF vs ARTISS and polyurethane foam) were determined for fibrin foam as compared to the fibrin sealant. Additionally, polyurethane foam was demonstrated significantly higher permeability compared to both fibrin foam and ARTISS (@ $p < 0.05$). Sample sizes: n = 14-16 (shear strength), n = 8 (compactibility and permeability), and n = 6-12 (porosity). ND: not determined.

Lastly, and to determine the kinetics of *in vivo* degradation, fluorescently conjugated fibrinogen was used to label both ARTISS fibrin sealant and fibrin foam as performed by Ludwig Boltzmann Institute in collaboration with Baxter. Each preparation was subcutaneously implanted in nude mice. As seen in Figure A1, there was no difference in the overall degradation rate of fibrin foam from that of ARTISS over the fourteen-day period. However, it was positive to see the biodegradability of fibrin foam *in vivo* of up to two weeks' time, which overlaps greatly with the wound healing process. These results coincide with previously performed *in vitro* degradation studies performed on fibrin sealants (internal Baxter research), which found their fibrin sealants remain within a degradative environment for approximately 14 days.

Cellular biocompatibility analyses of fibrin foam. An important consideration with the characterization of this novel biopolymer was ensuring the preservation of cellular biocompatibility. While ARTISS fibrin sealant is a commercially-available fibrin sealant and has been marketed for years, the permutations in matrix structure within fibrin foam could cause cellular distress. As seen in the literature, pore size environment is a determining factor in cell migration and proliferation.[15] Here, to assess cellular viability, a lactate dehydrogenase (LDH) assay was used. Primary human umbilical vein endothelial cells (HUVEC), primary normal human dermal fibroblasts (NHDF), and primary normal human epidermal keratinocytes (NHEK) were cultured on ARTISS and fibrin foam clots as well as polyurethane foam dressings. Polyurethane (PU) foam, a current therapy in acute and chronic wounds, was also analyzed in these experiments as its porous matrix is attributed to its resilience in wound healing applications, such as negative-pressure wound therapy. This colorimetric assay quantitatively measures LDH released into the media from damaged cells as a biomarker for cellular viability. The extracellular LDH in culture media, in combination with diaphorase, enzymatically converts tetrazolium into a red formazan product, which was measured spectrophotometrically.

As Figure 20 illustrates, several cellular conditions were analyzed at each time point. As expected, Media Alone, Cells + Media, ARTISS + Cells, Fibrin Foam + Cells, and Polyurethane Foam Alone conditions all resulted in low average absorbance levels at 2, 24, and 48 hour time points. This correlates to minimal cell death and high level of cell viability in each condition, including fibrin foam. Conversely, the LDH positive and Cell Lysis conditions resulted in increased levels of average absorbance, as these wells

contained high concentrations of LDH in the cell media (i.e. non-viable or dead cells). ARTISS and fibrin foam were both significantly different ($p < 0.05$) from the LDH positive condition, confirming cellular viability in each condition. PU + Cells begin to show increasing levels of absorbance (i.e. increased levels of LDH in supernatant) at 24 and 48 hours (Fig. 20 middle and lower panels). Compared to Media Alone, PU + Cells (NHDF, NHEK) show significant differences ($p < 0.05$) at 24 and 48 hour time points, which may denote increases in cell death when cells are seeded on PU foam dressings.

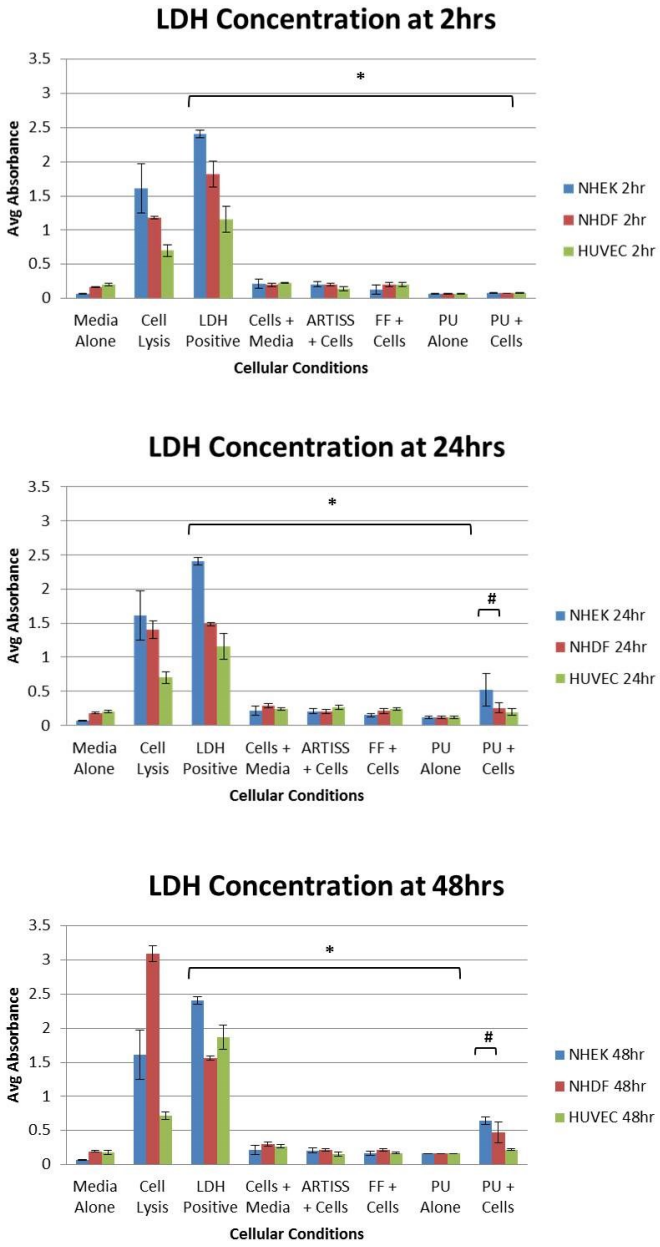

Figure 20. Lactate Dehydrogenase (LDH) Assay for Cellular Biocompatibility. HUVEC, NHDF, and NHEK cells were cultured on fibrin sealant and fibrin foam clots as well as polyurethane (PU) foam dressings for 2, 24, and 48 hour time points. ARTISS and fibrin foam (FF) were both significantly (*$p < 0.05$) different from the LDH positive condition, showing cell viability in each case. Compared to Media Alone, PU + NHEK and PU + NHDF show significant differences (#$p < 0.05$) at both 24 and 48 hour time points; this may denote cell death. Eight samples were performed for each group.

Additionally, cellular biocompatibility was determined on the basis of the metabolic state of the cells (Fig. 21). When cells are viable, they maintain a reducing

environment within the cytosol of the cell. Resazurin, the active ingredient of AlamarBlue (AB) reagent, is a non-toxic, cell permeable compound that is blue in color and non-fluorescent. Upon entering cells, resazurin is reduced to resorufin, a red-colored compound and highly fluorescent. Viable cells continuously convert resazurin to resorufin, increasing the overall fluorescence and color of the cell media.[124] Therefore, the amount of fluorescence produced is proportional to the number of viable and metabolically active cells.

Using this AlamarBlue assay, the metabolic activity of HUVEC, NHDF, and NHEK cells seeded on ARTISS, fibrin foam, or polyurethane foam was evaluated. The proliferation and metabolism of each cell type was indicated as the fold-increase of the AlamarBlue reagent at each time point (2, 24, 48, and 72 hours) using the excitation and emission filters of 570 nm and 585 nm, respectively.

In Figure 21, Media Alone, Cell Lysis, fibrin foam (FF) alone, and PU foam alone conditions all result in low fluorescence levels. This was expected as these conditions are void of viable cells. Cells Alone, FF + Cells, ARTISS + Cells, and PU Foam + Cells all begin to show a significant ($p = 0.0304$) increase in fluorescence at the 2 hour time point when compared to Media Alone. This significant difference carries across all time points leading to the conclusion of continuously proliferating and metabolizing cells present in these conditions, including fibrin foam. However, PU Foam + Cells had a significant decrease in fluorescence at 24 hours across all cell types when compared to Cells Alone ($p = 0.0304$). Cells, in this instance, may have inhibited surface adherence and migration into the polyurethane foam matrix, which would hinder their proliferation.

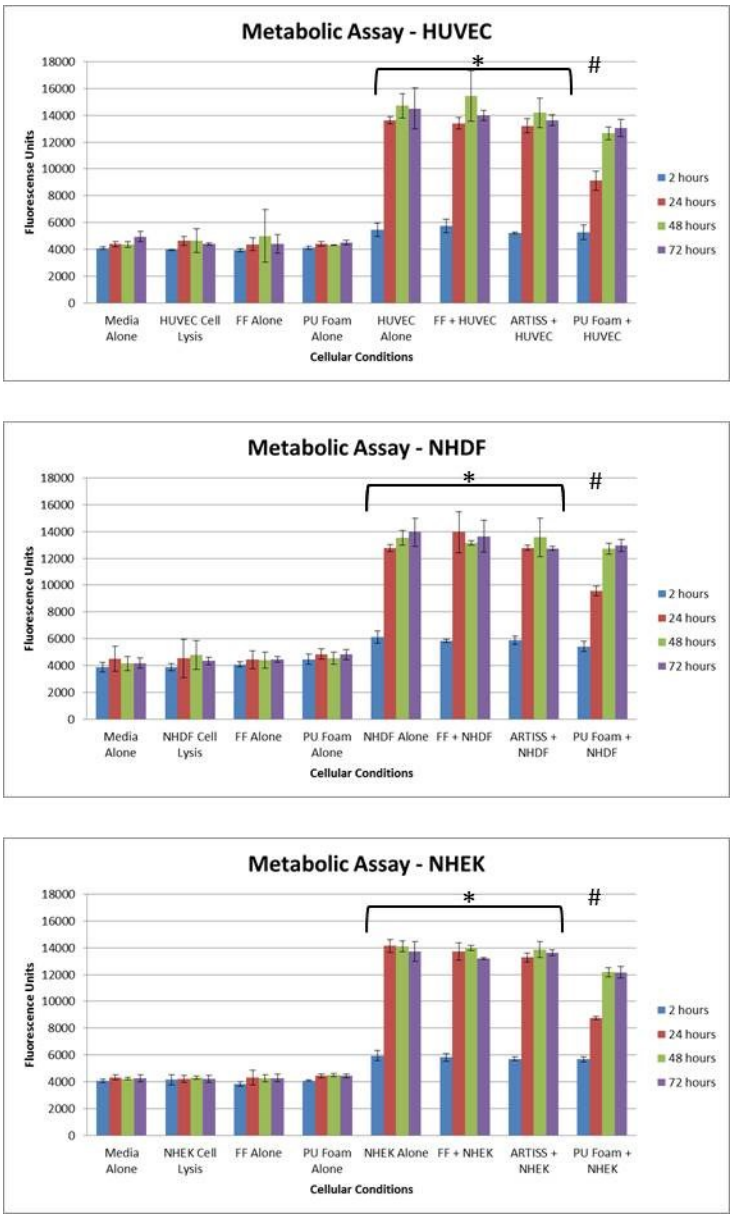

Figure 21. AlamarBlue Assay for Cellular Metabolic Activity. HUVEC, NHDF, and NHEK cells were cultured similar to panel A and Alamar Blue (AB) reagent was fluorescently analyzed at 2, 24, 48 and 72 hour time points. Media Alone, Cell Lysis, FF alone, and PU foam alone conditions all result in low fluorescence levels. Cells Alone, FF + Cells, ARTISS + Cells, and PU Foam + Cells all begin to show a significant (*p = 0.0304) increase in fluorescence at the 2 hour time point when compared to Media Alone. This significant difference carries across all time points (2, 24, 48, and 72 hours) leading to the conclusion of continuously viable and metabolizing cells present in these conditions, including fibrin foam. However, PU Foam + Cells had a noticeable decrease in fluorescence at 24 hours across all cell types. At 24 hours, PU Foam + Cells was significantly different (#p = 0.0304) when compared to Cells Alone. All samples were repeated for n = 4.

Additionally, cytoxicity of fibrin foam was assessed per ISO 10993-5.[118] The results of this experiment (Table 13) detail fibrin foam's biocompatibility once again. Taken together, these assays have shown that fibrin foam is biocompatible from both cellular viability and cellular metabolism assessments. Conversely, the current wound therapy product, polyurethane foam, displayed marked cellular death in the LDH assay, followed by a decreased rate of cellular proliferation in the AB assay after 24 hours of co-culture. This may be due to the more suitable pore size distribution of fibrin foam as compared to polyurethane foam or due to the extracellular matrix-like ligands present in the foam's structure.

Sample	Results/Score	Rating
Fibrin foam 1	0	Pass
Fibrin foam 2	0	Pass
Fibrin foam 3	0	Pass
Fibrin foam 4	0	Pass
Fibrin foam 5	0	Pass
Fibrin foam 6	0	Pass

Table 13. ISO 10993-5 Cytotoxicity Assessment of Fibrin Foam. Results from the ISO 10993-5 assessment of fibrin foam. All fibrin foam samples (n = 6) passed the cytotoxicity analysis. The positive control (n = 3) failed in all of its tests; while the negative control (n = 3) passed in all tests. Scoring and ratings are detailed in the Methods section.

Along with the quantitative analyses of cellular biocompatibility, two qualitative experiments were performed on fibrin foam. First, SEM images were taken of ARTISS fibrin sealant and fibrin foam clots that were seeded HUVEC, NHDF, and NHEK cells. These cells were cultured on the clots for 24 hours prior to imaging. As the images in Figure 22 show, endothelial, fibroblast, and keratinocyte cells spread and have morphology associated with viability on the ARTISS fibrin clots in panels A-C. When compared to the lower panels (D-F), the identical morphologies in the cell types are seen in and on the fibrin foam clots.

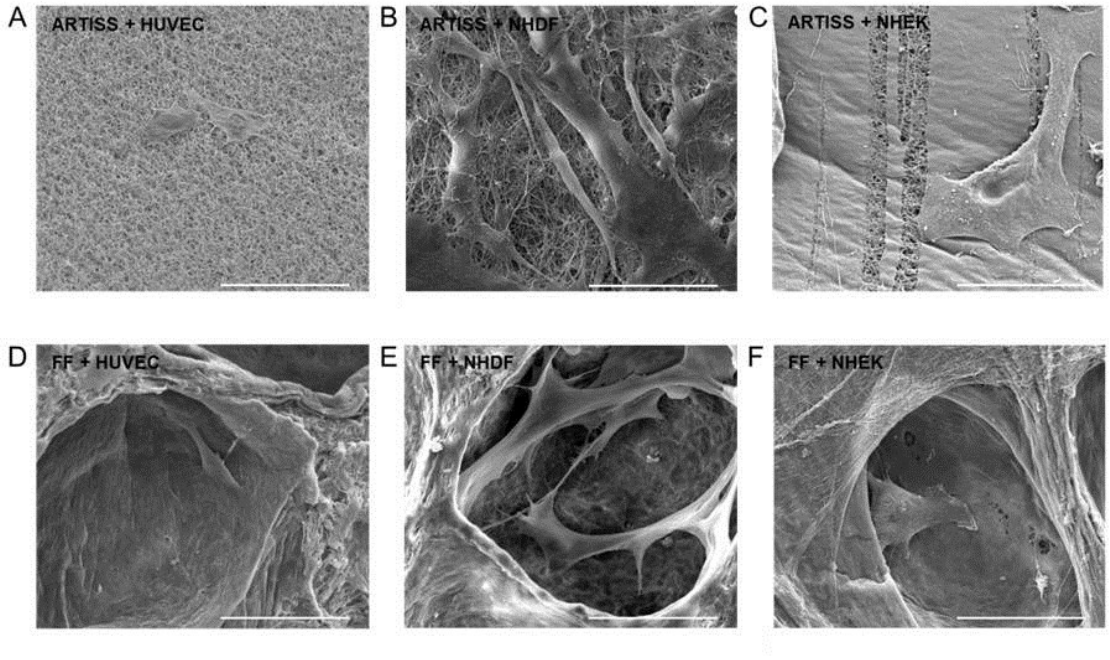

Figure 22. Cellular Interactions with Fibrin Foam. Cellular interactions with fibrin foam. Scanning electron microscopy images of ARTISS fibrin sealant (top) and fibrin foam (bottom) seeded with HUVEC (A, D), NHDF (B, E), and NHEK cells (C, F). Cells were cultured for 24 hours on the fibrin clots before fixation. Scale bars: 50 µm. FF: fibrin foam, HUVEC: human umbilical vein endothelial cells, NHDF: normal human dermal fibroblasts, NHEK: normal human epidermal keratinocytes. Images are representative of at least three separate images.

Additionally, cellular viability was assessed using confocal microscopy and live/dead cell stains. HUVEC, NHDF, and NHEK cells were seeded on fibrin foam clots and allowed to culture for 24 hours prior to imaging. After 24 hours, cells and clots were stained with live/dead stain and a wheat germ agglutinin stain (WGA, stained fibrin foam structure). Figure 23 confocal images show the vast majority of cells to be living (blue stain) within the fibrin foam matrix for each cell type used.

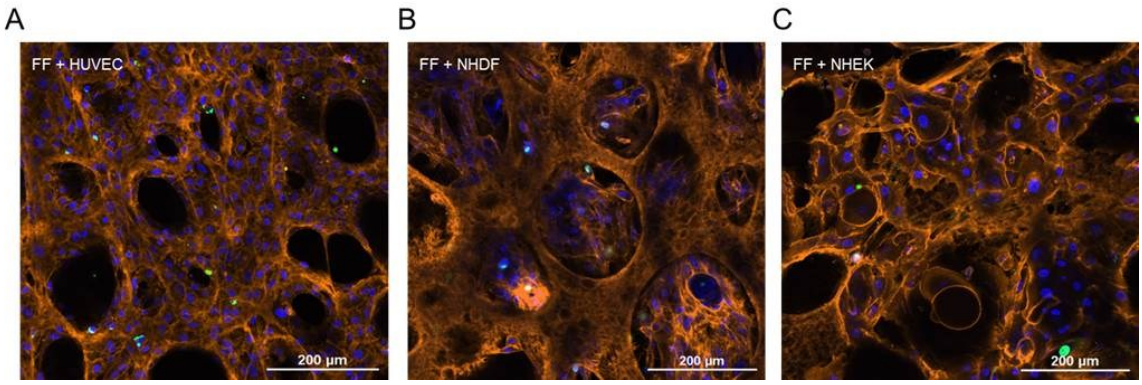

Figure 23. Cellular Viability Assessment of Fibrin Foam using Confocal Microscopy. Confocal images of fibrin foam seeded with A) endothelial cells (HUVEC), B) fibroblasts (NHDF), and C) keratinocytes (NHEK) following 24 hours of incubation at 37°C / 5% CO_2. Blue (live cell stain), green (dead cell stain), and orange (wheat germ agglutinin). FF: fibrin foam, HUVEC: human umbilical vein endothelial cells, NHDF: normal human dermal fibroblasts, NHEK: normal human epidermal keratinocytes. Scale bars: 200 µm. Images are representative of three separate experiments.

Aim 2: To evaluate the performance of fibrin foam as a novel dressing in acute wound and negative-pressure wound therapy settings.

Three-dimensional *in vitro* wound model. The structure and porosity of fibrin foam coupled with its biocompatibility and biodegradability make it a suitable candidate for wound therapy. Additionally, host cell migration into such wound scaffolds *in vivo* is crucial for such processes as angiogenesis and skin regeneration to occur. In this part of the research, a three-dimensional *in vitro* wound assay was employed to visually assess cellular migration into and onto fibrin foam.[125] For this *in vitro* assay, I utilized a three-dimensional (3D) model which mimics that of a skin wound environment. This allowed me to study the cellular migration of cells in the wound where previous 2D assays have sufficiently lacked. This 3D model was generated using a collagen matrix to mimic skin. Once the matrix was formed, HUVEC, NHDF, and NHEK cells were stained and seeded on the collagen before a wound was created in the matrix using a 2 mm biopsy punch.

The wound defect was filled with one of four treatments – collagen (control), ARTISS fibrin sealant, fibrin foam, or polyurethane foam.

At 24 and 48 hours after treatments were applied, the 3D wounds were fluorescently imaged. As seen in the top panel of Figures 24-26, the control-treated wounds had visibly poor cell migration onto their surface at both time points. The lack of fluorescent cells migrating onto the collagen-filled matrix is shown across all three cell types. Similarly, polyurethane (PU) foam-treated wounds (lower panels in figures) had marked failure of cellular adherence to its matrix or migration into the polyurethane foam dressing. From the fluorescent images of the PU foam-treated wounds, the presence of sloughed, or likely dead, cells that had settled into the bottom of foam matrix was noted – likely due to improper attachment to the synthetic polyurethane foam scaffold.

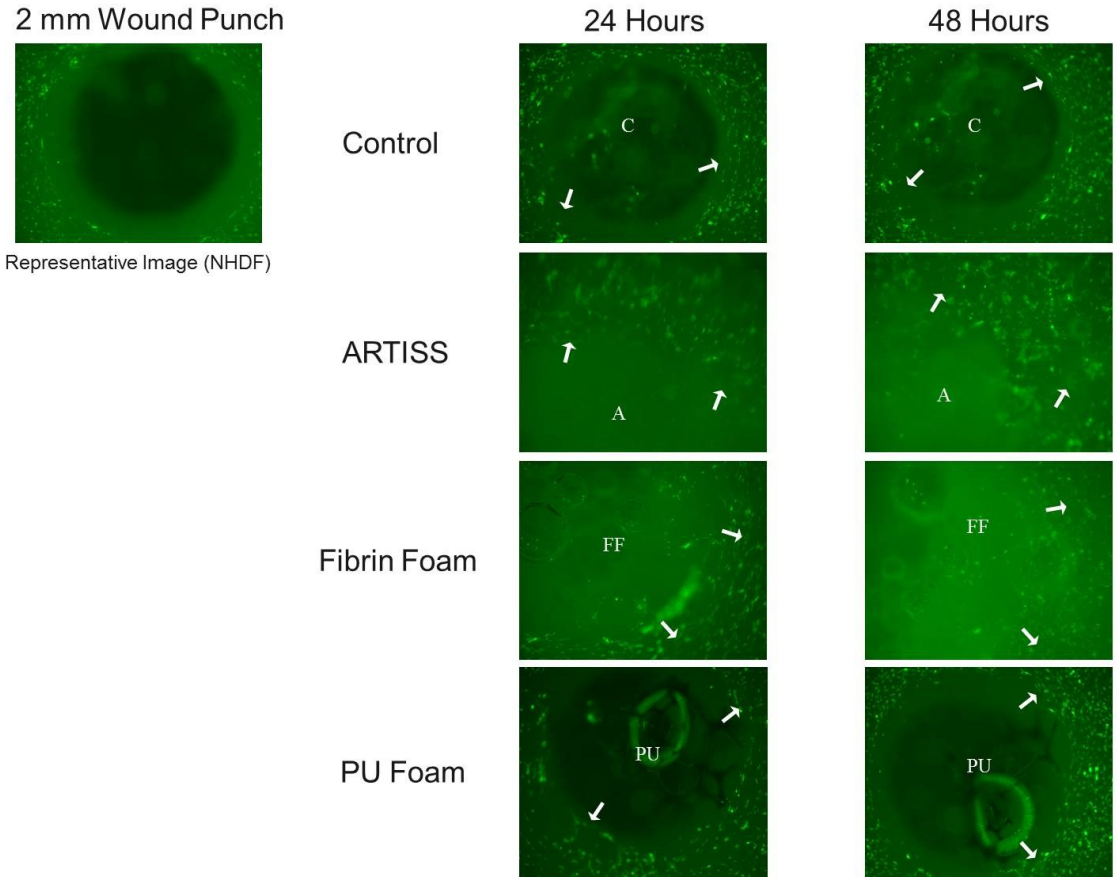

Figure 24. Three-Dimensional *In Vitro* Wound Assay (NHDF). Endothelial (HUVEC) cells, fibroblasts (NHDF) (shown), and keratinocytes (NHEK) stained with Vybrant DiO were analyzed for migration. Biopsy punch (2 mm) wounds were filled with control (PureCol EZ Gel), ARTISS fibrin sealant, fibrin foam, and polyurethane foam dressing. Migration was assessed at 24 and 48 hours into and onto wound treatments. Images are labeled with white arrows to denote location of wound periphery. A representative image of an unfilled wound is shown in the upper left corner. Location of treatments noted by abbreviations: C: Control; A: ARTISS; FF: Fibrin Foam; PU: Polyurethane foam dressing. Images were taken at 4x magnification. Images are representative of at least three separate samples.

Conversely to the control- and PU foam-treated wounds, moderate cell migration was seen at both time intervals for ARTISS fibrin sealant. When imaged, ARTISS led to a cloudy appearance in the wound cavity as is noted in its macroscopic form as well (Fig. 10). However, wound margins were still able to be marked (white arrows) for reference. Each cell type was able to adhere to the ARTISS fibrin matrix and was able to migrate

onto its surface by the 48 hour time interval. Lastly, fibrin foam-treated wounds showed and allowed for the greatest migration of cells into the foam-filled wound margin with all three cell types and at each time point. From the fluorescent images, migration of cells into and onto the fibrin foam scaffold can be seen.

Through the use of this assay, this research was able to recreate a three-dimensional collagen-based wound *in vitro* and test the efficacy and performance of several wound treatments. From a qualitative standpoint, fibrin foam-treated wounds were shown to allow for a more favorable migration environment throughout this 3D *in vitro* wound assay due to its fibrin matrix and porous structure.

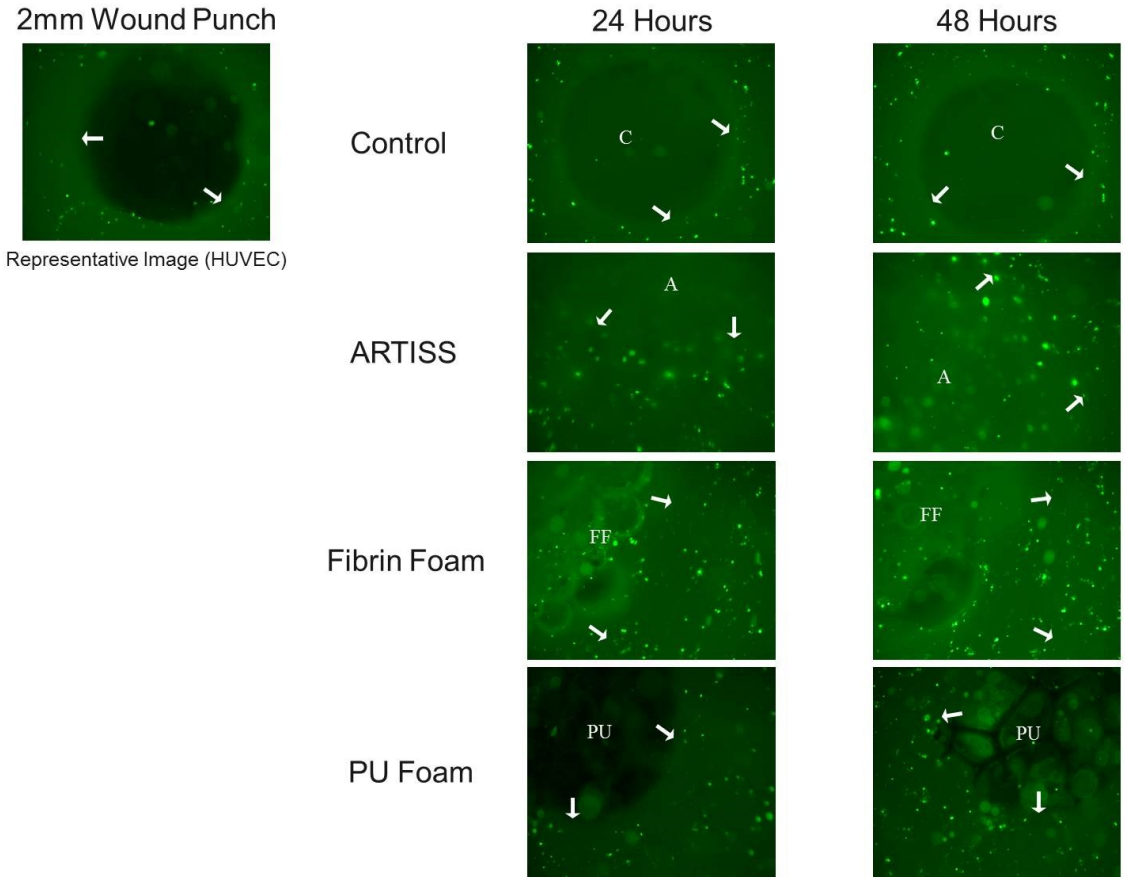

Figure 25. Three-Dimensional *In Vitro* Wound Assay (HUVEC). Three-Dimensional *In Vitro* Wound Assay. Endothelial (HUVEC) (shown) cells, fibroblasts (NHDF), and keratinocytes (NHEK) stained with Vybrant DiO were analyzed for migration from collagen matrix (PureCol EZ Gel) into 2 mm biopsy punch wound. Biopsy punch wounds were filled with control (PureCol EZ Gel), ARTISS fibrin sealant, fibrin foam, and polyurethane foam dressing. Migration was assessed at 24 and 48 hours into and onto wound treatments. Images are labeled with white arrows to denote location of wound periphery. A representative image of the unfilled wound is shown in the upper left corner. Location of treatments noted by abbreviations: C: Control; A: ARTISS; FF: Fibrin Foam; PU: Polyurethane Foam dressing. Images were taken at 4x magnification.

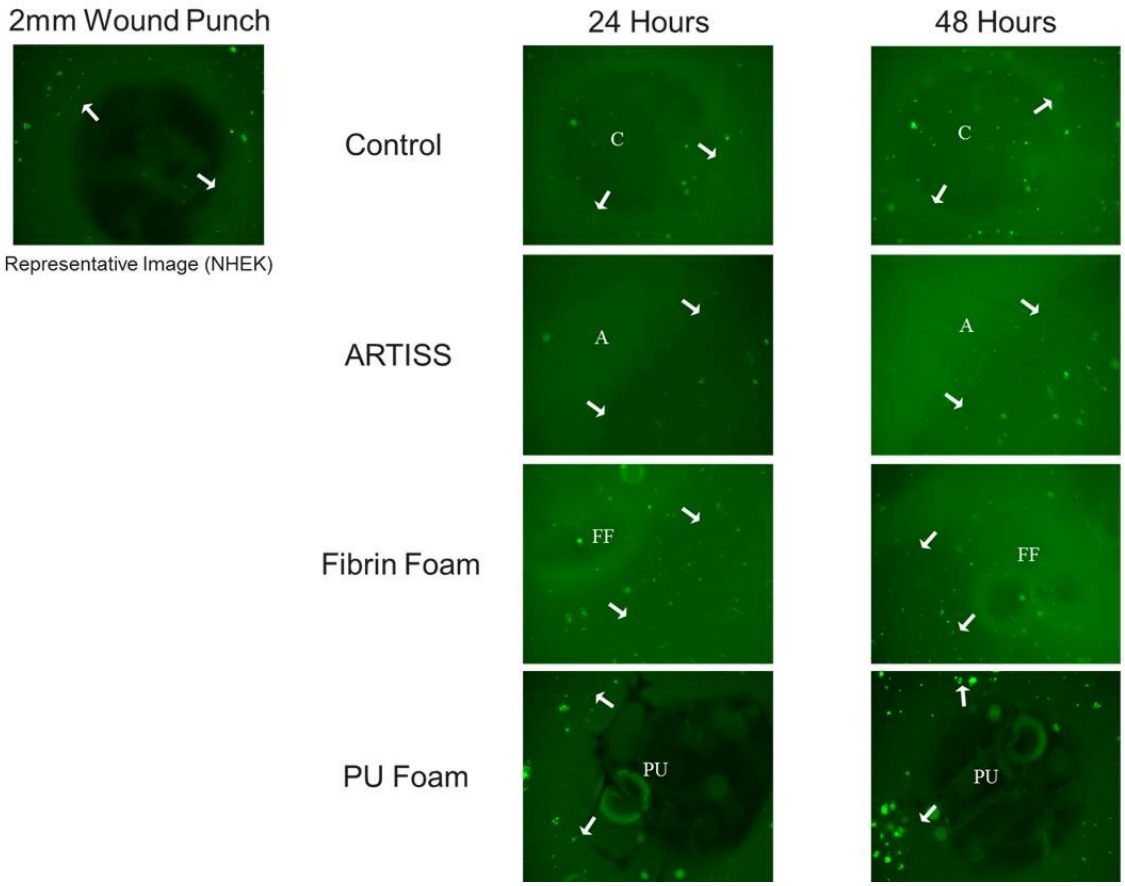

Figure 26. Three-Dimensional *In Vitro* Wound Assay (NHEK). Three-Dimensional *In Vitro* Wound Assay. Endothelial (HUVEC) cells, fibroblasts (NHDF), and keratinocytes (NHEK) (shown) stained with Vybrant DiO were analyzed for migration from collagen matrix (PureCol EZ Gel) into 2 mm biopsy punch wound. Biopsy punch wounds were filled with control (PureCol EZ Gel), ARTISS fibrin sealant, fibrin foam, and polyurethane foam dressing. Migration was assessed at 24 and 48 hours into and onto wound treatments. Images are labeled with white arrows to denote location of wound periphery. A representative image of the unfilled wound is shown in the upper left corner. Location of treatments noted by abbreviations: C: Control; A: ARTISS; FF: Fibrin Foam; PU: Polyurethane Foam dressing. Images were taken at 4x magnification.

Negative-pressure wound therapy (NPWT) feasibility using fibrin foam.

Negative-pressure wound therapy (NPWT) utilizes a vacuum system, which applies subatmospheric pressures ranging from 0 to -300 mmHg, to improve wound healing. This technique is often used in hard-to-close acute and chronic wounds because of its ability to seal the wound edges, continuously remove excess exudate from the site of

injury, and promote wound healing. NPWT involves the use of polyurethane foam or gauze dressings to cover and fill the wound site and serve as a permeable barrier. NPWT is ever-growing in popularity for patients with skin grafts, dehisced surgical wounds, and pressure ulcers as these clinical indications have increased during the 21st century.[126,127]

However, the disadvantage to treating such wounds with a polyurethane foam dressing is the need to debride the wounds every 2 to 3 days of vacuum treatment. During these few days, tissues are pulled and migrate into the non-biodegradable matrix of the polyurethane foam. This debridement step in NPWT leads to pain and irritation to the patient, re-injuring of the wound site, and an overall decrease in the wound healing rate.[128] Therefore, I wanted to test the feasibility of fibrin foam for use in a NPWT environment. Fibrin foam holds a porous matrix to allow for removal of exudate from the wound; however, fibrin foam also generates a fibrin scaffold for the migration of cells and tissues. Lastly, fibrin foam is a biodegradable and biocompatible matrix and therefore would not need to be debrided from NPWT-treated wounds.

For NPWT feasibility, full-thickness biopsy punch wounds were created in porcine skin samples. The wounds were filled with fibrin foam or ARTISS and allowed to cure over several time points. After curing, the NPWT device (KCI, Inc.) was attached, a protective plastic sheath was placed over the treated wound, and subatmospheric pressure (-200 mmHg) was applied to the wounds for 2-5 minutes. At each time point, images were taken. As Figure 25B and 25E shows, fibrin foam was able to withstand the negative pressure and remain in the wound cavity. To test the worst-case scenario (Fig. 25C, 25F), the protective sheath was removed and the direct pressure from the vacuum system was placed on top of the fibrin foam-treated wound. As seen at this

instance as well as the remaining time points, fibrin foam remained within the wounds after treated with the NPWT system. As shown in Figure 28, I also tested the feasibility of ARTISS fibrin sealant for use in NPWT. Similarly to fibrin foam, ARTISS remained in the wound cavity at 30 minute, 1 hour, and 2 hour time points.

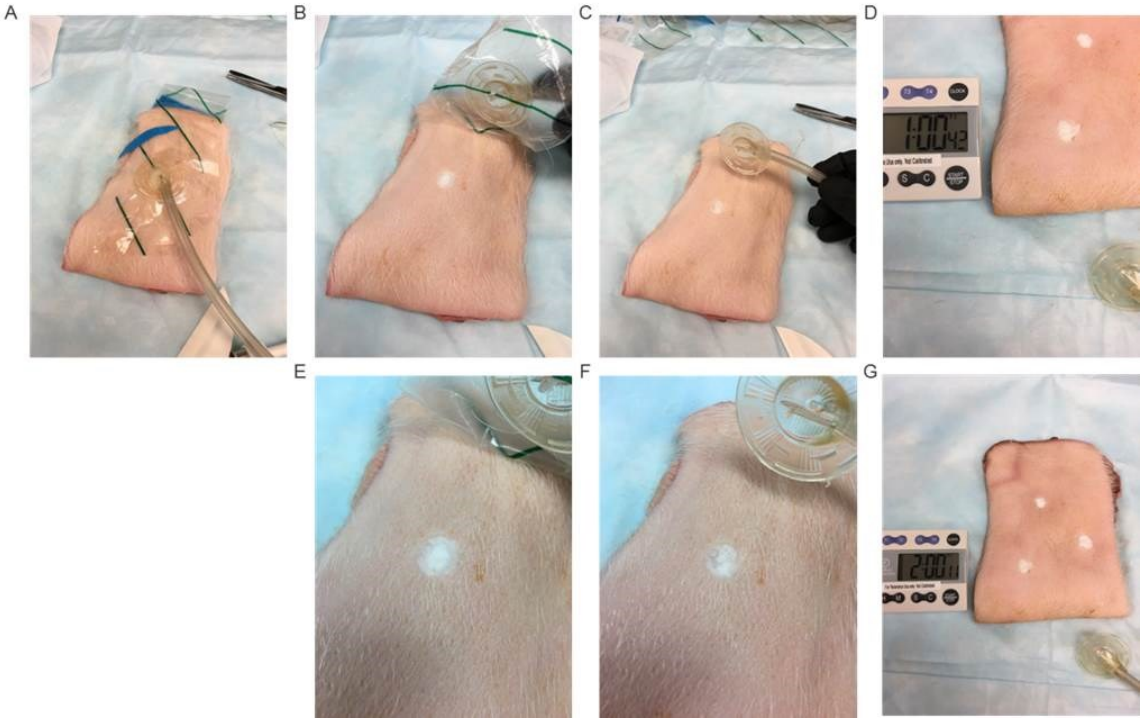

Figure 27. Negative-Pressure Wound Therapy Feasibility with Fibrin Foam. A) Negative-pressure wound therapy vacuum system apparatus attached to a 12-mm biopsy punch porcine skin wound treated with fibrin foam. B/E) Fibrin foam-treated wound after 30 minutes of set time followed by 2-5 minutes under negative pressure (-200 mmHg). C/F) Fibrin foam-treated wounds after 30 minutes of set time followed by application of vacuum directly onto wound. D/G) Fibrin foam-treated wounds after 1 hour and 2 hour set times, respectively, followed by application of vacuum treatment. In each instance, fibrin foam remained within wound cavities.

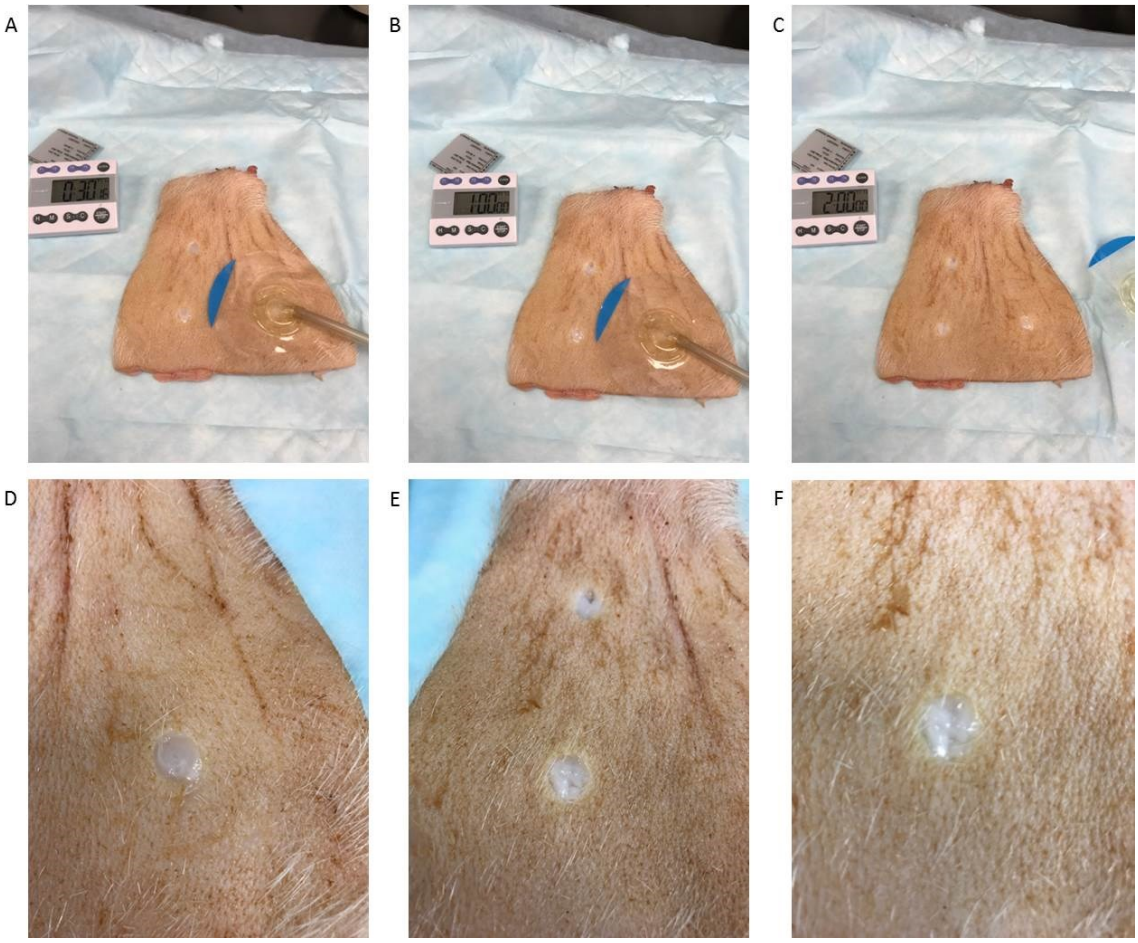

Figure 28. Negative-Pressure Wound Therapy Feasibility Testing with ARTISS. Negative-Pressure Wound Therapy Feasibility for ARTISS fibrin sealant. Images taken at 30 minutes, 1 hour, and 2 hours after ARTISS treatment of wound punch biopsies (A, B, C). At each time point, negative pressure (-200 mmHg) was applied for 2-5 minutes using negative pressure vacuum system. Wound images were taken after the application of NPWT (D, E, F). ARTISS remained in wounds at each time point after application of NPWT. Three wounds were treated at each time point.

***In vivo* murine model assessment of fibrin foam**. Since this research had characterized fibrin foam and shown the feasibility of the foam as a wound therapy *in vitro*, I wanted to evaluate its *in vivo* wound healing abilities. To accomplish this, I utilized a full-thickness murine wound biopsy punch model in collaboration with Loyola University Chicago and the W. Keith Jones Laboratory. The BKS.Cg-Dock7m +/+ Leprdb/J (db/-) mice (8-12 weeks of age) were anesthetized, and a 6 mm biopsy punch was used to make four excision wounds (1 cm apart) on the dorsal surface of the animal. Each of the four wounds was treated separately and covered using experimental materials and dressings, including ARTISS, fibrin foam (FF), polyurethane (PU) foam, and control (no treatment) (Figure 11).

To assess the wound closure of each treatment, a digital camera was used to take photographs of the wounds at days 0, 3, 7, 10, and 14. From the photographs taken, the wound area was measured. A wound was considered completely closed when the wound area was equal to zero (grossly). FIJI ImageJ imaging software was used to measure the wound area using manual technique as previously described.[119] Briefly, wound area was assessed by tracing the wound area with a fine-resolution computer mouse and calculating the pixel area within. The wound closure analysis was performed blinded and only the mouse identification number was known.

In general, the healing rate of fibrin foam-treated mice was greater than those of the other three treatments (Fig. 29). At day 7, fibrin foam-treated mice demonstrated significantly accelerated wound closure when compared to control ($p = 0.045$), ARTISS ($p = 0.007$), and PU ($p < 0.001$). Similar results were noted at day 14, when fibrin foam-treated wounds healed with wound closure significantly greater than the other treatment

groups ($p < 0.05$). This data indicates the fibrin foam wound therapy improved wound closure, which resulted in an overall better wound healing effect on the animals. Wound closure was also calculated based on percent wound closure based on day 0 wounds as 100% open. The results were identical as fibrin foam still showed significant ability to close the murine wounds compared to all other treatments (Fig. A2). Fibrin foam-treated wounds also yielded the most fully-closed wounds as detailed by the Loyola surgical staff at day 14. Fibrin foam had 5 fully-closed wounds (of 12 total mice) compared to 2 of control, 1 of ARTISS, and 0 of polyurethane foam (data not statistically significant).

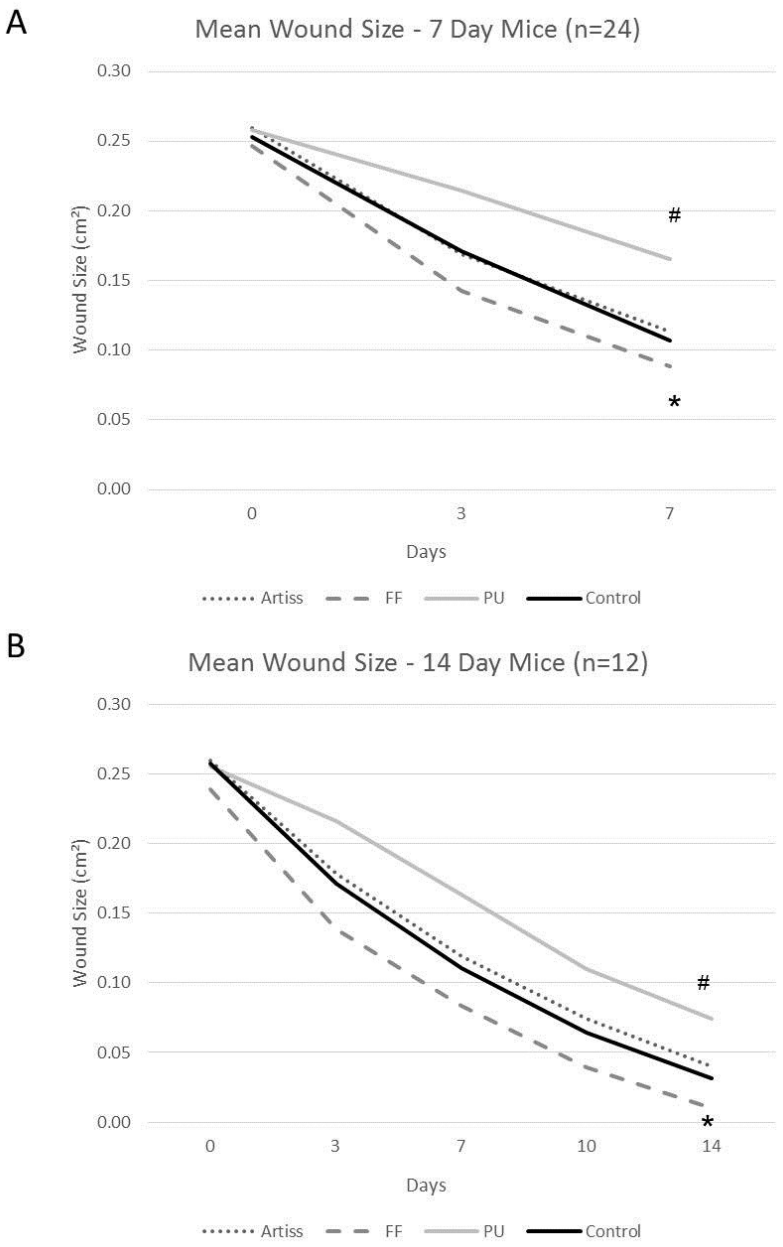

Figure 29. Fibrin Foam Performance in Murine Wound Model. A) Initial wound sizes (cm^2) were equivalent for the four treatments but significantly different subsequent days ($p < 0.001$ for days 3-14). By day seven, wounds treated with fibrin foam (FF) were smallest compared to all other treatments ($*p < 0.05$). Wounds were significantly larger for polyurethane foam (PU) compared to the other treatments ($\#p < 0.001$). C) At day 14, initial wound sizes were similar for all treatments. Similar to day 7, wounds were significantly larger for PU compared to all other treatments ($\#p < 0.001$) at day fourteen. Wounds treated with fibrin foam were significantly smaller compared to the other treatments ($*p < 0.05$). Twenty-four mice were analyzed for panel A and twelve mice were analyzed in panel B.

To obtain a further understanding into the tissue regeneration in the biopsy punch wound site, hematoxylin & eosin (H&E) and Masson's Trichrome staining were performed at Loyola to assess the cellular change of the skin throughout the wound model. At days 7 and 14, wounds were assessed on several histological parameters. The main histological parameters for wound healing were: reepithelialization, neovascular proliferation, acute and chronic inflammation, and collagen deposition. These parameters were scored on a 0-3 scale as shown in Table 8.[120] Additionally, epithelial maturation, granular tissue formation, and granular tissue maturation were assessed on a yes-or-no basis. The degree of granular tissue formation/maturation was determined by the structure and alignment of fibroblasts in the wound area.

Representative histological images of wounds from days 7 and 14 are shown in Figure 30. As the H&E staining details, fibrin foam-treated wounds had already begun the processes of reepithelialization and granular tissue formation by day 7 (Fig. 30C), and these wounds exhibited almost complete wound closure by day 14 (Fig. 30G). This was comparable to ARTISS and control based on histological samples. However, the polyurethane foam-treated wounds showed lack of epithelialization as clearly noted in Figure 30D and 30H. The polyurethane foam matrix is wedged within the wound cavity, and upon debridement, leads to re-injuring of the wound site.

Collagen deposition was also assessed using Masson's Trichrome stain. Figure 31 shows representative images of day 14 wounds from each treatment group. Control (31A) and fibrin foam (31C) treated wounds showed an abundant level of collagen deposition. This is in contrast to the polyurethane foam-treated wound (31D) which showed scant deposition of collagen by day 14 as these wounds failed to properly heal.

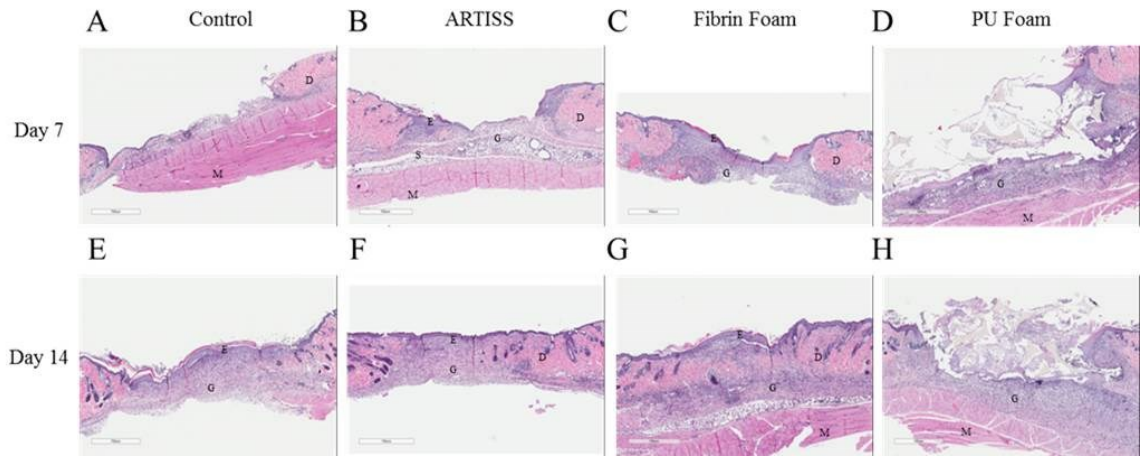

Figure 30. Histological Assessment of Murine Acute Wounds. Images of wound specimens from each wound treatment group at day 7 (top panel) and day 14 (bottom panel) using H&E stain. Sections were prepared and stained as per methods. A/E) Section from a wound from Control treatment group; B/F) Section from a wound from ARTISS treatment group; C/G) Section from a wound from Fibrin Foam treatment group; D/H) Section from a wound from Polyurethane Foam dressing treatment group. The scoring for the wound healing parameters for these samples with respect to reepithelialization, neovascular proliferation, and acute and chronic inflammation were, respectively: A) 0, 1, 0, 2 B) 2, 1, 1, 1 C) 2, 3, 1, 2 D) 1, 1, 3, 2 E) 3, 2, 1, 1 F) 3, 1, 1, 1 G) 3, 3, 1, 1 H) 0, 1, 3, 2. E: epithelium; D: dermis; G: granulation tissue; S: subcutaneous tissue; M: muscle. Scale bars: 700um.

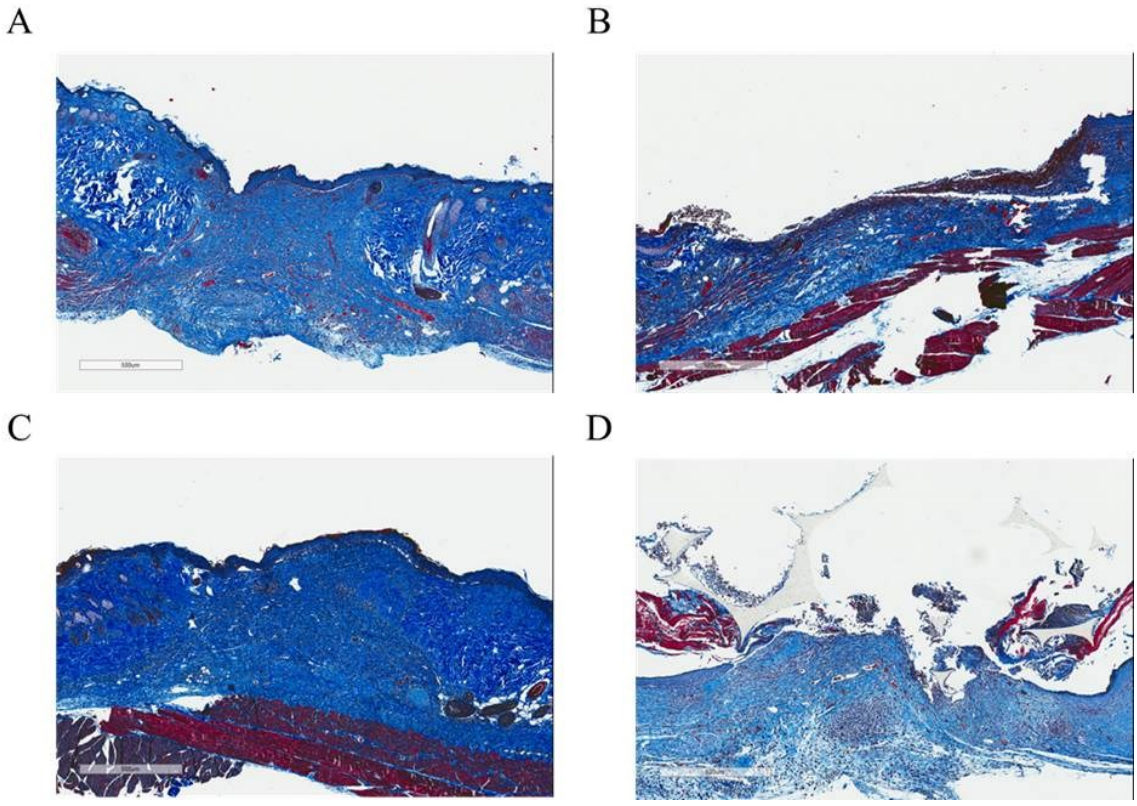

Figure 31. Collagen Deposition Analysis of Wound Samples. Images of day 14 wound specimens from each treatment group using Masson's Trichrome stain for collagen deposition. A) Section from control group wound B) Section from ARTISS group wound C) Section from fibrin foam group wound and D) Section from polyurethane foam group wound. The scoring of collagen deposition was, respectively: A) 3 B) 2 C) 3 D) 1. Scale bars: 500 μm.

The histological slides from Figures 30 and 31 were blindly assessed by a Loyola pathologist on the aforementioned parameters. The raw data of these results are found in Table A2 and A3, while the graphical data is shown below in Figures 32 and 33. Figure 32 details a comparison of the parameters – reepithelization, neovascular proliferation, acute and chronic inflammation, and collagen deposition – at days 7 and 14. While none of the comparisons were found to be significant, the data is useful for determining the cellular and wound-healing responses to the fibrin foam matrix and the other treatments.

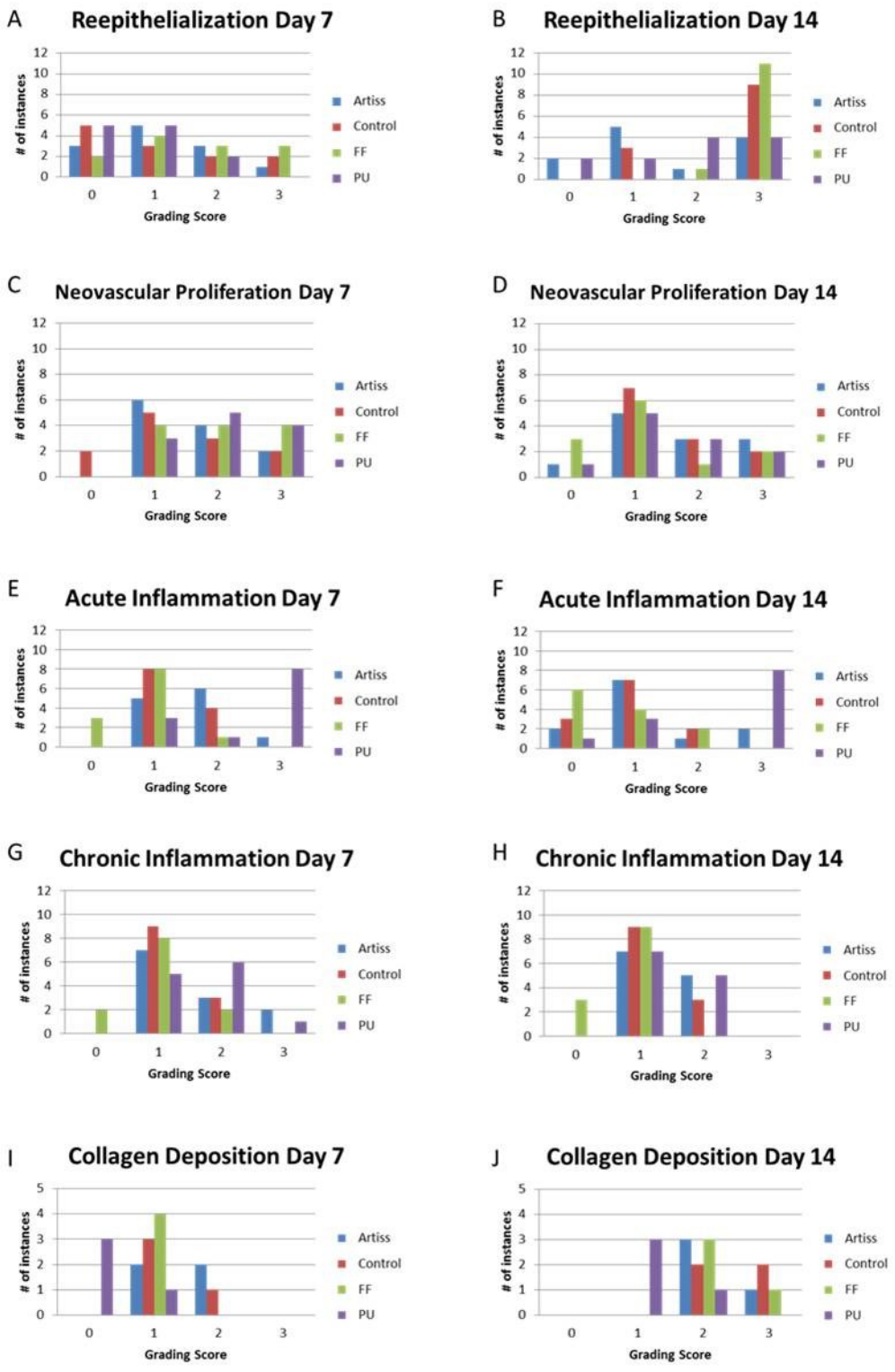

Figure 32. Histological Comparisons of Wounds at Days 7 and 14. Histological analyses at days 7 (A, C, E, G, I) and 14 (B, D, F, H, J) from Tables A2 and A3. n = 12 for all groups, except collagen deposition (n = 6).

From Figure 32, the parameters and scoring for the wounds treated by fibrin foam were further assessed. The green bars, representing fibrin foam-treated wounds, show a sharp increase in reepithelization from day 7 to day 14 (Fig. 32A, 32B). Additionally, these wounds have revascularization occurring at both time points, which is a hallmark of proper wound healing. Similarly, collagen deposition increased in fibrin foam wounds over the two week period. While inflammation is necessary in proper wound healing, an abundance or prolonged periods of inflammation can lead to improper or chronic wound healing. As shown in Figure 32E-H, fibrin foam wounds have scores of 0-1 for acute and chronic inflammation over the study. There were no signs of prolonged inflammation in the fibrin foam-treated wounds.

ARTISS and control treated wounds also showed similar results to fibrin foam in the five categories of Figure 32. Polyurethane foam, however, had distinct lack of proper wound healing parameters, including sustained inflammation and lack of collagen deposition over the two weeks.

Lastly, granular tissue formation and maturation as well as epithelial maturation were assessed. Figure 33 representatively details the results of that analysis. While no significance was observed, trends of increases in granular tissue maturation and epithelial maturation were noted for the fibrin foam-treated wounds over the 14-day study. Again, this signifies proper wound healing processes occurring within the wounds treated with fibrin foam.

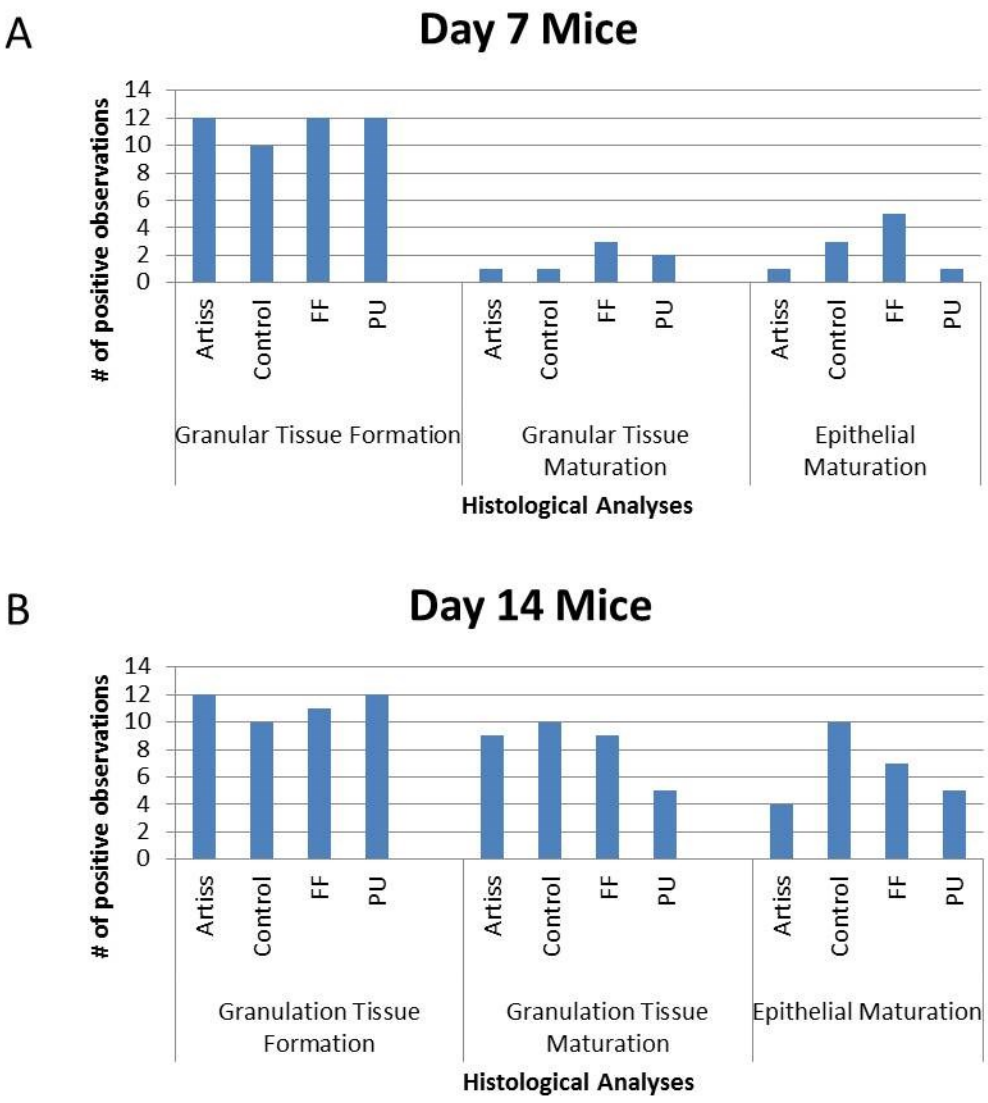

Figure 33. Quantification of Histological Data from Murine Model. Positive observations (YES/NO outcomes) for the histological and pathological parameters of epithelial maturation, granular tissue formation, and granular tissue maturation at days 7 and 14 from Tables A2 and A3 (n = 12 per group).

As shown, the polyurethane foam-dressed wounds produced the worst histological response as noted by the lack of reepithelialization and other features (Fig. 30). This result goes in line with the wound closure data (Fig. 29), which showed PU-treated wounds had the significantly poorest wound closure when compared to any other treatment ($p < 0.001$). This was due to the debridement of the wounds on dressing-change days – a typical clinical disadvantage to use of non-biodegradable dressings. I chose to analyze the debrided polyurethane foam on dressing-change days. In Figure 34, H&E staining of debrided polyurethane foam dressings was performed. The debrided dressings contained skin and tissue on the periphery as well as intercalated within the polyurethane foam matrix at both days 7 and 14. This confirmed previous observations in literature as to one of the key disadvantages of polyurethane foam dressing use in clinical situations – debridement.

From the combined *in vivo* analyses, the fibrin foam-treated wounds exhibited vastly improved wound healing and were able to provide an environment suitable for wound healing processes, such as reepithelialization and granulation tissue formation and maturation.

A

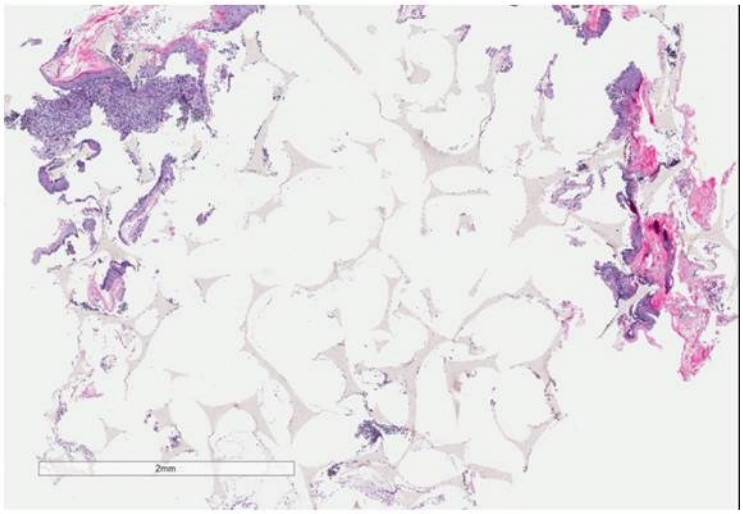

B

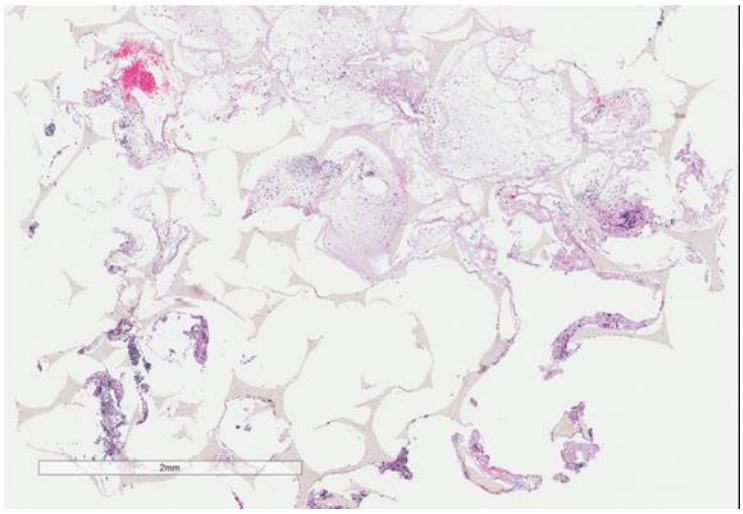

Figure 34. Histological Assessment of Debrided Polyurethane Foam Dressings. Images of A) day 7 and b) day 14 debrided polyurethane foam dressings from the polyurethane foam treatment group using H&E stain. Images show tissue embedded into the polyurethane foam matrix, which was debrided from each wound. Scale bars: 2 mm.

CHAPTER FIVE

DISCUSSION

Wound care is an impactful clinical and economical issue. In the United States alone, patients suffer from over 38 million acute and 6.5 chronic wounds each year.[8] Due to this ever-growing clinical problem, wound care has evolved significantly from gauze and sutures to regenerative dermal substitutes and implanted stem cells. Wound healing is a complex process that involves a vast array of cells, growth factors, and cellular matrices.[7,9] To treat the multifaceted wound healing process, tissue engineering researchers have devoted their efforts to finding an efficient and enhanced wound therapy. However, an optimal wound therapy still escapes the scientific and medical communities. Current research in the fields of tissue engineering and wound therapy are vying for the ideal therapy. This therapy must include the following features: biocompatible with tissues, biodegradable, mechanically suitable for wound cavity and movement, and permeable to cell and fluid transfer, among others. Certain scaffolds, such as collagen, polyesters, and fibrin have been studied in great detail.[10] Fibrin sealants, for instance, have been investigated as a wound healing matrix due to their functioning as a critical treatment methodology in hemostasis, inflammation, angiogenesis, and cellular interactions – all hallmarks of proper wound healing.[16]

In the present study, I describe a novel biopolymer – fibrin foam – that is generated through a patented aeration mixing process using a commercially-available

fibrin sealant.[24-27] Fibrin foam is created by manually passing fibrinogen and thrombin components through a porous, sintered mixing disc (Fig. 9A). Its foam-like consistency and porous structure are formed through the addition of air prior to mixing. Fibrin foam was characterized on several levels, including preparation and formulation, biocompatibility, and biomechanical strength. I also showed its use as a superior therapy in a murine wound model.

Initial tests on fibrin foam assessed the preparation and formulation to devise an optimal foam. I experimented with the number of manual passes to generate fibrin foam as well as the thrombin concentration and other additives. The requirements for the foam were that it must be easily handled during preparation, have a foam-like consistency, and have a pore size distribution < 200 μm. The manual mixing tests revealed a 4 IU thrombin fibrin foam generated from 6 passes through the Mix-F device to be the optimal foam (Fig. 13, Table 10). This foam met the requirements and would allow for ease of preparation by medical professionals in a wound therapy situation.

The biomechanical and structural properties of a biomaterial are crucial for use in wound care. Many studies have detailed the performance characteristics of effective wound therapies, including substantial tensile strength to remain in a wound cavity, but also the elasticity to move with the tissue throughout the healing process. I thereby assessed the tensile and wound closure strengths of fibrin foam. A decrease in strength was noted when compared to the fibrin sealant (Fig. 18A, 18C). This was hypothesized, however, as the aeration process leads to a more open matrix, which could cause this weakening effect on its structure. The elasticity of fibrin foam was significantly superior to that of the sealant (Fig. 18B).

Along with strength and elasticity, an optimal wound therapy must also have sufficient permeability and a porous structure to allow for both fluid and cellular movement. Shown in Table 12, structural analyses were performed on fibrin foam and ARTISS. Fibrin foam's compaction was significantly higher than that of ARTISS, which correlates to its aerated and porous state compared to the denser fibrin network of ARTISS. Fibrin foam also had increased porosity and permeability, as I would expect given its structure. These qualities are vast improvements from that of commercially-available fibrin sealants and are advantageous to promoting an enhanced wound healing response. Lastly, to examine the biodegradability of fibrin foam, an *in vivo* murine model was used to assess the degradation of fibrin foam over a two-week span. Similar degradation of fibrin foam was noted when compared to fibrin sealant; the porous structure of fibrin foam did not cause any increase (or decrease) in biodegradability, which gives confidence to the use of fibrin foam as an *in vivo* therapy (Fig. A1).

Next, I tested the *in vitro* biocompatibility of fibrin foam. Biocompatibility of the foam was expected, as its material composition is identical to the commercialized fibrin sealant, ARTISS, with demonstrated biocompatibility. However, the effects of aeration had not been previously studied. Thus, fibrin foam was confirmed as highly biocompatible through the use of SEM and confocal microscopy (Figs. 22, 23) as well as the cellular viability assays (Figs. 20, 21).

After characterizing the optimal preparation of fibrin foam, it was assessed in an *in vitro* wound assay using 3D collagen matrices. Fibrin foam qualitatively showed the greatest migration of cells into and onto its matrix. ARTISS also promoted migration of cells onto its surface; however, the more porous foam allowed for greater cellular

penetration into the wound space as compared to ARTISS (Figs. 24-26). Moving from these promising results from the characterization, I studied the use of fibrin foam as a novel wound therapy in an acute murine wound model. BKS.Cg-Dock7m +/+ Leprdb/J (db/-) mice were used due to their genetic background. These mice have the same genetic background as diabetic mice (db/db); however db/- mice do not exhibit the diabetic phenotype. The db/- mice were used as a gateway to study diabetic and impaired wound healing models in future animal work.

As seen from the murine model, at days 7 and 14, fibrin foam promoted significantly increased wound closure when compared to control and other wound treatments (Fig. 29). This superior ability of fibrin foam can be attributed to several factors. First, the fibrin-based foam is an optimal matrix for a wound site. Fibrin has been studied greatly for its interactions with extracellular matrices, keratinocytes, fibroblasts, and other major cellular components of the wound healing process.[16] These interactions are both integrin and non-integrin (e.g. VE-Cadherin, P-selectin, and I-CAM-1) receptor driven. Fibrin foam also possesses a pore size distribution that is applicable to the migration of these same wound healing cells and infiltration of cellular factors. Lastly, the inherent hemostatic ability of fibrin foam lends itself to actively supporting the pathways of hemostasis and the coagulation cascade – the first phase of wound healing.

The same trend and significance in wound closure was seen when wound closure was computed based on a percentage of day zero wound size (Fig. A2). Immunohistochemistry was analyzed to assess the host's reaction to the different wound treatments. The histological analysis showed an efficacious response to fibrin foam

(Figs. 30-33). While no significance was noted from analyzing the histological parameter scores of each treatment group, reepithelialization, granular tissue formation/maturation, and collagen deposition were all abundant in the fibrin foam-treated wounds.

Along with the in-depth comparisons of fibrin foam to its parent fibrin sealant, I also assessed the differences between fibrin foam and a current acute and chronic wound treatment, polyurethane foam. Polyurethane foam dressings are often used in these instances for their ability to provide a porous matrix (400-600 μm pores), which allows for high fluid and cellular transfer in a wound healing situation. A clinical drawback to these dressings is that they are non-biodegradable structures that must be debrided from wound sites at periodic time intervals.[126,127] In each of the characterization experiments as well as the *in vitro* and *in vivo* models, fibrin foam had significantly different attributes when compared to polyurethane foam, including its increased porosity, ideal pore size distribution, and better biocompatibility. This led to the testing of the feasibility of fibrin foam for use in negative-pressure wound therapy (NPWT). NPWT is a current vacuum-based wound therapy that utilizes polyurethane foam dressing or gauze as a wound healing treatment. The results, shown in Figure 27, detailed the ability of fibrin foam to remain within a wound cavity after application of subatmospheric pressure system. Fibrin foam was able to remain in the wounds over several time intervals as well.

The overall effectiveness of fibrin foam compared to the commercially-available fibrin sealant and polyurethane foam is, I believe, dependent on the hybridization of a fibrin-based scaffold and a structural matrix of pores suitable to sustain a wound healing environment. The fibrin portion of the foam allows it to facilitate the critical aspects of the wound healing process, such as cellular interactions and functioning in hemostasis

and angiogenesis. Additionally, the aeration process through the patented Mix-F mixing device allows for the generation of a porous scaffold with pore size distribution (100-250 μm), porosity, and permeability that is able to support cellular proliferation and migration that is not seen in either commercially-available fibrin sealants (0-50 μm) or polyurethane foam dressings (400-600 μm) (Fig. 35).

Taken together, this presented research has characterized a novel fibrin preparation. The optimal fibrin foam preparation has proven to meet and exceed the requirements needed for an effective wound therapy in today's clinical atmosphere. The fibrin-based biopolymer is: prepared with ease, biocompatible with cells and tissue, biodegradable *in vivo*, possesses mechanical strength and elasticity for wound closure, allows for fluid and cell infiltration, and reduces healing time – all hallmarks of an optimal wound therapy. These combined qualities were ever-apparent in the murine wound model, where fibrin foam was significantly superior to all other treatments and resulted in positive wound healing in all mice.

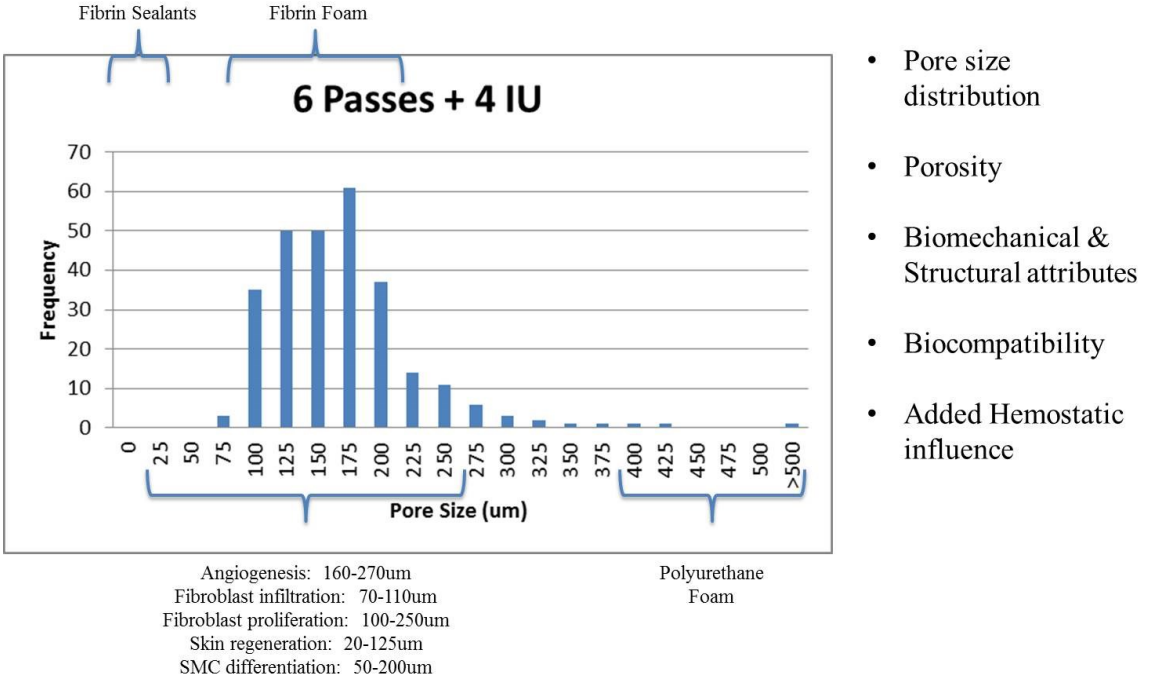

Figure 35. Fibrin Foam Functioning in Wound Healing. Fibrin foam (6 passes + 4 IU) preparation contains a pore size range from approximately 100-250 µm as compared to fibrin sealant (0-50 µm) and polyurethane foam dressings (400-600 µm). Due to this pore size spectrum within then fibrin foam matrix, key cellular processes could find fibrin foam a suitable environment. Additionally, fibrin foam contains specific wound-healing attributes and added hemostatic influence (derived from fibrin sealant components) that generates a suitable wound therapy. SMC: smooth muscle cell.

Future Directions.

The results from this dissertation research present several possibilities for further investigations. First, additional experiments can be done to delve deeper into the vast potential of fibrin foam and its preparation and formulation. Within this study, I was restricted to the Mix-F and Vyon-F devices to generate fibrin foam (Fig. 9). This mixing apparatus allowed for only a finite number of manual passes to be performed, while also limiting the constituents that could be passed through the porous Vyon-F. As mentioned, the addition of HSA and Tween 80 as well as increased thrombin concentrations were, in some instances, prevented by the mixing apparatus due to clogging.

Permutations to the Vyon-F porous disc (i.e. increasing its porous structure) could allow for mixing and aeration of more viscous preparations of fibrin foam. The addition of HSA, Tween 80, or other surfactants may allow for a far greater foaming process to occur during the mixing process. In preliminary work on fibrin foam, I assessed the total foamed volume as compared to the volume of constituents used to generate the foam. In these experiments, there was no noted increase in foam growth or expansion (data not shown). An expanding foam, however, even one with faster clotting abilities, would be a highly attractive medical therapy. Traumas that occur in combat, for instance, could use a foaming hemostat and wound healing agent for severe bleeds and amputations.

It must be noted that ultimately the foam presented in this research becomes a rigid structure due to the fibrin clot formation immediately following the mixing process and application. While drainage and coarsening occur within the foam, the fibrin structure holds strong until, and with *in vivo* situations, the fibrin is ultimately degraded by proteolysis and fibrinolysis. Thus, fibrin foam forms a quasi-foam – aeration and the presence of liquid/surfactant allows for the foam generation; however, after the initial mixing process (lasting only seconds), the fibrin fibers begin to clot yielding the set, foamed fibrin matrix.

While generating a larger foamed matrix or one that sets faster, could be beneficial to cover more wound space *in vivo* or stop a larger bleed, respectively, fibrin foam may also take on additional constituents to be used in a multitude of clinical applications. Fibrin sealants have been supplemented with living cells, growth factors, cytokines, and pharmaceutical drugs.[16,87,89,90] Future studies spiking fibrin foam with such growth factors, as platelet-derived growth factor (PDGF) or fibroblast growth factor

(FGF) could allow for improved wound healing over what has already been seen within this research. These factors would allow for the recruitment and activation of cells to promote a wound healing response at the site of fibrin foam application. Vascular endothelial growth factor (VEGF) is another potential candidate to supplement into fibrin foam. With VEGF, fibrin foam could have added abilities to promote increased neovascularization within a wound as well. Supplementation of wound-specific cell types, such as keratinocytes and fibroblasts, is another possibility for use of the foam.

Outside of the realm of wound healing, fibrin foam could be subjected to the addition of bone morphogenic protein (BMP) or human mesenchymal stem cells to aid in the regrowth of cartilage and bone and differentiation into osteoblasts, respectively. A final example could be the addition of antibiotics or other pharmaceutical drugs to fibrin foam. Antibiotics could be used to prevent bacterial infection in any number of surgical situations, while drugs, such as analgesics or anti-cancer medications could be added into fibrin foam for improved treatment of patients. The options for further additives are plentiful.

While the animal model showed significant results in favor of fibrin foam, there are some additional experiments that need to be performed to properly assess fibrin foam's efficacy *in vivo*. Mice are a highly-used species for animal models and translational research due to their ability to produce reproducible data, generate large sample sizes, and can be manipulated genetically with ease. Mice also share over 95% of genes with the human species. However, and in wound healing, mice heal through a contractile process as opposed to reepithelization (humans).[129] In the animal model, I was not as concerned with this caveat, as one of the key portions of this research was to

study the ingress of cells and tissues into the fibrin foam matrix and other treatments. Additionally and to adjust for possible error, treatments were blindly and evenly rotated on the dorsal surfaces of each mouse within the study. Future studies could also use a splinted-wound murine model whereby the epidermis is held back via splints to prevent the contractile healing response.[119] Instead, these mice are forced to heal by reepithelialization, which would better mimic the wound healing processes of humans. The shown animal model also utilized the BKS.Cg-Dock7m +/+ Leprdb/J (db/-) mouse strain, which has the same genetic background as their counterpart db/db mice that possess a diabetic phenotype.[119] These db/db mice would be subjects of further studies in a similar wound model. The db/db mice, in this instance, heal slower and have traits of chronic wound healing. Thus, the use of these mice would allow for preliminary *in vivo* research on fibrin foam as a chronic wound therapy, and this data could be compared back to their db/- littermates.

An additional animal study that would need to be performed to assess the validity of fibrin foam as a novel wound therapy would be a larger animal study. Pigs would be used, as porcine skin structure is highly similar to that of humans and correlates greatly. Alterations to the histological parameter assessment would also be performed, as this study lacked significance within the histology and pathology analyses of the treated wounds. These changes would include an expanded scoring scale for the histological parameters and immunohistochemical analysis of the wounds. The scoring scale used in this research were scored from 0-3 (Table 8) or on a yes-or-no basis. While these scales allowed for an overall assessment of the wound histology, a more detailed scale could elucidate differences among the treatments. Furthermore, the use of

immunohistochemistry to study the wound samples could be advantageous to gain a better understanding of the wound environment under each treatment. Antibodies, such as anti-Loricrin and CD28, could be utilized to stain for epidermal cell differentiation and angiogenesis, respectively.[130] Combined, these multiple animal studies would provide deep insight as to the efficacy and performance of fibrin in not only acute wounds, but chronic as well.

Fibrin foam was also tested for its use as a novel therapy in NPWT, since the foam showed superior wound healing abilities over the current dressing, polyurethane foam. While the *in vitro* feasibility results were positive, the next steps would require an animal model. A similar biopsy punch model performed on pigs would allow for the utilization of the actual NPWT vacuum system *in vivo*. Fibrin foam would be applied to the pigs after wounding, the vacuum system would be applied for several days, and wound healing would be compared to polyurethane foam. This experiment would be crucial for the overall efficacy assessment of fibrin foam for use as a therapy in a NPWT situation.

While fibrin foam seems to have abundant options in the clinical field, this research has also shown some other promising results for future applications. As shown in Figure 36, fibrin foam has the ability to be applied through laparoscopic applicators for use in minimally-invasive and endoscopic surgeries. With successful manipulations to the foam structure and/or clotting time, variations of the foam could be used laparoscopically in gastrointestinal anastomoses, perforated ulcer treatment, and hernia repair. Additionally, fibrin foam was able to be lyophilized and reconstituted to its native

fibrin foam structure. The lyophilization process could allow for a longer shelf life and quicker reconstitution, preparation, and application of fibrin foam at a wound site.

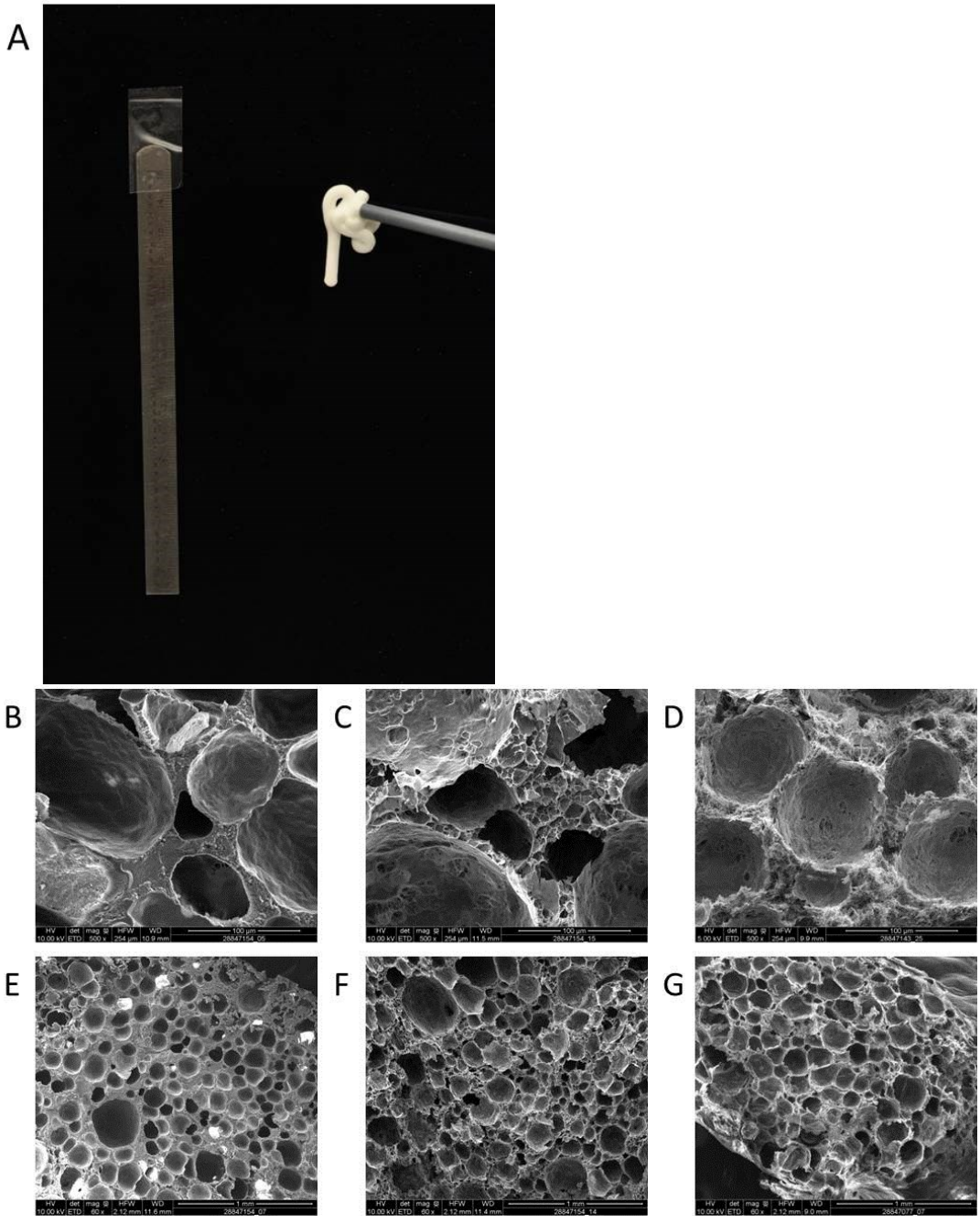

Figure 36. Additional Applications of Fibrin Foam. A) Fibrin foam usage through Baxter endoscopic applicator onto an inverted surface, such as used in minimally invasive surgeries. B/E) SEM images of lyophilized fibrin foam. C/F) SEM images of reconstituted fibrin foam. D/G) SEM images of native fibrin foam. Scale bars: 100 µm (B-D), 1 mm (E-G).

Throughout this combined research, I demonstrated that the biodegradable fibrin foam has unique macroscopic and microscopic structural characteristics from those of typical fibrin sealants. The foamed scaffold generates greater porosity, increased fluid permeability, and pore sizes suitable for cells and processes associated with a wound healing environment. Fibrin foam was also shown to be biocompatible and proved to be an efficacious and significantly superior acute wound healing treatment in both *in vitro* and *in vivo* model systems. This research sheds light on a novel fibrin matrix and its potential use as a wound therapy (Fig. 37). The results of this dissertation can also serve as the basis to develop innovative treatments – utilizing variants of fibrin foam – for specific surgical and regenerative medicine applications.

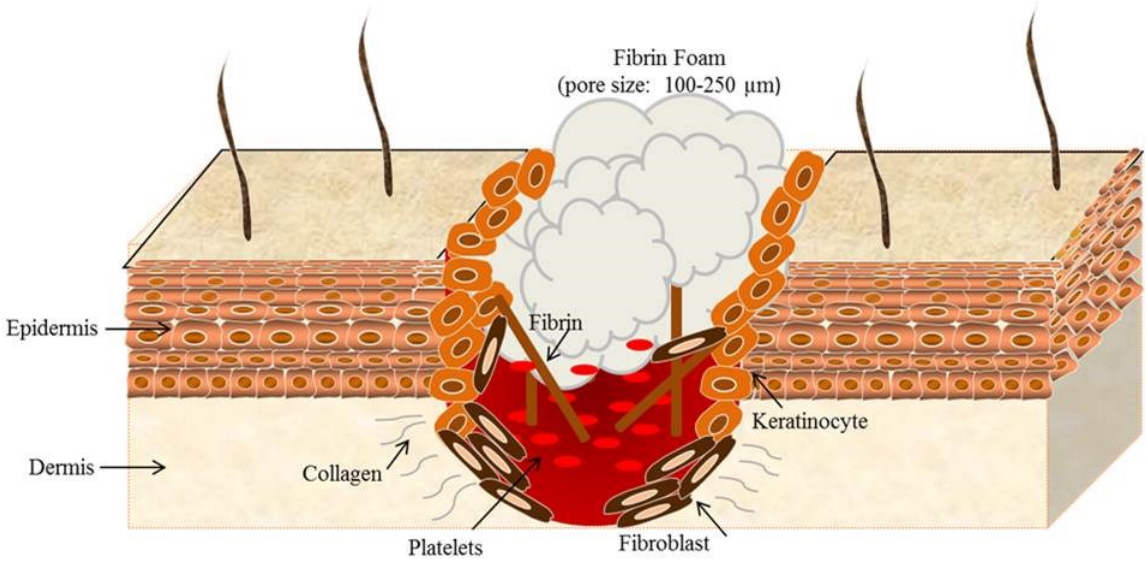

Figure 37. Fibrin Foam as a Novel Wound Therapy. An acute wound treated with the novel biopolymer, fibrin foam. With its pore size distribution, fibrin network, and wound-healing attributes, fibrin foam is a potential candidate for use in wound therapy.

Significance.

Wound healing products have been used in a variety of indications for many years. From acute lacerations to chronic pressure ulcers, wound healing products, such as

sutures and surgical sealants, have been the mainstay in this medical field. However, each wound healing treatment comes with its own set of caveats and flaws.[1] Sutures and staples can often lead to dehiscence or infection in wound closure space; while polyurethane foams can cause painful debridement from the tissues. An ageing population and increased occurrence of chronic wounds are additional trends that are affecting the wound healing field. Thus, the development and advancement of more efficacious and safe products is a substantial need for current and future patients. This research is significant because it served to improve the wound field by evaluating fibrin foam in two-fold – through characterization of its physical and biological properties, and analysis of the foam's use as an innovative wound therapy.

This research is impactful because it was the first to look at characterizing and understanding the unique set of qualities that fibrin foam possesses and how this knowledge could be translated to the medical field. The previously-mentioned attributes of the foam make it applicable for use in specific surgical and wound healing applications. The greater viscosity allows for fibrin foam to be applied on vertical or inverted surfaces, such as in laparoscopic surgeries or diabetic and pressure ulcer treatments. The foam's ability to polymerize independently of temperature is advantageous for a wide array of surgeries as the foam could be generated in the operating suite and be applied in a bodily cavity without the risk of altering the foam's structure and attributes.

Furthermore, the unique preparation method and characteristics of the foam alleviates some of the issues clinicians have with the current product and treatment options as well. The patented mixing device used for generation of the foam obviates the

need for gas-powered spray devices that are used in current surgeries to produce foam-like substances. These gas-powered spray devices are contraindicated for their use near open wounds and intravascular procedures due to the potential for thromboembolisms.[23] Fibrin foam allows for a similar foaming structure without the need for the additional surgical equipment.

This research has also provided a better understanding of novel aerated biopolymer – a fibrin-based foam – as a wound therapy agent as well. Fibrin and surgical sealants have been used as acute wound closure treatments for years. The benefits to fibrin sealants are that they mechanically seal the wound, aid in the hemostatic phase of wound healing, and are biocompatible and biodegradable. The foam's structure is important to understanding its potential significance in the wound healing field. Fibrin foam's open pore clot structure promoted migration and invasion of cells into the foam. This elicited an improved wound healing response when compared to current treatments. In the wound healing field, a specific treatment called negative-pressure wound therapy (NPWT) utilizes polyurethane foam or gauze to cover the wound site to treat acute and chronic wounds. Vacuum pressure is then applied to the site to mechanically seal the wound. However, discomfort, pain, and impaired wound healing can result from the use of the polyurethane foam or gauze dressings. Polyurethane foam dressing must be periodically debrided from the wound, a process which disrupts the wound and can remove healing tissue. Therefore, there is a critical need for a biodegradable wound dressing in this therapy. The research here evaluated fibrin foam for its use in NPWT. Fibrin foam's matrix and wound-healing ability are beneficial for cells and tissues to grow into the biodegradable foam under vacuum treatment.

While this research was centered on understanding how fibrin foam is generated, defining its key attributes, and assessing its function as a wound therapy in both acute wound and NPWT models, the significance of the research is much greater. The thorough analyses that were performed on fibrin foam will serve as a platform for the foam's use in other surgical fields. It is imperative to realize the foam's full potential while evaluating its concept as a wound healing treatment and beyond.

APPENDIX A

SUPPLEMENTAL DATA

Parameter	ARTISS fibrin sealant	Fibrin foam (6 Passes)	Fibrin foam (4 Passes)	Fibrin foam (8 Passes)	Fibrin foam (6 Passes + 20IU)	Fibrin Foam (6 Passes + 10% HSA)
R (clot formation, minutes)	0.6 ± 0.4	0.2 ± 0.0	0.2 ± 0.0	0.2 ± 0.1	0.2 ± 0.1	0.2 ± 0.1
K (degree of elasticity, minutes)	4.5 ± 1.8	0.8 ± 0.0	0.8 ± 0.0	0.8 ± 0.0	0.8 ± 0.0	0.8 ± 0.0
Maximum amplitude (MA; clot strength, mm)	85.0 ± 6.6	88.1 ± 1.8	87.3 ± 2.0	89.7 ± 1.0	86.4 ± 1.9	87.8 ± 0.9
G (shear modulus, kd/sec)	35.5 ± 18.9	38.0 ± 6.5	35.3 ± 7.4	43.8 ± 4.6	32.3 ± 5.5	36.2 ± 3.0
α-angle (clot kinetics, degrees)	49.8 ± 11.4	86.0 ± 0.7	84.4 ± 0.6	86.1 ± 0.4	87.5± 0.0	85.8 ± 0.3

Table A1. Thromboelastography Analysis of Fibrin Foam Preparations.
Thromboelastography (TEG) results obtained for fibrin foam and commercially-available fibrin sealant, ARTISS. Parameters measured included: fibrin clot formation (R), degree of elasticity (K), α-angle, and clot (MA) and shear strengths (G). Any other fibrin foam preparations not listed were not feasible for TEG analysis due to clotting and viscosity issues with the TEG test system.

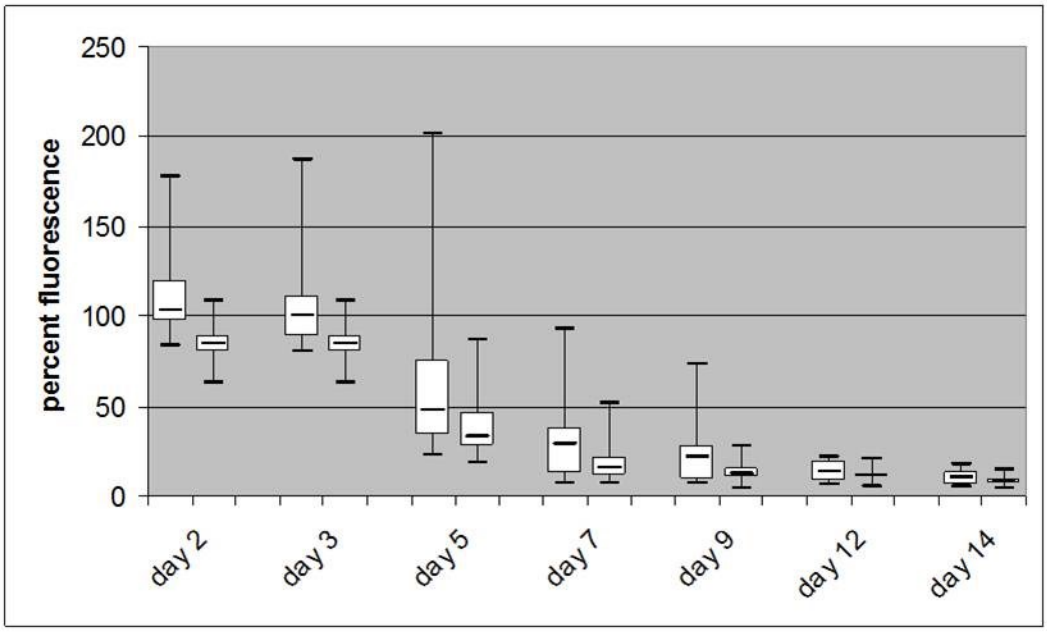

Figure A1. *In Vivo* Degradation Analysis of Fibrin Foam. Fluorescence of remaining ARTISS fibrin sealant (left boxes) or fibrin foam (right boxes) at each time point is presented in percent of day 0 fluorescence. Degradation of both materials followed a sigmoidal pattern over the observational period of 14 days. No significant differences in the degradation process were detected. n = 6 per group.

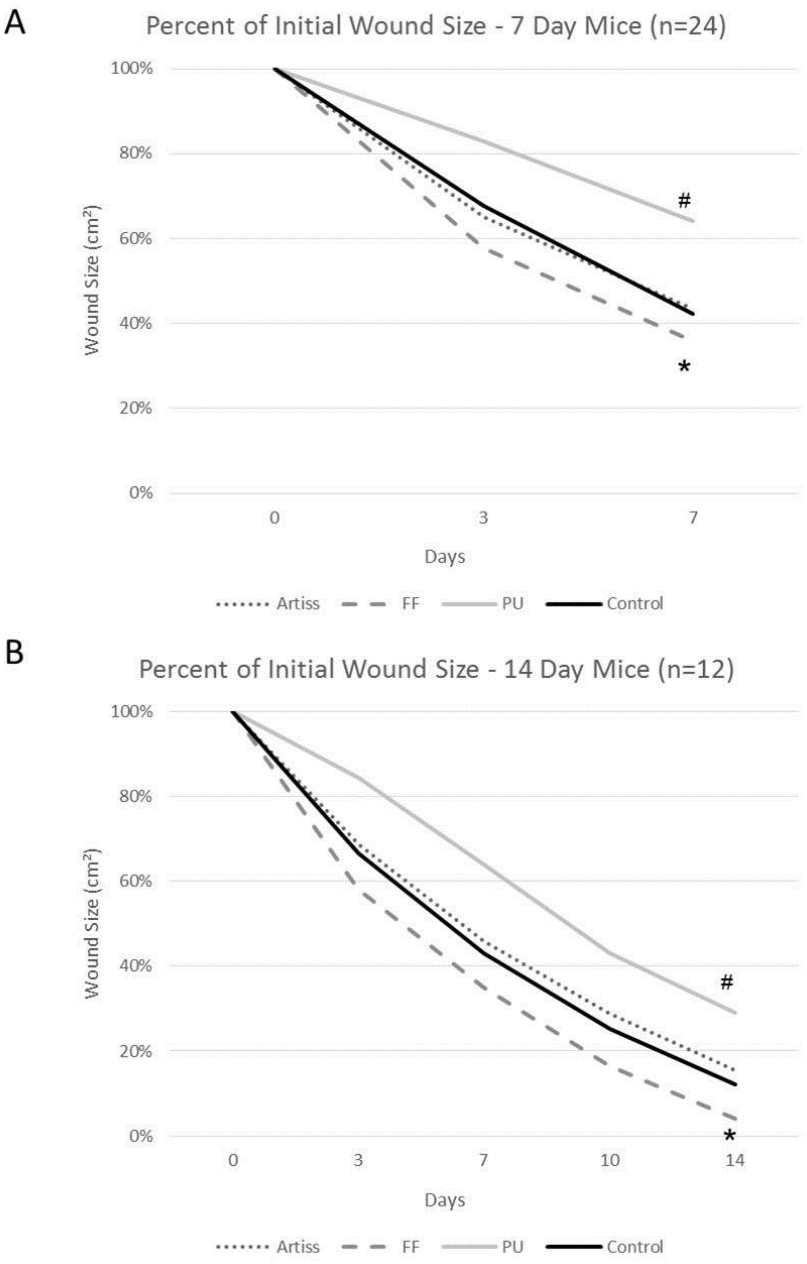

Figure A2. Wound Closure Assessment of Fibrin Foam. Initial wound sizes (considered 100% open) were equivalent for the four treatments but significantly different subsequent days ($p < 0.001$ for days 3-14). A) By day seven, wounds treated with fibrin foam (FF) were smallest compared to all other treatments ($*p < 0.05$). Wounds were significantly larger for polyurethane foam (PU) compared to the other treatments ($\#p < 0.001$). B) At day 14, initial wound sizes were similar for all treatments. Similar to day 7, wounds were significantly larger for PU compared to all other treatments ($\#p < 0.001$) at day fourteen. Wounds treated with fibrin foam were significantly smaller compared to the other treatments ($*p < 0.05$). Twenty-four mice were analyzed for panel A and twelve mice were analyzed in panel B.

n (%)	0	1	2	3
Reepithelization				
Artiss	3 (25.0)	5 (41.7)	3 (25.0)	1 (8.3)
Control	5 (41.7)	3 (25.0)	2 (16.7)	2 (16.7)
FF	2 (16.7)	4 (33.3)	3 (25.0)	3 (25.0)
PU	5 (41.7)	5 (41.7)	2 (16.7)	0 (0.0)
Neovascular proliferation				
Artiss	0 (0.0)	6 (50.0)	4 (33.3)	2 (16.7)
Control	2 (16.7)	5 (41.7)	3 (25.0)	2 (16.7)
FF	0 (0.0)	4 (33.3)	4 (33.3)	4 (33.3)
PU	0 (0.0)	3 (25.0)	5 (41.7)	4 (33.3)
Acute inflammation				
Artiss	0 (0.0)	5 (41.7)	6 (50.0)	1 (8.3)
Control	0 (0.0)	8 (66.7)	4 (33.3)	0 (0.0)
FF	3 (25.0)	8 (66.7)	1 (8.3)	0 (0.0)
PU	0 (0.0)	3 (25.0)	1 (8.3)	8 (66.7)
Chronic inflammation				
Artiss	0 (0.0)	7 (58.3)	3 (25.0)	2 (16.7)
Control	0 (0.0)	9 (75.0)	3 (25.0)	0 (0.0)
FF	2 (16.7)	8 (66.7)	2 (16.7)	0 (0.0)
PU	0 (0.0)	5 (41.7)	6 (50.0)	1 (8.3)
Collagen Deposition				
Artiss	0 (0.0)	2 (50.0)	2 (50.0)	0 (0.0)
Control	0 (0.0)	3 (75.0)	1 (25.0)	0 (0.0)
FF	0 (0.0)	4 (100.0)	0 (0.0)	0 (0.0)
PU	3 (75.0)	1 (25.0)	0 (0.0)	0 (0.0)

Table A2a. Day 7 Mice Histological Assessment.

	n (%) Yes
Epithelial Maturation	
Artiss	1 (8.3)
Control	3 (25.0)
FF	5 (41.7)
PU	1 (8.3)
Granulation Tissue Formation	
Artiss	12 (100.0)
Control	10 (83.3)
FF	12 (100.0)
PU	12 (100.0)
Granulation Tissue Maturation	
Artiss	1 (8.3)
Control	1 (8.3)
FF	3 (25.0)
PU	2 (16.7)

Table A2b. Day 7 Mice Histological Assessment.

n (%)	0	1	2	3
Reepithelization				
Artiss	2 (16.7)	5 (41.7)	1 (8.3)	4 (33.3)
Control	0 (0.0)	3 (25.0)	0 (0.0)	9 (75.0)
FF	0 (0.0)	0 (0.0)	1 (8.3)	11 (91.7)
PU	2 (16.7)	2 (16.7)	4 (33.3)	4 (33.3)
Neovascular proliferation				
Artiss	1 (8.3)	5 (41.7)	3 (25.0)	3 (25.0)
Control	0 (0.0)	7 (58.3)	3 (25.0)	2 (16.7)
FF	3 (25.0)	6 (50.0)	1 (8.3)	2 (16.7)
PU	1 (8.3)	5 (41.7)	4 (33.3)	2 (16.7)
Acute inflammation				
Artiss	2 (16.7)	7 (58.3)	1 (8.3)	2 (16.7)
Control	3 (25.0)	7 (58.3)	2 (16.7)	0 (0.0)
FF	6 (50.0)	4 (33.3)	2 (16.7)	0 (0.0)
PU	1 (8.3)	3 (25.0)	0 (0.0)	8 (66.7)
Chronic inflammation				
Artiss	0 (0.0)	7 (58.3)	5 (41.7)	0 (0.0)
Control	0 (0.0)	9 (75.0)	3 (25.0)	0 (0.0)
FF	3 (25.0)	9 (75.0)	0 (0.0)	0 (0.0)
PU	0 (0.0)	7 (58.3)	5 (41.7)	0 (0.0)
Collagen Deposition				
Artiss	0 (0.0)	0 (0.0)	3 (75.0)	1 (25.0)
Control	0 (0.0)	0 (0.0)	2 (50.0)	2 (50.0)
FF	0 (0.0)	0 (0.0)	3 (75.0)	1 (25.0)
PU	0 (0.0)	3 (75.0)	1 (25.0)	0 (0.0)

Table A3a. Day 14 Mice Histological Assessment.

	n (%) Yes
Epithelial Maturation	
Artiss	4 (33.3)
Control	10 (83.3)
FF	7 (58.3)
PU	5 (41.7)
Granulation Tissue Formation	
Artiss	12 (100.0)
Control	10 (83.3)
FF	11 (91.7)
PU	12 (100.0)
Granulation Tissue Maturation	
Artiss	9 (75.0)
Control	10 (83.3)
FF	9 (75.0)
PU	5 (41.7)

Table A3b. Day 14 Mice Histological Assessment.

REFERENCE LIST

1. BCC Research. Wellesley, M. Markets for Advanced Wound Management Technologies, PHM011H. (2014).

2. MedMarket Diligence, L., Worldwide Surgical Sealants, Glues, Wound Closure and Anti-Adhesion Markets, 2010-2017, Report #S190, February 2012, Foothill Ranch, CA.

3. Elsevier Business Intelligence. Bridgewater, N. U.S. Markets for Current and Emerging Wound Closure Technologies, Final Report #A138. (2012).

4. Frost & Sullivan, M.E., Global Wound Care Market Outlook: Analysis of Wound Care Technologies, Report MA50-54, October 2014, Mountain View, CA.

5. Life Science Intelligence, I., Global Markets for Specialty Surgical Wound Care Products in 2013: Surgical Sealants, Glues, Absorbable Hemostats, and Adhesion Prevention Products, Report #LSI-WW131WO, August 2013, Huntington Beach, CA.

6. Janis, J.E., Kwon, R.K. & Lalonde, D.H. A practical guide to wound healing. *Plast Reconstr Surg* **125**, 230e-244e (2010).

7. Broughton, G., 2nd, Janis, J.E. & Attinger, C.E. The basic science of wound healing. *Plast Reconstr Surg* **117**, 12S-34S (2006).

8. Sen, C.K.*, et al.* Human skin wounds: a major and snowballing threat to public health and the economy. *Wound Repair Regen* **17**, 763-771 (2009).

9. Janis, J.E. & Harrison, B. Wound healing: part I. Basic science. *Plast Reconstr Surg* **133**, 199e-207e (2014).

10. Ehrenreich, M. & Ruszczak, Z. Update on tissue-engineered biological dressings. *Tissue Eng* **12**, 2407-2424 (2006).

11. Pruitt, B.A., Jr. & Levine, N.S. Characteristics and uses of biologic dressings and skin substitutes. *Arch Surg* **119**, 312-322 (1984).

12. Smith, D.J., Jr. Use of Biobrane in wound management. *J Burn Care Rehabil* **16**, 317-320 (1995).

13. Lorenti, A. Wound Healing: From Epidermis Culture to Tissue Engineering. *Cell Bio* **1**, 17-29 (2012).

14. Hu, M.S.*, et al.* Tissue engineering and regenerative repair in wound healing. *Ann Biomed Eng* **42**, 1494-1507 (2014).

15. Loh, Q.L. & Choong, C. Three-dimensional scaffolds for tissue engineering applications: role of porosity and pore size. *Tissue Eng Part B Rev* **19**, 485-502 (2013).

16. Laurens, N., Koolwijk, P. & de Maat, M.P. Fibrin structure and wound healing. *J Thromb Haemost* **4**, 932-939 (2006).

17. Bennett, J.S. Platelet-fibrinogen interactions. *Ann N Y Acad Sci* **936**, 340-354 (2001).

18. Martinez, J., Ferber, A., Bach, T.L. & Yaen, C.H. Interaction of fibrin with VE-cadherin. *Ann N Y Acad Sci* **936**, 386-405 (2001).

19. Flick, M.J., Du, X. & Degen, J.L. Fibrin(ogen)-alpha M beta 2 interactions regulate leukocyte function and innate immunity in vivo. *Exp Biol Med (Maywood)* **229**, 1105-1110 (2004).

20. Guadiz, G., Sporn, L.A. & Simpson-Haidaris, P.J. Thrombin cleavage-independent deposition of fibrinogen in extracellular matrices. *Blood* **90**, 2644-2653 (1997).

21. Rybarczyk, B.J., Lawrence, S.O. & Simpson-Haidaris, P.J. Matrix-fibrinogen enhances wound closure by increasing both cell proliferation and migration. *Blood* **102**, 4035-4043 (2003).

22. Ikari, Y., Yee, K.O. & Schwartz, S.M. Role of alpha5beta1 and alphavbeta3 integrins on smooth muscle cell spreading and migration in fibrin gels. *Thromb Haemost* **84**, 701-705 (2000).

23. Corporation, B.H. ARTISS, Fibrin Sealant Product Information. http://www.ARTISSadherence.com/int/index.html. . Vol. 2015 (2017).

24. Delmotte, Y.A. U.S. Patent #8,512,740. Fibrin Foam and Process for Making. (2013).

25. Delmotte, Y.A. Fibrin Foam and Process. (2014).

26. Delmotte, Y.A. U.S. Patent #8,641,661 B2. Mixing system, kit and mixer adapter. (2014).

27. Delmotte, Y.A. Devices for mixing and extruding medically useful compositions. Vol. U.S. Patent #7,766,919 B2 (2010).

28. Stevens, J., Brossard, G., Blom, A., Douteur, A. & Delmotte, Y. A Novel Sintered Porous Micromixer for the Effective Mixing of Biologics and Scale Model Investigation of Micromixing Mechanisms. *J Appl Fluid Mech* **5**, 91-100 (2012).

29. Fore, J. A review of skin and the effects of aging on skin structure and function. *Ostomy Wound Manage* **52**, 24-35; quiz 36-27 (2006).

30. Grice, E.A. & Segre, J.A. The skin microbiome. *Nat Rev Microbiol* **9**, 244-253 (2011).

31. Mackie, R.M. *Clinical Dermatology*, (Oxford Press, New York, NY, 2004).

32. Burns, D.A., Breathnach, M.S., Cox, N., Griffiths, C.E. *Rook's Textbook of Dermatology*, (Blackwell Publishing, Oxford, UK, 2004).

33. Fitzpatrick, J.E., Morelli, J.G. *Dermatology Secrets*, (Mosby Publishing, Philadelphia, PA, 2006).

34. Jarbrink, K.*, et al.* Prevalence and incidence of chronic wounds and related complications: a protocol for a systematic review. *Syst Rev* **5**, 152 (2016).

35. Yates, C.C., Hebda, P. & Wells, A. Skin wound healing and scarring: fetal wounds and regenerative restitution. *Birth Defects Res C Embryo Today* **96**, 325-333 (2012).

36. Broughton, G., 2nd, Janis, J.E. & Attinger, C.E. Wound healing: an overview. *Plast Reconstr Surg* **117**, 1e-S-32e-S (2006).

37. Witte, M.B. & Barbul, A. General principles of wound healing. *Surg Clin North Am* **77**, 509-528 (1997).

38. Pohlman, T.H., Stanness, K.A., Beatty, P.G., Ochs, H.D. & Harlan, J.M. An endothelial cell surface factor(s) induced in vitro by lipopolysaccharide, interleukin 1, and tumor necrosis factor-alpha increases neutrophil adherence by a CDw18-dependent mechanism. *J Immunol* **136**, 4548-4553 (1986).

39. Lawrence, W.T. & Diegelmann, R.F. Growth factors in wound healing. *Clin Dermatol* **12**, 157-169 (1994).

40. Kurkinen, M., Vaheri, A., Roberts, P.J. & Stenman, S. Sequential appearance of fibronectin and collagen in experimental granulation tissue. *Lab Invest* **43**, 47-51 (1980).

41. Diegelmann, R.F. Analysis of collagen synthesis. *Methods Mol Med* **78**, 349-358 (2003).

42. Grotendorst, G.R., Soma, Y., Takehara, K. & Charette, M. EGF and TGF-alpha are potent chemoattractants for endothelial cells and EGF-like peptides are present at sites of tissue regeneration. *J Cell Physiol* **139**, 617-623 (1989).

43. Demidova-Rice, T.N., Hamblin, M.R. & Herman, I.M. Acute and impaired wound healing: pathophysiology and current methods for drug delivery, part 1: normal and chronic wounds: biology, causes, and approaches to care. *Adv Skin Wound Care* **25**, 304-314 (2012).

44. Demidova-Rice, T.N., Hamblin, M.R. & Herman, I.M. Acute and impaired wound healing: pathophysiology and current methods for drug delivery, part 2: role of growth factors in normal and pathological wound healing: therapeutic potential and methods of delivery. *Adv Skin Wound Care* **25**, 349-370 (2012).

45. Sullivan, T.P., Eaglstein, W.H., Davis, S.C. & Mertz, P. The pig as a model for human wound healing. *Wound Repair Regen* **9**, 66-76 (2001).

46. Wang, X., Ge, J., Tredget, E.E. & Wu, Y. The mouse excisional wound splinting model, including applications for stem cell transplantation. *Nat Protoc* **8**, 302-309 (2013).

47. Sullivan, S.R.*, et al.* Validation of a model for the study of multiple wounds in the diabetic mouse (db/db). *Plast Reconstr Surg* **113**, 953-960 (2004).

48. Gale, A.J. Continuing Education Course #2: Current Understanding of Hemostasis. *Toxicol Pathol* **39**, 273-280 (2011).

49. Colvin, B.T. Physiology of haemostasis. *Vox Sang* **87 Suppl1**, 43-46 (2004).

50. Monroe DM, H.M., Roberts HR. *Molecular biology and biochemistry of the coagulation factors and pathways of hemostasis. Williams Hematology. 8th ed*, (McGraw-Hill Professional Publishing, New York NY, 2010).

51. Hoffman, M. & Monroe, D.M. Coagulation 2006: a modern view of hemostasis. *Hematol Oncol Clin North Am* **21**, 1-11 (2007).

52. Esper, R.J.*, et al.* Endothelial dysfunction: a comprehensive appraisal. *Cardiovasc Diabetol* **5**, 4 (2006).

53. Zucker-Franklin, D. *Megakaryocyte and platelet structure. In: Hoffman, R.; Benz, EJ.; Shattil, SJ.; Furie, B.; Silberstein, LE.; McGlave, P., editors.*, (Churchill Livingstone, New York, 2000).

54. Andrews, R.K. & Berndt, M.C. Platelet physiology and thrombosis. *Thromb Res* **114**, 447-453 (2004).

55. Ashby, B., Daniel, J.L. & Smith, J.B. Mechanisms of platelet activation and inhibition. *Hematol Oncol Clin North Am* **4**, 1-26 (1990).

56. Heemskerk, J.W., Bevers, E.M. & Lindhout, T. Platelet activation and blood coagulation. *Thromb Haemost* **88**, 186-193 (2002).

57. Ruggeri, Z.M. Platelet adhesion under flow. *Microcirculation* **16**, 58-83 (2009).

58. Ruggeri, Z.M. & Mendolicchio, G.L. Adhesion mechanisms in platelet function. *Circ Res* **100**, 1673-1685 (2007).

59. Kirchhofer, D. & Nemerson, Y. Initiation of blood coagulation: the tissue factor/factor VIIa complex. *Curr Opin Biotechnol* **7**, 386-391 (1996).

60. Lane, D.A., Philippou, H. & Huntington, J.A. Directing thrombin. *Blood* **106**, 2605-2612 (2005).

61. Dahlback, B. Blood coagulation. *Lancet* **355**, 1627-1632 (2000).

62. Lasne, D., Jude, B. & Susen, S. From normal to pathological hemostasis. *Can J Anaesth* **53**, S2-11 (2006).

63. Triplett, D.A. Coagulation and bleeding disorders: review and update. *Clin Chem* **46**, 1260-1269 (2000).

64. Kahn, M.L.*, et al.* A dual thrombin receptor system for platelet activation. *Nature* **394**, 690-694 (1998).

65. Moss, R. Management of Surgical Hemostasis: An Independent Study Guide. *AORN, Inc.* (2013).

66. Lijnen, H.C., D. . *Molecular and cellular basis of fibrinolysis. Hematology Basic Principles and Practice*, (Churchill Livingstone, New York, 2000).

67. Szymanski, L.M., Pate, R.R. & Durstine, J.L. Effects of maximal exercise and venous occlusion on fibrinolytic activity in physically active and inactive men. *J Appl Physiol (1985)* **77**, 2305-2310 (1994).

68. Huber, K., Christ, G., Wojta, J. & Gulba, D. Plasminogen activator inhibitor type-1 in cardiovascular disease. Status report 2001. *Thromb Res* **103 Suppl 1**, S7-19 (2001).

69. Xiao, Q., *et al.* Plasminogen deficiency accelerates vessel wall disease in mice predisposed to atherosclerosis. *Proc Natl Acad Sci U S A* **94**, 10335-10340 (1997).

70. Ugarova, T.P. & Yakubenko, V.P. Recognition of fibrinogen by leukocyte integrins. *Ann N Y Acad Sci* **936**, 368-385 (2001).

71. Yakovlev, S., Zhang, L., Ugarova, T. & Medved, L. Interaction of fibrin(ogen) with leukocyte receptor alpha M beta 2 (Mac-1): further characterization and identification of a novel binding region within the central domain of the fibrinogen gamma-module. *Biochemistry* **44**, 617-626 (2005).

72. Richardson, D.L., Pepper, D.S. & Kay, A.B. Chemotaxis for human monocytes by fibrinogen-derived peptides. *Br J Haematol* **32**, 507-513 (1976).

73. Gross, T.J., Leavell, K.J. & Peterson, M.W. CD11b/CD18 mediates the neutrophil chemotactic activity of fibrin degradation product D domain. *Thromb Haemost* **77**, 894-900 (1997).

74. Thiagarajan, P., Rippon, A.J. & Farrell, D.H. Alternative adhesion sites in human fibrinogen for vascular endothelial cells. *Biochemistry* **35**, 4169-4175 (1996).

75. Liu, H.M., Wang, D.L. & Liu, C.Y. Interactions between fibrin, collagen and endothelial cells in angiogenesis. *Adv Exp Med Biol* **281**, 319-331 (1990).

76. Farrell, D.H. & al-Mondhiry, H.A. Human fibroblast adhesion to fibrinogen. *Biochemistry* **36**, 1123-1128 (1997).

77. Becker, J.C., Domschke, W. & Pohle, T. Biological in vitro effects of fibrin glue: fibroblast proliferation, expression and binding of growth factors. *Scand J Gastroenterol* **39**, 927-932 (2004).

78. Samudrala, S. Topical hemostatic agents in surgery: a surgeon's perspective. *AORN J* **88**, S2-11 (2008).

79. Spotnitz, W.D. & Burks, S. Hemostats, sealants, and adhesives: components of the surgical toolbox. *Transfusion* **48**, 1502-1516 (2008).

80. Spotnitz, W.D. & Burks, S. State-of-the-art review: Hemostats, sealants, and adhesives II: Update as well as how and when to use the components of the surgical toolbox. *Clin Appl Thromb Hemost* **16**, 497-514 (2010).

81. Fraser, I.S., Porte, R.J., Kouides, P.A. & Lukes, A.S. A benefit-risk review of systemic haemostatic agents: part 2: in excessive or heavy menstrual bleeding. *Drug Saf* **31**, 275-282 (2008).

82. Undas, A. & Ariens, R.A. Fibrin clot structure and function: a role in the pathophysiology of arterial and venous thromboembolic diseases. *Arterioscler Thromb Vasc Biol* **31**, e88-99 (2011).

83. Di Cera, E., Dang, Q.D. & Ayala, Y.M. Molecular mechanisms of thrombin function. *Cell Mol Life Sci* **53**, 701-730 (1997).

84. Wood, J.P., Silveira, J.R., Maille, N.M., Haynes, L.M. & Tracy, P.B. Prothrombin activation on the activated platelet surface optimizes expression of procoagulant activity. *Blood* **117**, 1710-1718 (2011).

85. Weisel, J.W. Structure of fibrin: impact on clot stability. *J Thromb Haemost* **5 Suppl 1**, 116-124 (2007).

86. Chiu, C.L., Hecht, V., Duong, H., Wu, B. & Tawil, B. Permeability of three-dimensional fibrin constructs corresponds to fibrinogen and thrombin concentrations. *Biores Open Access* **1**, 34-40 (2012).

87. Spotnitz, W.D. Fibrin Sealant: The Only Approved Hemostat, Sealant, and Adhesive-a Laboratory and Clinical Perspective. *ISRN Surg* **2014**, 203943 (2014).

88. Gugerell, A.*, et al.* High thrombin concentrations in fibrin sealants induce apoptosis in human keratinocytes. *J Biomed Mater Res A* **100**, 1239-1247 (2012).

89. Dickneite, G., Metzner, H., Pfeifer, T., Kroez, M. & Witzke, G. A comparison of fibrin sealants in relation to their in vitro and in vivo properties. *Thromb Res* **112**, 73-82 (2003).

90. Curie, L.J., Shapre, J.R., Martin, R. The Use of Fibrin Glue in Skin Grafts and Tissue-Engineered Skin Replacements: A Review. *Plast Reconstr Surg* **108**, 1713-1726 (2001).

91. Lee, M.G. & Jones, D. Applications of fibrin sealant in surgery. *Surg Innov* **12**, 203-213 (2005).

92. Janmey, P.A., Winer, J.P. & Weisel, J.W. Fibrin gels and their clinical and bioengineering applications. *J R Soc Interface* **6**, 1-10 (2009).

93. Wong, C., Inman, E., Spaethe, R. & Helgerson, S. Fibrin-based biomaterials to deliver human growth factors. *Thromb Haemost* **89**, 573-582 (2003).

94. Briganti, E.*, et al.* A composite fibrin-based scaffold for controlled delivery of bioactive pro-angiogenetic growth factors. *J Control Release* **142**, 14-21 (2010).

95. Dhivya, S., Padma, V.V. & Santhini, E. Wound dressings - a review. *Biomedicine (Taipei)* **5**, 22 (2015).

96. Sood, A., Granick, M.S. & Tomaselli, N.L. Wound Dressings and Comparative Effectiveness Data. *Adv Wound Care (New Rochelle)* **3**, 511-529 (2014).

97. Branski, L.K., Pereira, C.T., Herndon, D.N. & Jeschke, M.G. Gene therapy in wound healing: present status and future directions. *Gene Ther* **14**, 1-10 (2007).

98. O'Brien, F.J.*, et al.* The effect of pore size on permeability and cell attachment in collagen scaffolds for tissue engineering. *Technol Health Care* **15**, 3-17 (2007).

99. O'Brien, F.J., Harley, B.A., Yannas, I.V. & Gibson, L.J. The effect of pore size on cell adhesion in collagen-GAG scaffolds. *Biomaterials* **26**, 433-441 (2005).

100. Lorenzetti, O.J., Fortenberry, B., Busby, E. & Uberman, R. Influence of microcrystalline collagen on wound healing. I. Wound closure of normal excised and burn excised wounds of rats, rabbits, and pigs. *Proc Soc Exp Biol Med* **140**, 896-900 (1972).

101. Longaker, M.T.*, et al.* Studies in fetal wound healing. IV. Hyaluronic acid-stimulating activity distinguishes fetal wound fluid from adult wound fluid. *Ann Surg* **210**, 667-672 (1989).

102. Madihally, S.V. & Matthew, H.W. Porous chitosan scaffolds for tissue engineering. *Biomaterials* **20**, 1133-1142 (1999).

103. Osathanon, T.*, et al.* Microporous nanofibrous fibrin-based scaffolds for bone tissue engineering. *Biomaterials* **29**, 4091-4099 (2008).

104. Livesey, S.A., Herndon, D.N., Hollyoak, M.A., Atkinson, Y.H. & Nag, A. Transplanted acellular allograft dermal matrix. Potential as a template for the reconstruction of viable dermis. *Transplantation* **60**, 1-9 (1995).

105. Macchiarini, P.*, et al.* Clinical transplantation of a tissue-engineered airway. *Lancet* **372**, 2023-2030 (2008).

106. Hollister, S.J. Porous scaffold design for tissue engineering. *Nat Mater* **4**, 518-524 (2005).

107. Nair, R., Shukla, S. & McDevitt, T.C. Acellular matrices derived from differentiating embryonic stem cells. *J Biomed Mater Res A* **87**, 1075-1085 (2008).

108. Weaire, D., Hutzler, S. *The Physics of Foams*, (Oxford University Press, New York, 1999).

109. Saint-Jalmes, A., Langevin, D. Time evolution of aqueous foams: drainage and coarsening. *J Phys Condens Matter* **14**, 9397-9412 (2002).

110. Saint-Jalmes, A. Physical chemistry in foam drainage and coarsening. *Soft Matter* **2**, 836–849 (2006).

111. Hilgenfeldt, S., Koehler, S.A., Stone, H.A. Dynamics of Coarsening Foams: Accelerated and Self-Limited Drainage. *Physical Review Letters* **86**, 4704-4707 (2001).

112. Cooper, A. & Kennedy, M.W. Biofoams and natural protein surfactants. *Biophys Chem* **151**, 96-104 (2010).

113. *Biomedical Foams for Tissue Engineering Applications*, (Woodhead Publishing Series in Biomaterials, New York, 2014).

114. International, A. ASTM F2458-05: Standard Test Method for Wound Closure Strength of Tissue Adhesives and Sealants. *2010 Annual Book of ASTM Standards.* (2010).

115. Solomon, C., Ranucci, M., Hochleitner, G., Schochl, H. & Schlimp, C.J. Assessing the Methodology for Calculating Platelet Contribution to Clot Strength (Platelet Component) in Thromboelastometry and Thrombelastography. *Anesth Analg* **121**, 868-878 (2015).

116. Sugo, T.*, et al.* Fibrinogen Niigata with impaired fibrin assembly: an inherited dysfibrinogen with a Bbeta Asn-160 to Ser substitution associated with extra glycosylation at Bbeta Asn-158. *Blood* **94**, 3806-3813 (1999).

117. Undas, A.*, et al.* Altered plasma fibrin clot properties and fibrinolysis in patients with multiple myeloma. *Eur J Clin Invest* **44**, 557-566 (2014).

118. ISO 10993-5. Biological Evaluation of Medical Products. (2009).

119. Galiano, R.D., Michaels, J.t., Dobryansky, M., Levine, J.P. & Gurtner, G.C. Quantitative and reproducible murine model of excisional wound healing. *Wound Repair Regen* **12**, 485-492 (2004).

120. Abramov, Y.*, et al.* Histologic characterization of vaginal vs. abdominal surgical wound healing in a rabbit model. *Wound Repair Regen* **15**, 80-86 (2007).

121. Glidden, P.F., Malaska, C. & Herring, S.W. Thromboelastograph assay for measuring the mechanical strength of fibrin sealant clots. *Clin Appl Thromb Hemost* **6**, 226-233 (2000).

122. Hickerson, W.L., Nur, I. & Meidler, R. A comparison of the mechanical, kinetic, and biochemical properties of fibrin clots formed with two different fibrin sealants. *Blood Coagul Fibrinolysis* **22**, 19-23 (2011).

123. Khorshidi, H., Raoofi, S., Bagheri, R. & Banihashemi, H. Comparison of the Mechanical Properties of Early Leukocyte- and Platelet-Rich Fibrin versus PRGF/Endoret Membranes. *Int J Dent* **2016**, 1849207 (2016).

124. Al-Nasiry, S., Geusens, N., Hanssens, M., Luyten, C. & Pijnenborg, R. The use of Alamar Blue assay for quantitative analysis of viability, migration and invasion of choriocarcinoma cells. *Hum Reprod* **22**, 1304-1309 (2007).

125. Xie, Y.*, et al.* Development of a three-dimensional human skin equivalent wound model for investigating novel wound healing therapies. *Tissue Eng Part C Methods* **16**, 1111-1123 (2010).

126. Shweiki, E. & Gallagher, K.E. Assessing a safe interval for subsequent negative pressure wound therapy change after initial placement in acute, contaminated wounds. *Wounds* **25**, 263-271 (2013).

127. Shweiki, E. & Gallagher, K.E. Negative pressure wound therapy in acute, contaminated wounds: documenting its safety and efficacy to support current global practice. *Int Wound J* **10**, 13-43 (2013).

128. Hunter, J.E., Teot, L., Horch, R. & Banwell, P.E. Evidence-based medicine: vacuum-assisted closure in wound care management. *Int Wound J* **4**, 256-269 (2007).

129. Perez, R. & Davis, S.C. Relevance of animal models for wound healing. *Wounds* **20**, 3-8 (2008).

130. Gupta, A., Kumar, P. Assessment of the histological state of the healing wound. *Plastic and Aesthetic Research* **2**, 239-242 (2015).

VITA

The author, Adam R. Marek, was born in Chicago, Illinois on October 27th, 1987 to Robert and Tracy Marek. He received his Bachelor of Science in Chemistry from the University of Illinois at Urbana-Champaign in May 2010. After his undergraduate career, Adam came to Loyola University Chicago in pursuit of graduate education. He was welcomed into the Master of Science in Molecular and Cellular Biochemistry Program in August 2010. He later joined the laboratory of Nancy J. Zeleznik-Le, Ph.D., where he performed his research on the novel interaction of Mixed Lineage Leukemia (MLL) protein and a cohesin complex protein, Nipped B-like, and their impact on MLL-based leukemias.

After completing his M.S. in August 2012, Adam continued his journey at Loyola. He was accepted into both the Doctor of Philosophy in Molecular Pharmacology and Therapeutics Program as well as the Master of Business Administration Program at Loyola University's Quinlan School of Business. Adam finished his M.B.A. in Operations Management in August 2013 while simultaneously completing his Ph.D. coursework. Under the guidance of Richard H. Kennedy, Ph.D., Adam was fortunate to have the opportunity to pioneer an industrial research program for the university. He performed his doctoral research at Baxter Healthcare Corporation beginning in August 2014. There, he spent his years researching fibrin sealants – one of the mainstays in Baxter's surgical portfolio.

His research focused on the characterization of an aerated fibrin sealant and how this biopolymer performed as an innovative wound therapy. Throughout his years at Baxter, Adam was able to learn a great deal from his industry mentors and colleagues, including his main advisors, Shawn F. Bairstow, Ph.D. and John J. Barry, Ph.D. Alongside his daily activities at Baxter, Adam also served as an Adjunct Instructor at Benedictine University. There, Adam taught Exercise Pharmacology to graduate students in the Master of Science in Clinical Exercise Physiology Program. He served in this position from 2014 to 2016. After completing his Ph.D., Adam plans to pursue a career in the medical industry where he hopes to fully utilize his technical and business backgrounds.